# The copper sulphide mineralization of the Zinkgruvan deposit, Bergslagen, Sweden

*Karolina Bjärnborg*

**Examensarbeten i Geologi vid**
**Lunds universitet - Berggrundsgeologi, nr. 240**
**(45 hskp/ECTS)**

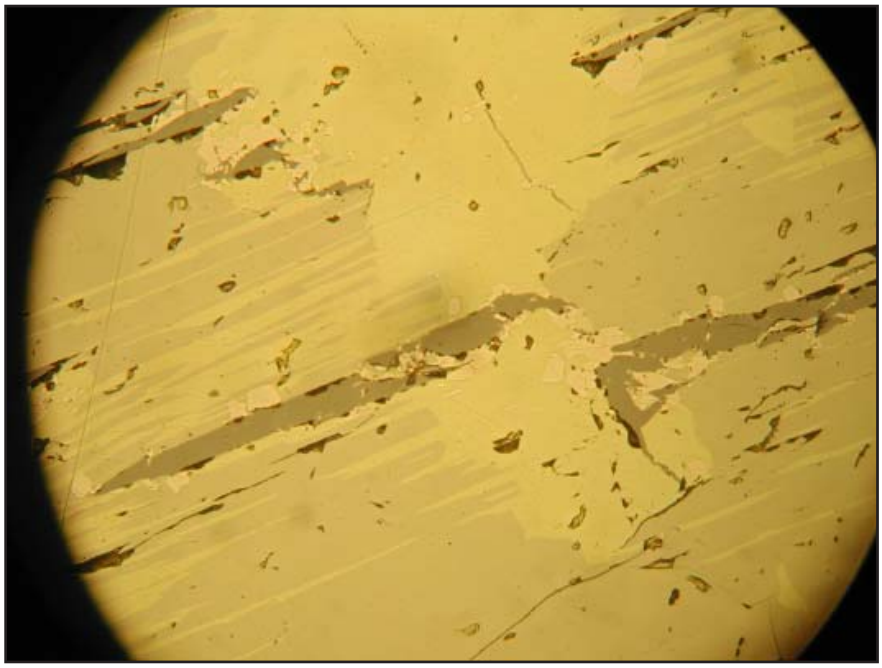

**Geologiska institutionen**
**Centrum för GeoBiosfärsvetenskap**
**Lunds universitet**
**2009**

# The copper sulphide mineralization of the Zinkgruvan deposit, Bergslagen, Sweden

Master Thesis

Karolina Bjärnborg

Department of Geology
Lund University
2009

# Contents



**Cover Picture:** Chalcopyrite with cubanite lamellae and magnetite-filled fractures (DBH2992 102.47 m).

# Contents, continuation

# The copper sulphide mineralization of the Zinkgruvan Deposit, Bergslagen, Sweden

KAROLINA BJÄRNBORG

Bjärnborg, K., 2009: The copper sulphide mineralization of the Zinkgruvan deposit, Bergslagen, Sweden. *Examensarbeten i geologi vid Lunds universitet*, Nr. 240, 62 pp. 45 ECTS.

**Abstract:** At Zinkgruvan, Sweden, zinc, lead and silver are mined from a stratiform ore body. It is considered syngenetic and situated in metavolcanic and metasedimentary rocks. A fault, the Knalla fault, separates the Zinkgruvan deposit into two parts. In the western part, Knalla, the ore is severely deformed, whereas in the eastern part, Nygruvan, a distinct layering occurs. In the western part of Knalla, stratigraphically below the Zn-Pb-Ag-ore, a copper sulphide mineralization occurs, predominantly in a marble unit. According to plans mining of the mineralization will start in the coming years.

The study is devoted to determining the occurring ore minerals and their distribution. In addition, the host minerals of the elements As, Sb, Bi and Hg are determined. Optical microscopy and scanning electron microscopy including energy dispersive X-ray analyses are the main tools of the study.

The study has showed that the dominating ore minerals in the copper sulphide mineralization are chalcopyrite and cubanite. Sphalerite, magnetite, cobalt-rich pentlandite and other Fe-Ni sulphides are common. Breithauptite, cobaltite, valleriite, bornite and a number of smaller arsenic- and antimony containing minerals occur. The ore minerals mostly occur in aggregates of varying size but also as discrete grains. Most ore minerals occur as both. The main exceptions are the Fe-Co-Ni-sulphides which only occur in the aggregates and the As- and Sb- containing minerals (except for breithauptite and cobaltite), which normally occur as intergrowths outside the aggregates. The richer the mineralization is, the larger and more numerous are the aggregates. In the richest part of the mineralization, the amounts of ore minerals exceed the amount of host rock minerals. Most of the ore minerals occur both in the weakly and strongly mineralized samples. The number of different minerals does not increase with increasing degree of mineralization.; merely the amounts of the ore minerals increase.

Cobaltite is the dominating As-containing mineral, but arsenopyrite and other minor As- and Sb- phases occur. Antimony foremost occurs in breithauptite but also in gudmundite, tetrahedrite and costibite. Bismuth mainly occurs as rounded grains in the host rock but rarely occurs as larger grains of metallic bismuth or as part of the mineral parkerite. Mercury has been proved in silver filled fractures. The two latter elements have a restricted distribution.

The chalcopyrite aggregates dominate the copper mineralization in most of the ore body, found in the carbonate horizon. In the underlying quartz-feldspar leptite sequence the degree of mineralization is low. Some parts of the marble have sections with a different host-rock mineralogy, such as high content of skarn minerals. There, the ore minerals occurring differs from the normal.

Chemically most of the ore minerals are relatively constant in composition; no significant difference can be demonstrated among the three studied cores, irrespective of stratigraphic position. Exceptions are cobalt-rich pentlandite, sphalerite and tetrahedrite, where significant variations in composition have been proved.

**Keywords:** Zinkgruvan, copper sulphide mineralization, chalcopyrite, cubanite

*Karolina Bjärnborg, Department of Geology, GeoBiosphere Science Centre, Lund University, Sölvegatan 12, SE-223 62 Lund, Sweden. E-mail: karolina.bjarnborg@gmail.com*

# Kopparsulfidmineraliseringen i Zinkgruvan, Bergslagen, Sverige

KAROLINA BJÄRNBORG

Bjärnborg, K., 2009: The copper sulphide mineralization of the Zinkgruvan deposit, Bergslagen, Sweden. *Examensarbeten i geologi vid Lunds universitet*, Nr. 240, 62 sid. 45 högskolepoäng.

**Sammanfattning:** I Zinkgruvan, Sverige, bryts zink, bly och silver ur en stratiform malmkropp. Denna anses vara syngenetiskt avsatt och återfinns i metavulkaniska och metasedimentära bergarter. En förkastning, Knallaförkastningen, delar malmförekomsten i två delar. Den västra delen, Knalla, är kraftigt deformerad medan den östra, Nygruvan, har en väl utvecklad lagring. Stratigrafiskt under Zn-Pb-Ag- malmen i västra delen av Knalla finns en kopparsulfidmineralisering. Denna är företrädesvis belägen i marmor. Brytningsstart planeras inom de närmaste åren.

I undersökningen skall de förekommande malmmineralen och deras fördelning bestämmas. Vidare omfattar studien ett klarläggande av i vilka mineral grundämnena As, Sb, Bi och Hg återfinns. De huvudsakliga undersökningsmetoderna utgörs av optiskt mikroskopering och svepelektronmikroskopering inklusive energidispersiv röntgenanalys.

Studien har visat att de dominerande malmmineralen i kopparsulfidmineraliseringen är kopparkis och kubanit. Zinkblände, magnetit, koboltrik pentlandit och andra Fe-Co-Ni-sulfider är vanliga. Breithauptit, koboltglans, valleriit, bornit samt ett antal mindre arsenik- och antimoninnehållande mineral återfinns. Malmmineralen sitter främst i aggregat av varierande storlek, men återfinns även som enstaka spridda korn. De flesta malmmineralen kan återfinnas på båda sätt. Undantagen är Fe-Co-Ni sulfider som enbart förekommer i aggregaten och As- och Sb- innehållande mineral (bortsett från breithauptit och koboltglans) som normalt förekommer som kristaller invuxna i varandra men utanför aggregaten. Desto rikare mineraliseringen blir, desto större och fler blir de aggregat i vilka främst kopparsulfiderna är lokaliserade. I de rikaste delarna överväger mängden malmmineral mängden bergartsbildande mineral. Vanligen kan de flesta malmmineral återfinnas i fattiga såväl som rika prov. Antalet olika mineral som återfinns ökar inte med ökande malmhalt utan det är främst mängden av respektive mineral som ökar.

I mineraliseringen återfinns Arsenik främst i koboltglans men även i arsenikkis och andra As- och Sb-förande faser som finns i små mängder. Antimon återfinns främst i breithauptit, men även i gudmundit, tetrahedrit och kostibit. Vismut sitter som små droppformade korn i värdbergarten men även i ett fåtal fall som större korn eller som del i mineralet parkerit. Kvicksilver återfinns i silverfyllda sprickor. De två senare elementen har, av vad studien kunnat visa, en relativt begränsad utbredning.

Kopparkisaggregaten dominerar mineraliseringen i större delen av malmen, som är belägen i en karbonathorisont. Kvarts-fältspatsleptit, som överlagras av marmorn, är mycket svagt mineraliserad. I vissa delar av marmorn finns inlagringar av andra bergarter, t.ex. skarnbergarter. De malmmineral som återfinns där skiljer sig från det normala.

De flesta malmmineralen är relativt konstanta i sin sammansättning. Detta gäller både mellan de tre undersökta borrkärnorna och inom en och samma borrkärna oavsett placering i stratigrafin. Undantag utgörs av koboltrik pentlandit, zinkblände och tetrahedrit, där en signifikant kemisk variation har påvisats.

**Nyckelord:** Zinkgruvan, kopparsulfidmineralisering, kopparkis, kubanit

*Karolina Bjärnborg, Geologiska Institutionen, Centrum för GeoBiosfärsvetenskap, Lunds Universitet, Sölvegatan 12, 223 62 Lund, Sverige. E-post: karolina.bjarnborg@gmail.com*

# 1 Introduction

The Zinkgruvan community, which was built up around the zinc mine, is located around 50 km south of Örebro in the Bergslagen ore district, Sweden (Fig. 1). The zinc-lead deposit, which has been mined since the 19th century, is a stratiform deposit of Precambrian age occurring in a metavolcanic-metasedimentary unit. Sphalerite and galena are the main minerals of the deposit, but silver is also important and is a third mining product. In the lower part of the stratigraphic unit hosting the zinc-lead ore, there is a copper sulphide mineralization. It is planned to be mined for production in the coming years. A dolomitic marble is the main host rock of the copper mineralization. Chalcopyrite is the dominating ore mineral but also cubanite, bornite, magnetite, pentlandite and sphalerite are common.

During the study, ore microscopy was used frequently. It is an important method in the study of an ore or mineralization and differs from petrographic microscopy by the use of a reflected light source. Ore minerals are mostly opaque and are more or less impossible to identify under the transmitted light microscope. In reflected light the optical properties, such as colour, reflectivity and anisotropy of the opaque minerals can be distinguished, and the minerals can thereby be identified.

The copper mineralization has so far not been investigated in detail and there are still many questions to ask. Hopefully this study can shed light on some of the mineralogical and microscopic aspects.

## 1.1 Purpose and questions of issue

It is important to investigate a mineralization, not only for mineralogical interest, but it also gives significant information for the valuation and the ore-processing further ahead. There is an interest to know, in which minerals the interesting elements occur and how these are distributed. Some compounds and elements give penalty fees during the production of the metals, due to the extra effort and costs in refining. Hence it is important to know where to expect these.

The purpose of the study is to investigate the mineralogy of the copper mineralization of the Zinkgruvan formation. The main aspects are to study the ore minerals; the major as well as the minor minerals, their internal relations and distribution. Another important aspect is to investigate where to find the penalty giving elements bismuth, antimony, arsenic and mercury; in which minerals and assemblages they normally occur. Both morphological and chemical analyses are of importance for the study.

The following questions of issue were formulated:

- Which are the main ore minerals in the copper mineralization and how are these distributed?
- Which minerals containing bismuth, antimony, arsenic or mercury can be found in the mineralization and how are they distributed?
- Is there a variation in the chemical composition of the minerals and within the mineralization?

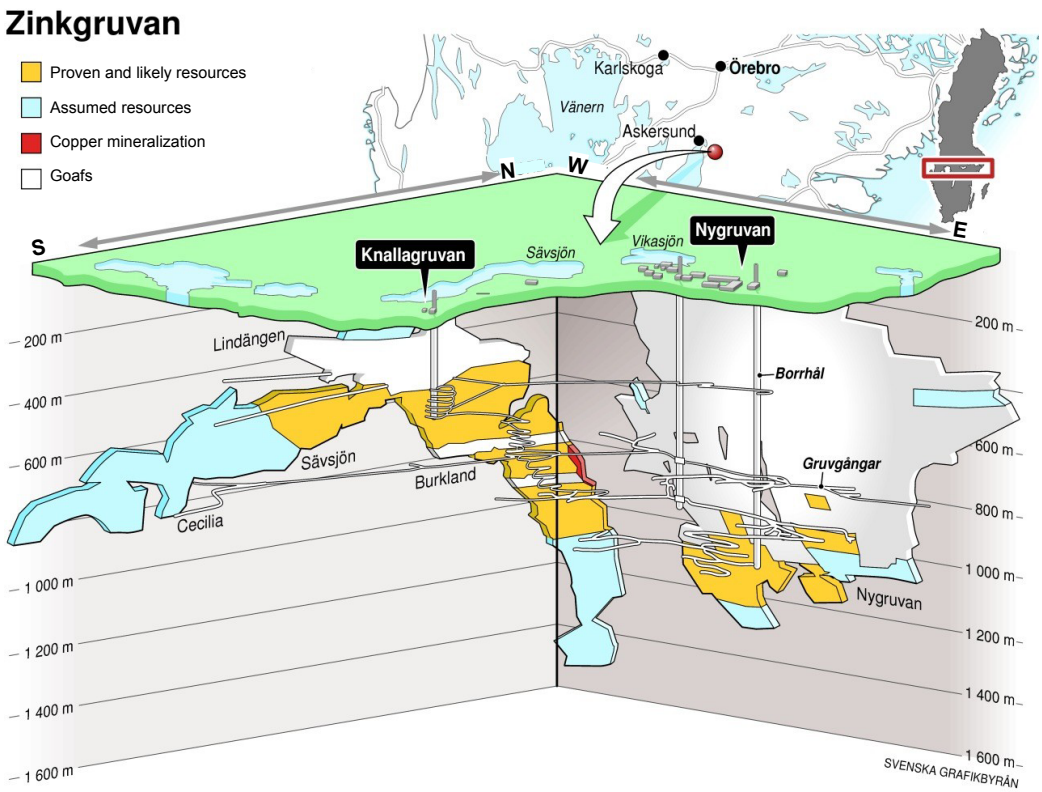


*Fig. 1.* The geographical location of Zinkgruvan mine and the ore bodies within the mine (used with permission from Zinkgruvan Mining AB; Lars Malmström and Stefan Sandberg). The copper mineralization is here represented by its richest parts, for the current copper ore model, see Fig. 7.

# 2 Ore geology – an introduction

Ore is an economical term for a mineralization that is commercially worth to produce with current techniques. Both gemstones, certain rock types and metalliferous minerals can constitute an ore, but the latter is the most common. The phases in which metals are mainly found are oxides (such as magnetite and hematite) and sulphides (e.g. sphalerite). They are thereby referred to as ore minerals. Ore minerals are mostly opaque and are studied in reflected light microscopes.

There are two main types of ores. *Syngenetic* ores are those, which are formed simultaneously with the rock, in which it occurs. *Epigenetic* ores have formed in a later process than the host rock in which the deposit is situated. Ores can be either *discordant*, such as veins, or *concordant*, e.g. stratiform (Evans 1993). The syngenetic ores are concordant and stratiform, which means that they often are restricted to a certain part of the strata. However, all concordant deposits do not necessarily have to be syngenetic.

Ores can be found in most types of host rock environments. Sulphides crystallise mainly from aqueous fluids. Some of the ore forming processes are related to certain plate tectonic settings, e.g. along divergent margins and subduction zones (Wenk & Bulakh 2004), where there are abundant heat transport and circulating hydrothermal solutions. Summaries of the main types of ore follow.

*Magmatic ores* are not very common. Crystal fractionation, where heavy (ore) minerals such as magnetite, sink through the melt to the bottom of the magma chamber, is one possible ore forming process. It occurs in mafic and ultramafic intrusions. Another possible ore forming process is when magma separates into two immiscible melts, where the denser melt sinks to the bottom of the magma chamber. The heavier melt might contain metal sulphides, which leads to the formation of an ore (Wenk & Bulakh 2004).

Hydrothermal ore formation is more common. *Plutonic hydrothermal deposits* are e.g. pegmatites, where fluids and heavy metal ions have been enriched during the crystallisation of the magma and are crystallised as veins and dykes with decreasing temperature. Also skarn is a type of plutonic hydrothermal deposits. It is a metasomatic rock that forms at the contact between marble or limestone and an intruding granite. During initial metamorphism, calcium and magnesium from the marbles together with silica, aluminium and sodium from the granite are expelled and into supercritical fluids creating zones with calc-silicate minerals and often accumulations of ore minerals (Wenk & Bulakh 2004).

On the sea floor, where vents spread hydrothermal solutions into the sea water, *volcanogenic massive sulphides* might develop. Black smokers are of this type (Wenk & Bulakh 2004). Shallow volcanic rocks underlie the future deposit, generating heat for the hydrothermal water. The solutions are moving upwards through feeder veins and when the fluids reach the sea water, ore minerals precipitate as sediments on the sea floor. Generally the precipitation of the different minerals depends on the temperature, leading to zoned deposits.

*Hydrothermal-sedimentary deposits* form in low temperature environments. Metal-rich hydrothermal solutions, from volcanic, plutonic or metamorphic processes, penetrate into the sedimentary rocks and change the composition of the pore fluids. With further burial of the sediments the pressure is increasing, leading to recrystallisation of the rocks and precipitation of sulphide minerals (Wenk & Bulakh 2004). These deposits are often stratiform.

Regional metamorphic processes, faulting and later intrusions can remobilise the ore. When this occurs, the primary structures are often modified or lost (Evans 1993). Also, weathering and oxidation can create oxidised ores situated above the primary ore, which are often enriched in metals and thus form important deposits (Wenk & Bulakh 2004).

In ore microscopy, the minerals are determined and the morphology and texture of the grains are studied, which might give important information about the ore paragenesis. The appellations of textures and structures are similar to those in petrographic studies. During the study the following listed terms are frequently used (Ramdohr 1980).

*Aggregate* is an extended accumulation of ore mineral grains, which bounds with each other (Fig. 2A). When two or more grains, often of different composition, share borders, it is called an *intergrowth*. These can be complex, such as a *myrmekite type of intergrowth* (Fig. 2B), which is an interfingering intergrowth of at least two different minerals. A *symplectite type of intergrowth* is similar to myrmekite type, but is much finer. An *emulsion* is a type of intergrowth where small often rounded grains of one mineral is situated inside another much larger and more abundant mineral (Fig. 2C). *Lamellae* are periodically repeated bands of different minerals (Fig. 2D). The formation of the two latter has long been debated; they might form due to exsolution processes.

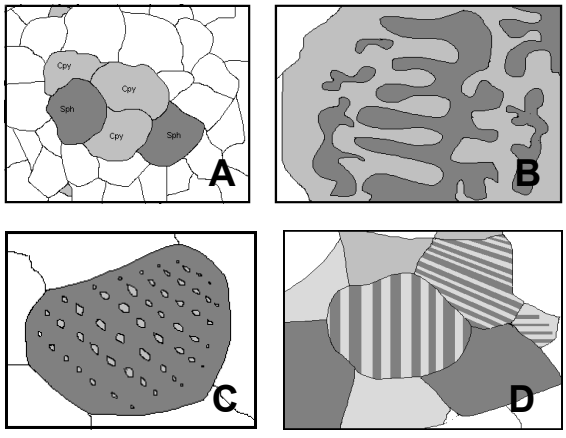


*Fig. 2.* Simple sketches of ore textures. **A.** Aggregate. **B.** Myrmekite type of intergrowth. **C.** Emulsion. **D.** Lamellae

# 3 The Bergslagen ore province

The Bergslagen ore province is situated in south central Sweden and extends approximately from Falun in the north to Norrköping in the south and from Filipstad in the west to the Swedish coast in the east. The area has a long history of mining, close to a thousand years, and was for a long time the most important mining district in Sweden. Today, many of the old mining sites are abandoned due to either exhaustion or economic reasons. However, with rising metal-prices, some of these deposits might become important again. A few deposits in the area are still in production, *Zinkgruvan* in the south and *Garpenberg odalfält* and *Garpenberg norra* in the north (eg. Allen et al. 1996).

## 3.1 Geologic background

Metavolcanic- and metasedimentary rocks, together with intrusive rocks of three different generations make up most of the Bergslagen ore province. The metavolcanic and metasedimentary rocks were deposited on a still unknown basement around 1.85–1.9 Ga (Welin et al. 1980; Lundström 1987; Oen et al. 1982). Intrusions of gabbros to granites occurred prior to 1.85 Ga (Welin et al. 1980). The area was subjected to regional deformation and metamorphism shortly afterwards, deforming the primorogenic intrusive rocks together with the metavolcanic and metasedimentary rocks. During or slightly after the metamporphic period serorogenic granites were formed (eg. Lundqvist 1979). There are also yet younger intrusions, with ages around 1.65–1.73 Ga. It is suggested that the second and third phases in fact make up a continuous phase of intrusions (Åberg & Strömberg 1984). Around 0.9–1.0 Ga steep NNW-ESE and E-W striking dolerite dykes intruded the rocks (Lundström 1987).

The oldest phase of metamorphism is the synvolcanic metasomatism and contemporous contact metamorphism. The second phase is a regional metamorphism of low-pressure type, which reached upper amphibolites facies in the central parts of Bergslagen. The metamorphic grade is closer to greenschist facies in the eastern and western parts. Post-metamorphic fracture zones occur in the area (Lundström 1987).

## 3.2 The Svecofennian orogeny

Northern Europe, or Scandinavia, is located on the Baltic Shield, which was formed during the Proterozoic period. In the east and northeast, Archean rocks, forming the Archean craton, make up most of the bedrock. The central part of the Baltic Shield is called the Svecofennian domain, whereas the southwest part is named the Southwest Scandinavian domain. The rocks are generally getting younger towards the southwest and the bedrock in the southernmost parts of Sweden is late Proterozoic to Phanerozoic (eg. Gaál & Gorbatschev 1987). Much of the Baltic Shield was formed in the Svecofennian orogeny. Many models with the aim to explain the course of events during the Svecofennian orogeny have been proposed. The first tectonic model based on plate-tectonic concepts was proposed by Hietanen (1975) and since then the topic has been vividly discussed. In the following sections, the formation of the Bergslagen ore province is in focus.

The model of Gaál & Gorbatschev (1987) proposes two Archean (Saamian and Lopian) and one Proterozoic crust formation periods including numerous intrusions. However, in a later study Bogdanova & Bibikova (1993) show that in the Belomorian Belt (NE Baltic Shield) rocks, earlier considered to have formed during the early Archean Saamian orogeny, have late Archean Lopian ages.

In the central parts of the shield during the proterozoic, an arc of volcanic belts; the Bergslagen ore district in the south together with the Skellefte zone in the north, is located with its opening toward the west. According to Gaál and Gorbatschev (1987) this makes up a Proterozoic continental margin; perhaps an embayment in an Archean craton. Sediments, forming the Bothnian Basin, are deposited in the embayment. During this time large amounts of plutonic rocks intrude. Three periods of intrusion are recognised; early-, late- and post-orogenic, where the former two approximately marks the timing of periods with deformation and metamorphism.

Nironen (1997) instead proposes a model with microcontinents colliding with the Archean craton. Earlier the Archean craton was opened up, creating an ocean. The microcontinents, made up from island arc complexes, are accreted through subduction during two major periods. The Skellefte zone, hosted by one microcontinent is accreted during the first while the one hosting the Bergslagen ore district is accreted during the later period. The Bothnian Basin marks an intervening period of sedimentation on a seafloor under which the other two plates are partially subducted.

The most recent model for the formation is proposed by Lahtinen et al. (2005). It is partly based on the older model by Nironen (1997). Five orogenies with some overlap in time are suggested to have formed the shield. Microcontinents and island arcs become attached to the Archean craton through subduction in varying directions during several different events. Bergslagen is at that time situated at a microcontinent, which possibly was located close to a cratonic environment. The microcontinent collides and is accreted to the Svecofennian complex around 1.87–1.89 Ga. The already existing part of the Svecofennian had formed in a series of slightly earlier, similar accretions. This leads to an evolution similar to that in the Himalayas or the Andes. Due to a change in plate motions, extensional basins are formed in the microcontinent hosting Bergslagen around 1.84–1.86 Ga. This also leads to intrusions and migmatisation.

## 3.3 The ores of Bergslagen

In Bergslagen, iron, manganese and sulphide ores can mainly be found in felsic metavolcanic rocks with intercalated horizons of limestone and dolostone. There is a close relation between the iron and sulphide ores

(Frietsch 1982a). The wall rocks of the ores have been severely altered into sodium or potassium rich rocks, probably due to the synvolcanic metasomatism. This alteration is more or less restricted to the deposits (Frietsch 1982b). The ores of Bergslagen are thought to have formed in an exhalative sedimentary environment with seafloor hydrothermal processes (Oen et al. 1982). The proximity to the volcanic centres varies among the deposits and the ores are thought to have formed when the volcanic activity of the region waned (Allen et al. 1996).

Earlier, the sulphide ores of Bergslagen were divided into the Åmmeberg type and Falun type (e.g. Geijer 1964; Magnusson 1953). The ores of the central parts of Bergslagen were of the Falun type; such as Falun, Garpenberg, Saxberget and Stollberg (Sundblad 1994). Åmmeberg type represented the ores of the southern parts; such as Zinkgruvan (Åmmeberg), Tunaberg, Vena and Utö deposits (Henriques 1964).

The division of the two, mainly sulphide, ore types were mainly based on the idea that there were two different periods of granite intrusions with associated ore formation (Magnusson 1953). With time, the idea of the ore forming processes changed, into the assumption that all of the ores in Bergslagen have a similar volcano-sedimentary origin and that no clear division between the deposits exists (eg. Oen et al. 1982; Hedström et al. 1989). However, studies of the isotopic lead composition in the major ores of Bergslagen (Sundblad 1994) show that there is a difference between deposits of the former Åmmeberg type (with the exception of the easternmost parts) and Falun type.

According to Allen et al. (1996), it is not probable that all the deposits have the same origin, and there are also differences in the physical characteristics of the deposits of Bergslagen. The ores can be divided into "stratiform ash-siltstone" hosted deposits which are more or less the Åmmeberg type and "volcanic-associated, limestone-skarn" hosted deposits of the former Falun type (Allen et al. 1996). In the metavolcanic units of Bergslagen occasional marble horizons exist (compare to Fig. 3).

Differences between the litho-stratigraphic sequence in the western and eastern part of Bergslagen have been known for long, and can be interpreted to reflect the distance to the volcanic centres (Lundström 1987). In addition, the Falun type of ore are associated with magnesium metasomatosed rocks. This association is not found with the Åmmeberg type (e.g. Magnusson 1953). Thus, the issues around the genesis of the ores of Bergslagen are still not answered.

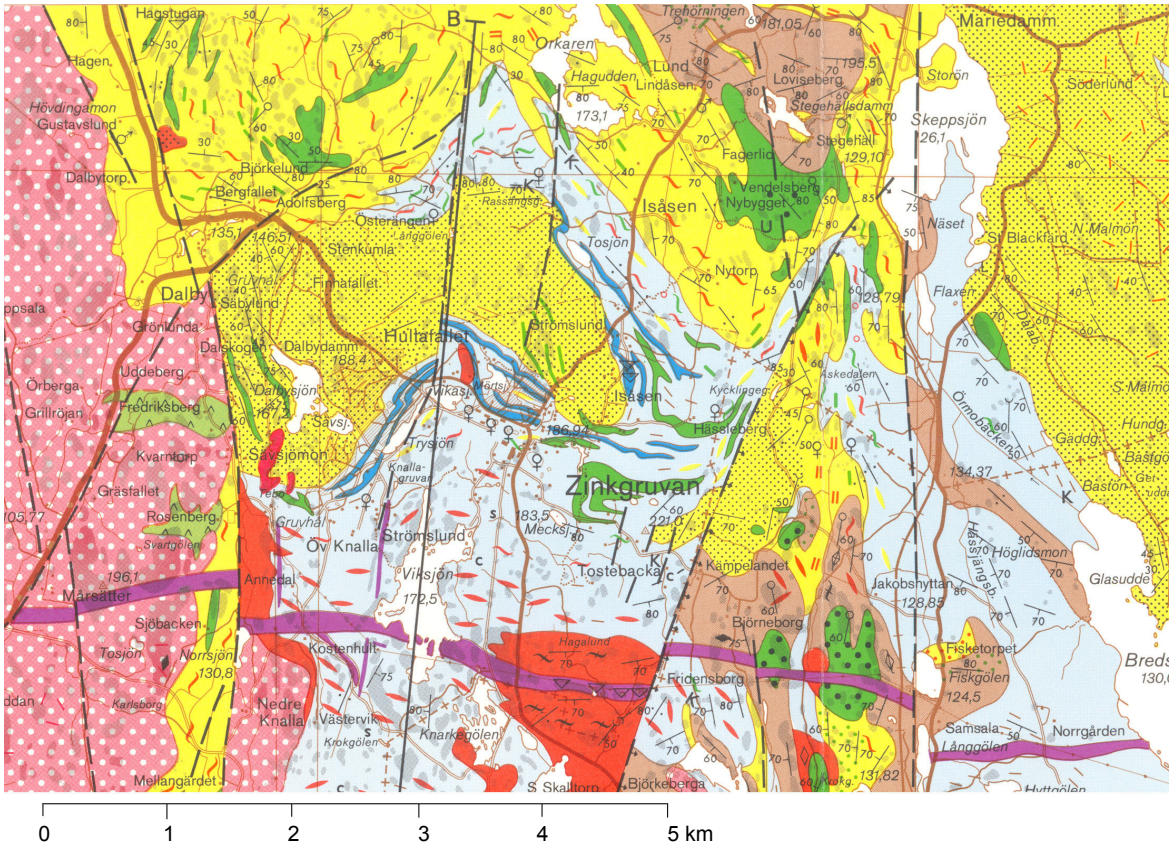


*Fig. 3.* Geological map of the area around Zinkgruvan (edited from SGU ser Af nr. 165, 9F Finspång SV). Used with permission from Sveriges geologiska undersökning (SGU). Yellow = metavolcanic rocks, yellow (spotted) = altered metavolcanic rocks, light blue = metasedimentary rocks, blue = marble, green = mafic rocks, brown = early granitic rocks, red = late granitic rocks, light green = younger monzonitic-monzodioritic rocks, pink (spotted) = post orogenic granitic rocks, red-pink = younger granitic rocks, purple = dolerite dikes. For further information on the rock types the SGU legend should be used.

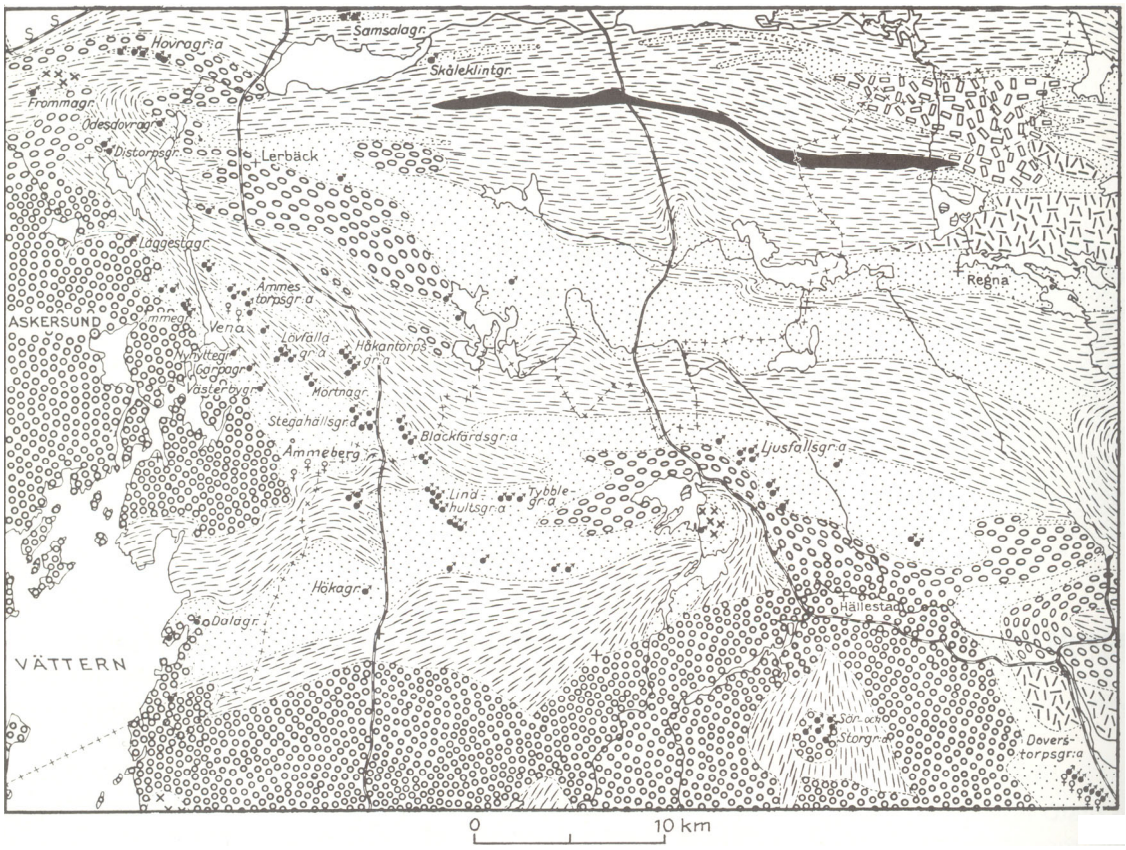


*Fig. 4.* The deposits and mineralizations of Åmmeberg area. Oxide deposits are marked with ♂, sulphide deposits are marked with ♀ (Törnebohm 1881; reprinted in Magnusson et al. 1973).

# 4 The Zinkgruvan area

## 4.1 Local geology

The Zinkgruvan deposit is situated in an area in which metasedimentary and metavolcanic rocks of Svecofennian age are important (Fig. 3). This is similar to the rest of Bergslagen. Zircon dating from rhyolite in the area yields ages around 1.9 Ga (1901±18 and $1889\pm^{35}_{24}$ Ma) which corresponds in age to other ore bearing volcanic rocks of Bergslagen (Kumpulainen et al. 1996). The metasedimentary and metavolcanic rocks are deformed and metamorphosed in the amphibolite facies (Henriques 1964).

There are three generations of plutonic rocks in the area; early, late and post-orogenic intrusive rocks (Hellingwerf 1996). Mafic early intrusive rock are not very common in the area, granitic rocks are more abundant and occur as larger massifs southeast of Zinkgruvan (Fig. 3). The late granite occurs as small massifs south of Zinkgruvan (Fig. 3). The age of this granite has been debated (Karis & Wikström 1991).

The Askersund granite, or Filipstad granite, is post-orogenic and occurs as large massifs of feldspar-phenocryst bearing granite (Fig. 3) in which enclaves of mafic rock types are common (Karis & Wikström 1991). Post-orogenic intrusions of monzodioritic-gabbroitic rocks occur as E-W oriented bodies further south of the area. South of the Zinkgruvan deposit dolerite dikes (Fig. 3) striking E-W occur. They are younger than the above mentioned rocks but are faulted together with the surrounding rocks. The faults are probably coeval with the lake Vättern fault system (Karis & Wikström 1991) around 10 km west of the area. The basement, on which the supracrustal rocks were deposited is unknown (Hedström et al. 1989).

## 4.2 The history of Zinkgruvan

The mineralized bedrock of the Zinkgruvan, or Åmmeberg, area has been known since the 14th century. Iron was the main mining product during the first centuries of ore mining in the area. The most important mine was *Västerby Storgruva*, situated northwest of Zinkgruvan (Fig. 4, the Zinkgruvan deposit is marked as Åmmeberg). At the end of 18th century and the beginning of the 19th century cobalt and copper were mined at *Vena gruvfält*, situated west of lake Åmmelången (northwest of Västerby storgruva in Fig. 4). In the middle of 19th century there was an increasing interest in zinc and the area around Zinkgruvan was investigated. After a few years of small scale mining the Belgian company *Vieille Montagne* bought the mines in 1857 (Gunnarsson & Gunnarsson 2007). This was the start of the larger scale of mining in the area and still, 150 years later, the mine is open and in production. The Zinkgruvan deposit is the largest in the area, but at least two separate ore bearing horizons occur;

the Zinkgruvan deposit in the upper part of the volcanosedimentary succession and Marketorp in the lower part of the same unit (Kumpulainen et al. 1996). Also Ingelsby deposit, where sulphides such as chalcopyrite, sphalerite and galena are found, is localised in the area. It is situated in a contact zone between amphibolite and volcanic rocks (Karis & Wikström 1991).

## 4.3 The Zinkgruvan Deposit

The zinc-lead deposit of Zinkgruvan is situated in the upper parts of a metavolcanic-metasedimentary sequence, which is folded and faulted together with the surrounding rocks (Fig. 3). The strata has become overturned and the original bedding is more or less vertical. It comprises mainly metavolcanic rocks interlayered with chemically precipitated rocks, such as marble, skarn and chert (Hedström et al. 1989). The metavolcanic rocks are traditionally referred to as leptite. The modern view of leptite can be summarised as fine-grained supracrustal, felsic to intermediate, supracrustal rocks probably of a volcanic origin (eg. Karis & Wikström 1991).

Underlying the metavolcanic-metasedimentary sequence, potassium enriched, sodium depleted, metavolcanic rocks are found (Fig. 5). In the local nomenclature this rock type is referred to as quartz-feldspar leptite due to its characteristic high content of quartz and microcline. It is located mainly to the north and east of Zinkgruvan (Fig. 3). The potassium enrichment in the foot wall rock is caused by alteration as hydrothermal fluids circulated in the sea floor (e.g. Hellingwerf 1996; Hedström et al. 1989).

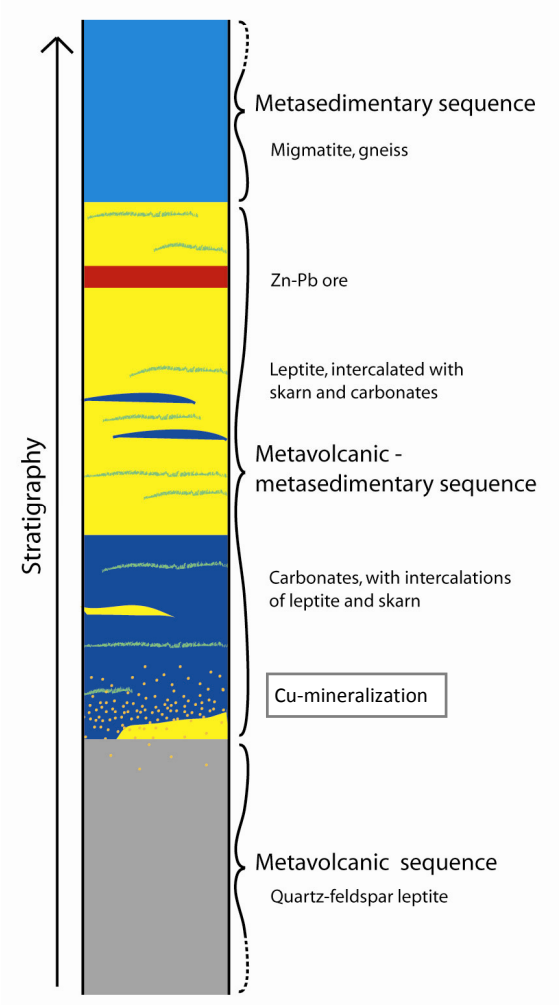


*Fig. 5.* Simplified figure of the general stratigraphy in western part of Knalla, Zinkgruvan. The green layers represent sections rich in skarn minerals. For legend, see Fig. 6.

On top of the metavolcanic-sedimentary sequence, in the youngest part of the stratigraphy, there are mainly metasedimentary rocks (Fig. 5). Migmatite and gneiss of sedimentary origin dominate (Hedström et al. 1986). In between the upper two sequences Fe rich rocks with pyrrhotite and e.g. biotite occur (Fig. 6).

The Zinkgruvan deposit comprises tabular, sheet like ore bodies, which together are approximately five km long and continue at least 1300 m below ground level (Hedström et al. 1989). The ore bearing zone is 5–25 m thick. On the east side of the Zinkgruvan deposit, a few additional narrow ore beds occur (Henriques 1964). The ore bearing sequence generally consists of alternating bands of mineralized and non-mineralized metavolcanic and metasedimentary rocks. A banded structure normally occurs in this disseminated ore (Henriques 1964). The banded structure is predominantly caused by varying amounts of garnet, diopside, tremolite, calcite, vesuvianite and clinozoisite (Hedström et al. 1989).

Two adjacent layers of zinc-lead ore are distinguished, the main ore and the parallel ore (Henriques 1964). The folded ore bearing sequence has also been faulted, resulting in two separate ore bodies. To the west is Knalla and to the east is Nygruvan, separated by the Knalla fault (Figs. 1 & 3). Nygruvan generally has a developed stratification, which cannot be seen in the more folded and deformed Knalla. The stratigraphical foot wall is the structural hanging wall in that part of the mine, which is not the case in Nygruvan. Further, the parallel ore cannot be found in Knalla (Hedström et al. 1989).

Sphalerite followed by galena are the main sulphide minerals in the zinc-lead ore. Native silver occurs sporadically, and is one of the three mining products. Chalcopyrite also occurs, mostly as inclusions in sphalerite. In the eastern part of Knalla, two additional massive ore lenses are found above and below the main ore. These two lenses are totally dominated by sphalerite (Hedström et al. 1989).

## 4.4 The copper mineralization

The copper mineralization is situated in the eastern part of Knalla, named Burkland, close to the Knalla fault (Figs. 1 & 7). Another copper mineralization, more deformed and of smaller extent, is located in the Sävsjön area, Knalla (Fig. 1). The mineralization is hosted by a serpentine marble with a varying content of dolomite and calcite. The marble unit is situated in the lower part of the metasedimentary-metavolcanic sequence, generally close to the potassium enriched

metavolcanic rocks (Figs. 5 & 6). Chalcopyrite is the main sulphide mineral and occurs as disseminations together with some pyrrhotite and sphalerite. The sulphides are mostly situated in silicate veins in the marble. These contain biotite, talc and diopside. The silicate veins can be followed down into the quartz-microcline rock although decreasing in extent (Hedström et al. 1989).

The copper mineralization has its maximum width and thickness at around 700 to 1100 m below ground level and gradually tapers both upwards and downwards (Fig. 7). Its total vertical extension is unknown but exploration drillings have indicated the mineralization at a depth of 1500 m. To the west the mineralization pinches out and to the east it is terminated by the Knalla fault, or pinches out (Fig. 6). It has a NE-SW strike, a NNE plunge of 60° and dips around 80° between 600–700 m and around 45° at 1000 m below ground level (Lundin mining).

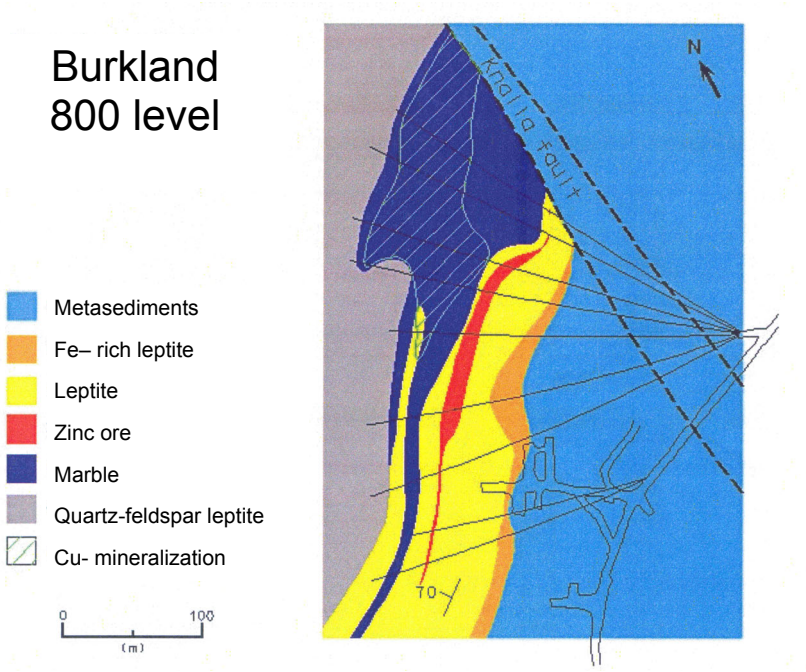


*Fig. 6.* Sketch of the stratigraphy of the ore bearing sequence in the western part of Knalla, at 800 m level (Used with permission from Zinkgruvan Mining AB; Lars Malmström and Stefan Sandberg).

## 4.5 The ore forming processes

The Zinkgruvan deposit is thought to be a syngenetic ore of hydrothermal origin, which has developed in a calm, deep subaqueous environment. This interpretation is based on the lack of sedimentary structures and the fine banding of the ore zone (Hedström et al. 1989). During the sedimentation of exhalative products from distal volcanoes also carbonates, chert, sulphides and oxides were precipitated from the sea water. Hydrothermal fluids circulated in the underlying sediments leaching various ions from the rock and saturating the fluid with these ions. The fluids rose from the underlying sediments up through vents in the sea floor leading to a saturation of the sea water and thus the precipitation of certain compounds. The circulation of hydrothermal fluids has also caused depletion and alteration of the underlying rock. As earlier described this rock is today the quartz-feldspar leptite foot wall rock with abnormal potassium contents. Possibly, the circulation was initialised due to fractures and faults caused by the intrusion of mafic sills and dikes (Hedström et al. 1989).

There is thought to be three different vent areas in the Zinkgruvan deposit, which were active during different periods of time (Hedström et al. 1989). Together they were active during the time needed to accumulate approximately 1000 m of sediments. At some periods of time the precipitation even exceeded the sedimentation of exhalative and terrestrial erosion products (Hedström et al. 1989).

The eastern part of Knalla, where the copper mineralization is located, is interpreted to be the position of one vent. The degree of alteration of the foot wall rock increases toward the copper mineralization. Further, the combined ore zone of the Zinkgruvan deposit has a pronounced zonation of chalcopyrite, galena, sphalerite and pyrrhotite. The copper mineralization principally occurs in the stratigraphic lower positions whereas the zinc-lead ore is situated higher up. Also the ratio zinc/lead in Nygruvan is increasing away from the copper mineralization and thereby from the interpreted vent area. This is consistent with the solubilities of the minerals involved. The temperature of the hydrothermal fluids seems to have been the controlling factor of the sulphide precipitation (Hedström et al. 1989).

The Zinkgruvan deposit, being a stratiform deposit situated in a metavolcanic-metasedimentary environment, can be considered an intermediate of massive volcanogenic sulphide deposit and a sediment hosted exhalative (SEDEX) deposit (Hedström et al. 1989). One type of SEDEX deposit is the Broken Hill type deposit, Australia, with which Zinkgruvan and the Bergslagen ore district in general share many similarities (Walters 1998). The characteristics of a Broken Hill type deposit is an underlying quartz-feldspar rich rock, an overlying metasedimentary unit and in between metasedimentary and metavolcanic rocks hosting a sulphide ore. Furthermore, the depositional environment is rift-related tectonic and the rocks have been metamorphosed into amphibolite- to granulite facies. Possibly, the Broken Hill type deposits were formed from circulating hydrothermal solutions in a deep rift basin, leading to the precipitating of sulphides on the sea floor (Plimer 1986, in Pirajno & Bagas 2008).

# 5 Method

## 5.1 Sample selection

Cross sections of the central parts of the mineralization were constructed to achieve a representative plot of the mineralization. The cross sections are represented by three drill cores distributed in a plane, which is close to vertical and cuts the mineralization at a large angle. Thus the width of the mineralization appears wider than it actually is. In the mineralized area, the vertical distances between the cores are about 50 m (Fig. 7).

The Zinkgruvan mine is divided into a number of mining areas, one example being Burkland, which forms part of Knalla (Fig. 1). Further the mining areas are divided into different vertical areas named after the depth of each area. The vertical areas have a number of levels, linked with ramps, where the base level is the lowest and thereby the first level. The cores used in the study come from the Burkland 800 m area, where the mineralization is rich and at its widest (Figs. 6 & 7).

The cores used were already drilled at the start of this study. DBH2992 is the central core, used as a reference core. DBH2993 is the uppermost core whereas DBH2955 is the lowermost core. The starting point of the two upper cores is approximately the same, the eastern part of the third level in the 800 m area in Burkland. This corresponds to at depth of 692 m according to the local coordinate system. The lower core has a starting point at the second level in the 800 m area in Burkland, at a depth of 727.1 m. DBH2992 has a diameter of 60 mm whereas DBH2993 and DBH2995 have a diameter of 42 mm.

DBH2993 is drilled upwards at an angle around 20° and passes through the mineralization at a depth of 658–663 m. The cutting angle toward the mineralization is 52° horizontally and 13° vertically. DBH2992 is drilled with a downward dip of around 10°, reaches the mineralization at 709 m and exits at 713 m depth. It cuts the ore with 38° degrees horizontally and 10° vertically. DBH2955 has a starting downward dip of around 13.3° and pass through the mineralization at a depth of 751–757 m below ground. The vertical dip of the drill core, with which the mineralization is cut, is 14°. The horizontal cutting angle is 30°.

Samples were selected at regular distances in the mineralized part of the cores to decrease the statistic bias and to reduce the risk of preferring a certain type of mineralization. The additional criterion, that the sample must contain ore minerals visible with the naked eye, might give a deviation of ±5 cm from the originally chosen sample point. Mineralized parts of the cores are normally chemically analysed by Zinkgruvan Mining (see section 5.2.1). The samples selected for this study are restricted to the zones marked for analysis. This selection was not only a choice of convenience but also a way to simplify further comparisons of the results from this study and results from the chemical analyses.

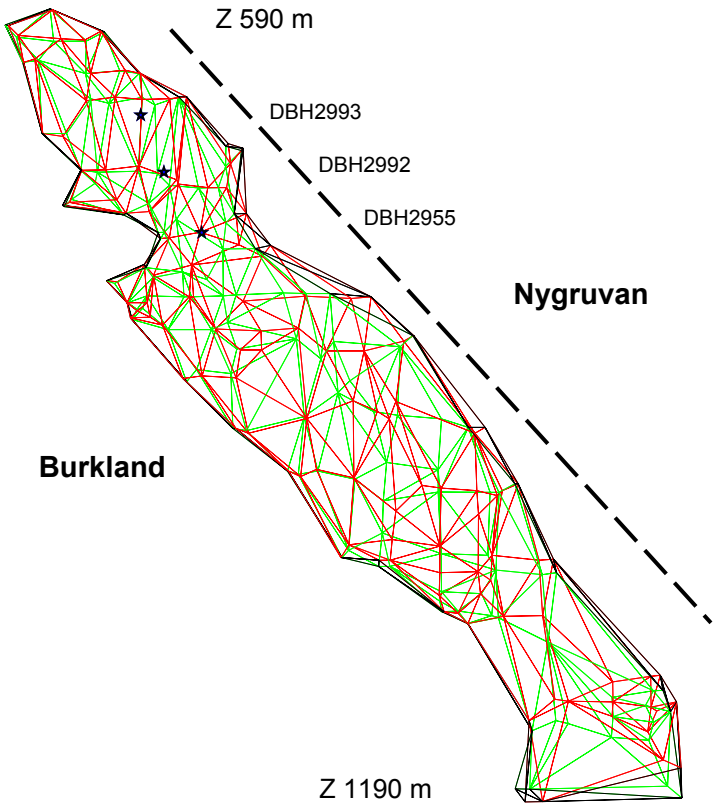


*Fig. 7.* Triangulation model of the copper mineralization ( ≥ 2 % Cu) in Burkland, Knalla (2008-12-31), with drill cores marked as stars. The model is veiwed from the side (towards the northwest), showing the length of the mineralization; thereby the width cannot be observed. The spaced line represents the Knalla fault, (Used with permission from Zinkgruvan mining AB; Lars Malmström and Stefan Sandberg).

The mineralized zone of the drill cores was divided into intervals of equal length, where a sample was chosen in the middle of each section. DBH2992, the reference core, was first divided into one meter intervals. Two sections were then merged into one, due to excessive amounts of samples, and every second sample was then chosen for this study. Thereby the length of each section, and the spacing of the samples is two metres. An extra sample five metres from both ends of the mineralized zone was collected. The two other cores, DBH2993 and DBH2955, were divided into intervals with a length of five metres. A sample from the centre of each section was collected. Additional samples, five metres before and after the mineralized zone, were also collected.

The sections were measured with a gauge to attain as exact intervals as possible. Reference points already marked on the drill cores were used for these measurements. Due to the loss of core during drilling the reference points are not exact. Uncertainties for this reason are bigger in the reference core than the two other cores. A hammer was used for the sample collection.

The method leads to varying sizes of the samples; this should however not be of any significance for this study.

The 45 samples were prepared as polished thin sections at the Mineralogisch-Petrografisches Institut, Universität Hamburg, Germany, by Peter Stutz. A small hand sample of each thin section was also prepared. Each thin section covers an area of around 2x3 cm.

### 5.1.1 Logging of the cores

The intervals, into which the drill cores were split, were studied and described according the following parameters: type of rock, main structure, ore minerals and other minerals of interest, the distribution of these and also an approximate estimate of the percentage of copper minerals. The whole reference core, DBH2992, was also studied and mapped carefully for understanding of the stratigraphy. The two other cores, DBH2993 and DBH2955, were already mapped by Zinkgruvan Mining AB and additional information about these two cores has been collected from the already existing notes. From the data collected during mapping and logging, summarising logs are compiled (Appendix 1).

### 5.1.2 Chemical analyses

Chemical analyses were performed for Zinkgruvan Mining at ACME Analytical Laboratories, Vancouver, Canada. The method used is ICP-ES, G7AR program where 23 elements are measured (Lundin Mining). This is a normal procedure for the drill cores. The data attained from the drill cores of this study has been used to produce graphs of the chemical variation of a number of elements (Fe, Zn, Cu, Co, Ni and Sb) in the cores. The sections analysed approximately correlates with the samples collected for microscopic study.

## 5.2 Microscopy work

### 5.2.1 Optic microscopy

Studies of the thin sections were mainly performed in an optical microscope, Nikon Eclipse E400 POL. The host rock and its mineral composition, texture and structure were studied with transmitted light. The mineralogy, distribution, structures, morphology and intergrowths of the opaque phases were studied in reflected light. The samples were studied in air with 5x, 10x and 50x objective lenses. For photographic purposes a digital camera was fixed on the microscope.

### 5.2.2 Electron microscopy

To complement the optic microscopy, energy dispersive X-ray (EDS) analysis were performed in a scanning electron microscope (SEM). A backscatter detector (BSE) was used to provide images of the sample. The study was carried out on a Hitachi S3400 N, located at the Department of Geology in Lund. EDS analyses were mainly used to study the chemical variations in different phases but also to determine phases, which were indistinguishable in the optical microscope and to investigate complex intergrowths. The software used was INCA, Suit version 4.06, Oxford Instruments. This was done with point identifications of the mineral phases and element mapping of larger, complex areas.

The samples were coated with carbon. During the study an acceleration voltage of 17.5 keV was used. For standardisation the compounds listed in Table 1 were used, also the standards were obtained at 17.5 keV. The standard devices are; no.210-24, Taylor Corporation, Stanford, USA and no.1494, Micro Analysis Consultants, St. Ives, USA. As Sb standard, a pure breithauptite crystal from Zinkgruvan copper sulphide mineralization (sample 1556 275.1 m) was chosen. The elements molybdenum (Mo) and lead (Pb) were not standardised, even though they were expected. No suitable standards without a sever overlap of the peaks in the spectra were available. Thus, correct values are difficult to obtain. Instead, default standards inherent in the Oxford INCA system were used. The instrument set-up was standardized with pure cobalt (INCA quant optimization procedure).

In the reference core seven samples were chosen for EDS analyse. In the two other cores three samples were chosen in each core. From the data collected in the SEM/EDS studies, tables and graphs of the mineral chemical compositions were compiled (Appendix 4). In most cases only analyses having total sums between 97 and 103 wt% were used. However, sometimes analyses within these limits could not be obtained. Contents of e.g. O, Pb, Mo and Ag cause either too high or low values. The analyses with values outside the limits are marked grey in the tables of Appendix 4.

When determining the minerals both optical and chemical analyses and data have been used and compared. All minerals identified optically have been correlated with chemical data. Crystallographic determinations have not been made, thus the name is only based on the chemical composition and optical properties.

Table 1: The standards used during SEM work.

| Element | Standard | Source |
|---|---|---|
| Ag | $Ag_2S$ | no. 210-24 |
| As | GaAs | no.1494 |
| Bi | $Bi_2Se_3$ | no.1494 |
| Co | Co | no. 210-24 |
| Cu | $CuFeS_2$ | no.1494 |
| Fe | $Fe_2O_3$ | no. 210-24 |
| Ni | NiO | no.1494 |
| S | $Fe_2S$ | no. 210-24 |
| Sb | NiSb | Zinkgruvan |
| Zn | ZnS | no.1494 |

# 6 Results

## 6.1 A general description of the mineralization

The copper mineralization is nearly completely restricted to the marble unit of the metasedimentary-metavolcanic unit of the Zinkgruvan deposit (Fig. 5). The cores are drilled from the stratigraphical hanging wall of the mineralization. Thus, the core starts close to the hanging wall and ends close to the foot wall (Fig. 6). Above the marble unit, leptite is generally found. Under the marble unit there is generally quartz-feldspar leptite, in between those leptite sometimes occurs (Figs. 5 & 6). In DBH2992 (Appendix 1) the quartz-feldspar leptite is not reached but the core ends in marble intercalated with leptite and skarn (Fig. 5, for comparison). The thin leptite section is absent in the other two cores. In the marble unit, thin intercalations of leptite, quartzite and skarn are common.

The marble contains varying amounts of calcite and dolomite leading to two sometimes distinguishable types. The calcite-rich marble consists mainly of calcite and serpentine but also minor amounts of dolomite and other minerals. The serpentine and calcite grains give a patchy black and white look to the rock type. The grain size is around 1–2 mm. Serpentine skarn areas appear magnetic and probably magnetite occurs among the serpentine grains creating this effect. In the following text, this rock type is referred to as calcite-skarn dominated marble (Appendix 1).

The dolomite rich marble contains minor amounts of calcite and serpentine. Serpentine and calcite are sometimes distributed as small islands in the dolomite ground mass. The colour of this rock is light grey and the grain size is around 5 mm. In between the two types of marbles, there are of course intermediate rock types. There are sometimes alternating bands of the two marble types, but there might also be simple mixtures of calcite and dolomite. It is often difficult to determine which carbonate dominates. Commonly, the texture of the marble is weakly gneissic to massive, but there is sometimes a stronger gneissic texture. Some intervals are sheared, which is also the case in the quartz-feldspar leptite unit (Appendix 1C).

### 6.1.1 The mineralization in DBH 2992

The main rock type of the drill core interval is marble, where leptite and skarn parties can be found in the last meters of the core. The core is restricted to the marble unit and never reaches the quartz-feldspar leptite unit. Dolomite-rich marble and calcite-rich marble alternate throughout the core (Appendix 1A) and there are some skarn intervals within the marble.

The degree of mineralization appears to increase gradually in the core (Appendix 1A). The first inter-

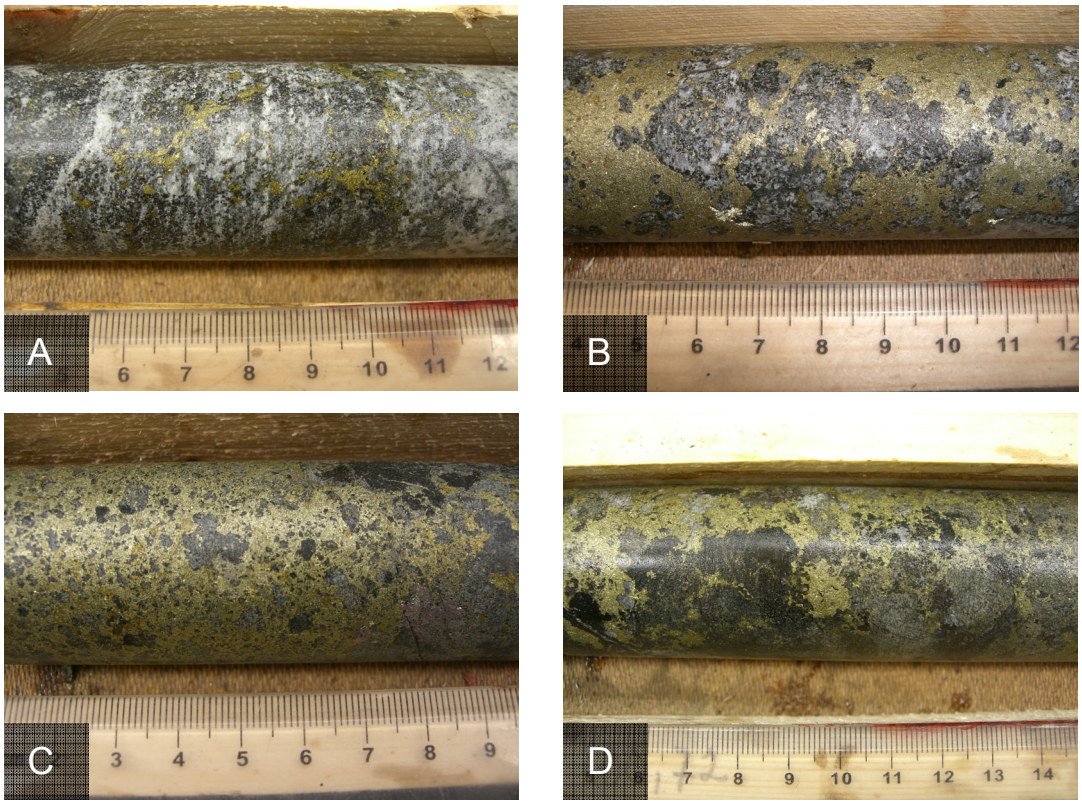


*Fig. 8 A-D.* Type images of the different properties of the copper mineralization in DBH2992. The scale is in cm. **A.** Chalcopyrite aggregates and networks in a mainly calcite-skarn dominated marble (106.00 m). **B.** Chalcopyrite aggregates and networks in a calcite-skarn dominated marble (97.80 m). **C.** Rich chalcopyrite network in a carbonate host rock (100.00 m). **D.** Chalcopyrite aggregates in a skarn host rock (100.80 m).

vals are rather similar in composition, with ore minerals mostly distributed as separate grains, fracture fillings and minor aggregates (Fig. 8A). As the degree of mineralization increases, the aggregates increase in size and start to form networks covering areas up to several centimetres (Fig. 8B). The aggregates are mainly composed of chalcopyrite and cubanite and are often magnetic. A mineral, similar to pyrrhotite, occurs in the aggregates. Sphalerite and breithauptite can be found, often in close connection with each other.

When the richest zone is reached at 99 m, the degree of mineralization is around 50 %. The ore is then close to massive and forms close networks (Fig. 8C). The host rock can be seen through small rounded gaps (Fig. 8C) and is mainly marble, but also skarn (Appendix 1A). Apart from the otherwise common chalcopyrite and cubanite, large grains of sphalerite with breithauptite are common in these parts.

In the skarn parties, in the richest part of the mineralization, there are a higher number of different ore minerals. Apart from the minerals mentioned above, nickel minerals, molybdenite, cobaltite and arsenopyrite can be found. The area covered with ore minerals is not as extensive as in the almost massive ore, but still high and might reach around 20 %. The mineralization is patchy and large aggregates are common (Fig. 8D). In the richer zone the mineralization varies among almost massive types, skarn types and large aggregates in marble.

On the foot wall side of the rich zone, the main host rock is again marble and the ore minerals mainly form aggregates and networks (Fig. 8A). The amount of ore minerals gradually decreases toward the foot wall, however the decrease is not as elongated as the increase on the stratigraphical hanging wall side. The host rock shows a gradual transition into leptite (Appendix 1A). There are broad and thin bands of leptite in the marble, varied with bands of skarn. In the last meters, the degree of mineralization is low and only single sparsely distributed grains of chalcopyrite and bornite occur.

### 6.1.2 The mineralization in DBH 2955

Also in the core DBH2955 the mineralization is mainly found in the marble (Appendix 1B). The amount of dolomite relative to serpentine-calcite in the marble varies. Skarn is found as a unit in the central parts of the core. There is a gradual increase in the degree of mineralization in the core and the highest concentrations are reached in the stratigraphical lower parts, around 115 m, of the marble (Appendix 1B). Only minor amounts of ore minerals can be found in the underlying quartz-feldspar leptite unit.

The ore minerals found, and their distribution, are similar to those found in DBH2992 with the exception that bornite is more important. The proportions are however uncertain due to extensive oxidation of the ore minerals. In the intervals with a low degree of mineralization, ore minerals such as chalcopyrite, cubanite and bornite are found. The minerals occur mostly as small aggregates but occur also as separate grains. As the degree of mineralization increases also pyrrhotite, sphalerite, cobaltite, nickel minerals, breithauptite and magnetite occur. Networks and large aggregates of the sulphide minerals become more common as the degree increases. In the richest parts, the mineralization has mainly changed into extensive networks and impregnation types. The degree of mineralization decreases rather rapidly away from the rich zone and in the few last metres of the core the host rock is quartz-feldspar leptite, with only traces of ore minerals.

### 6.1.3 The mineralization in DBH 2993

In the core DBH2993 the quartz-feldspar leptite unit is reached rather early (Appendix 1C). Half of the core is represented by mainly calcite marble, with a small interval of leptite. The ore minerals are more evenly distributed compared to the other cores. There is a small increase in ore minerals, but the amounts of ore minerals in the richest zone (maximum around 15 %) is not as high as in the other two cores. The stratigraphical lower half of the core consists of quartz-feldspar leptite and the amount of sulphide minerals is low, with sections without any visible ore minerals. The quartz-feldspar leptite is often severely sheared.

The ore minerals are similar in all three cores. In this core chalcopyrite and cubanite dominate, pyrrhotite, magnetite, bornite, cobaltite, sphalerite, nickel minerals and arsenopyrite occur. The distribution with increasing amounts of different minerals as the degree of mineralization increase is similar to the other cores.

### 6.1.4 Microscopic study of the host rock types

Microscopy studies of the host rock (Appendix 2) have revealed that the marble contains, apart from the carbonate minerals, varying amounts of serpentine, phlogopite and chlorite. This agrees with previous microscopic studies of the marble (Henriques 1964). The dominating minerals are always carbonates. As dolomite is very hard to distinguish from calcite, the term carbonates is used. The carbonate grains are transparent and show a distinct twinning. In some cases they appear dusty, most likely due to some sort of alteration. The texture is often equigranular with rather large, isometric and polygonal grains but some sections have carbonates with irregular grain shapes and varying grain size.

Serpentine occurs as pseudomorphs after olivine. These are rounded and often grouped together (Fig. 9). Olivine can still be found in some samples, either as whole, non-altered grains, or as remaining small grains (Fig. 10). The serpentine replacement first occurs along fractures. If olivine remains, the grains are transparent and have a high lustre, but in the serpentine-altered grains the transparency and the lustre are slightly lower. In some cases, the serpentine is yellow or green, often in bands or areas (Fig. 9). Spot analysis of the olivine shows that it had a forsteritic composition, around $(Mg_{1.64}Fe_{0.34}Mn_{0.04})SiO_4$. The serpentine

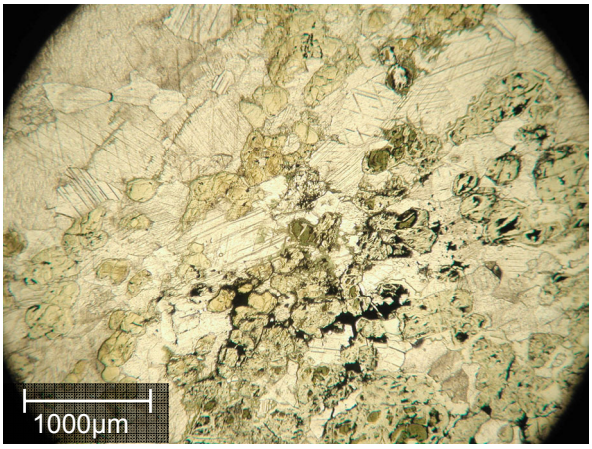


*Fig. 9.* Marble with carbonates and serpentine pseudomorphs (yellow and green) oriented in bands (DBH2992 96.50 m).

is also Mg-rich. Graphite occurs in the pseudomorphs after olivine.

The mica has a weak green colour, shows a faint pleochroism from transparent to weak green and has high interference colours. Spot analysis showed that the composition of the mica is close to phlogopite. Both tabular and rounded grains of mica occur in the thin sections. The rounded grains have lower interference colours and appear to show a relief relative to the surrounding minerals. Chlorite often partly replaces the mica, resulting in green rims on the grains and in lower interference colours. Apart from replacing mica, chlorite also occurs as tabular grains clustered together. In the marble, diopside is sometimes found. Diopside occurs as rather large and irregularly shaped grains, which are transparent and have high interference colours.

Sometimes the magnesium-rich spinel pleonaste (Fig. 10) occurs in the marble. Rather frequently, magnetite is found as small rounded inclusions in pleonaste or pleonaste occurs as inclusions in magnetite. When the content of magnetite inclusions in pleonaste is high, the transparency is low and the grain sometimes appears opaque.

The quartz-feldspar leptite consists of an equigranular groundmass of quartz and microcline with some biotite and small amounts of titanite (Fig. 11). The grain size is smaller than in the marble. The titanite, which is brown, occurs as small rounded grains either spread out in the sample or clustered together. It often has small rounded inclusions of titanium dioxide. The biotite is light brown and shows a distinct pleochroism. It is mostly gathered into bands. Sometimes small grains with a high relief, possibly zircon, occur.

In the samples with a skarn host rock diopside, mica and carbonates dominate. The grains, especially of diopside and carbonate, are commonly severely altered. Fractures or veins commonly occur in these samples, which are filled with quartz, carbonates or some unidentified altered phase. Sections of this type are e.g. DBH2992 100.65 m, 108.73 m, DBH2955 67.60 m and 77.60 m (Appendix 1 and 2).

There are biotite-rich samples, in which also quartz, diopside and light mica are common constituents, such as DBH2992 110.71 m, DBH2955 62.60 m, DBH2993 104.40 m and partly 114.40 m (Appendix 1 and 2). The biotite sometimes have inclusions of a high relief mineral, probably zircon, surrounded by haloes of radiation damage. The ore minerals of the latter group differs from the other sections.

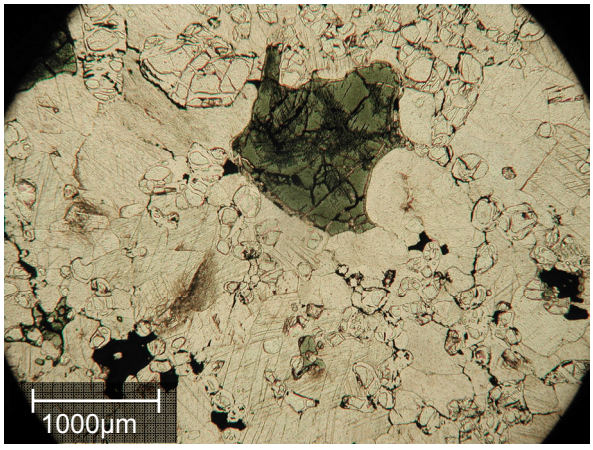


*Fig. 10.* Pleonaste (green) surrounded by carbonates, olivine (high relief) and ore minerals (DBH2955 55.10 m).

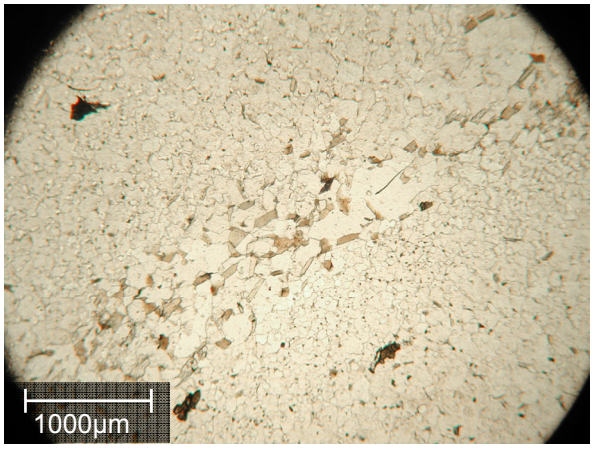


*Fig. 11.* Quartz-feldspar leptite with a band of coarse-grained quartz and biotite (brown) (DBH2993 119.40 m).

*Fig. 12 A-H (p 19).* **A.** Chalcopyrite aggregate with a distinct cleavage (DBH2955 107.60 m). **B.** Chalcopyrite (yellow) with cubanite lamellae (beige) (DBH2992 78.80 m). **C.** Cubanite lamellae, compare the bireflectance to 11B (DBH2955 107.60 m). **D.** Sphalerite star in a chalcopyrite grain with sharp magnetite filled fractures (DBH2992 80.70 m). **E.** Fine flame-like texture of sphalerite in chalcopyrite with magnetite filled fractures (DBH2993 79.40 m). **F.** Fine-grained (light pink) pentlandite along fine fractures filled with magnetite in chalcopyrite (DBH2992 80.70 m). **G.** Fine-grained flame-like pentlandite situated in cubanite lamellae in chalcopyrite (DBH 299292.74 m). **H.** Argentopentlandite (light brown) oriented parallel to the cleavage in chalcopyrite (DBH2992 98.60 m).

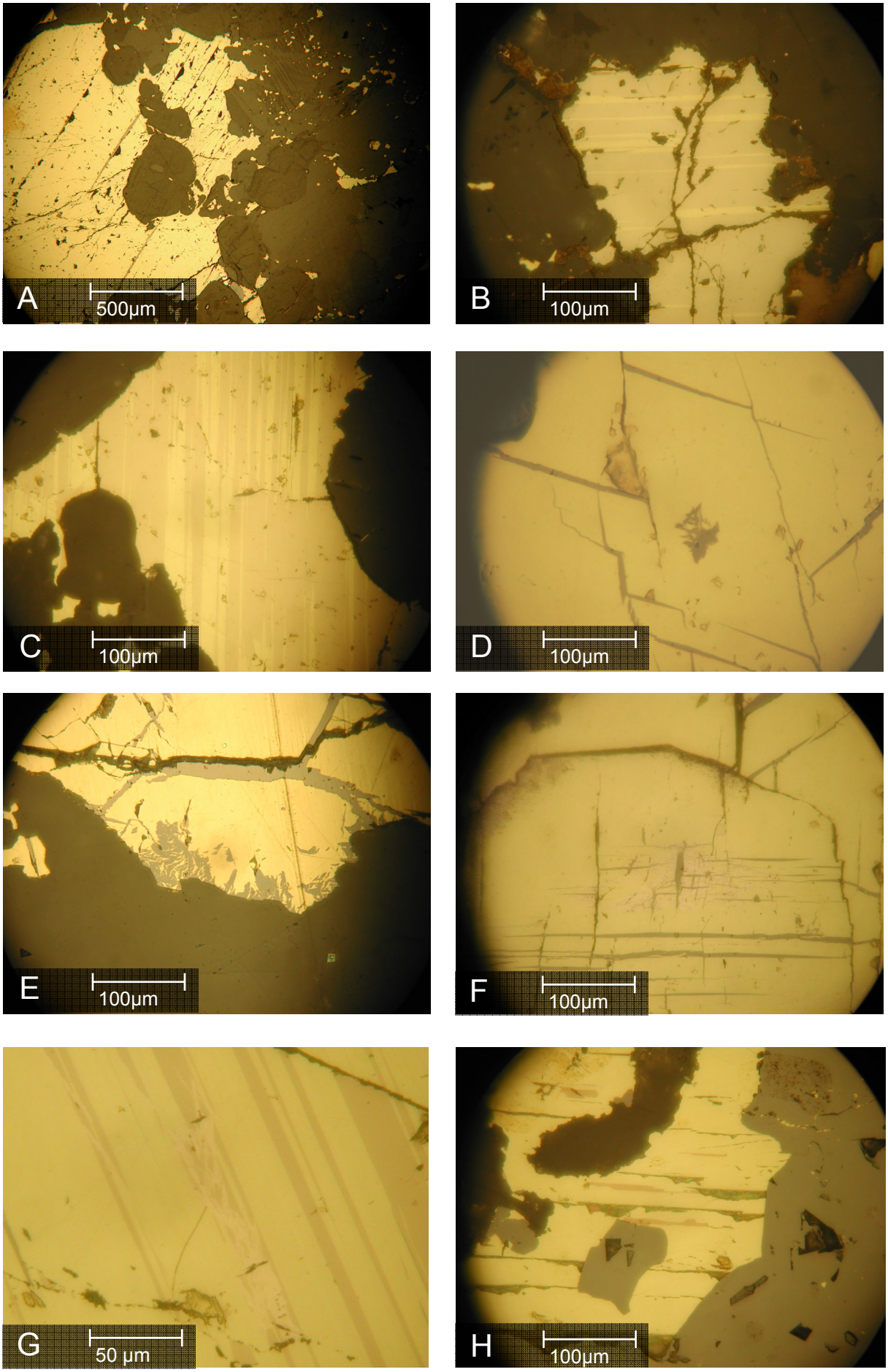
A
500µm
B
100µm
C
100µm
D
100µm
E
100µm
F
100µm
G
50 µm
H
100µm

## 6.2 The mineral assemblages of the mineralization

The copper mineralization is made up of small and large aggregates of mainly copper sulphides occurring in a marble host rock. In the host rock, small grains of various ore minerals are distributed. Small aggregates of other sulphides, such as sphalerite, galena, cobaltite and breithauptite are common. This can be observed at the macroscopic as well as at the microscopic scale. However, the microscopic scale reveals the mineral composition and textures. In this section, the occurrence and textures of the ore minerals are discussed, whereas the information about the individual minerals and their properties can be found in section 6.4. A list of the ore minerals and their stoechiometric chemical composition can be found in Appendix 3.

### 6.2.1 Chalcopyrite aggregates

The most common mineral assemblage in the samples is granular chalcopyrite aggregates. These vary in size from 1–20 mm and have an irregular shape (Figs. 12A, 14C & D). Generally the larger the aggregates are, the higher is the number of different minerals they contain. Chalcopyrite, which is the most common mineral in the aggregates, occurs as relatively large grains, around 100–500 μm in diameter. The grains are polygonal to rounded and are often isometric. In the chalcopyrite, cubanite lamellae are common (Fig. 12B and C), but cubanite also occurs as individual crystals. Normally the number of chalcopyrite grains clearly exceeds the number of cubanite grains, but there are some exceptions (e.g. DBH2993 99.40 m).

Fractures along the cubanite lamellae, and thus parallel to the cleavage of the chalcopyrite, are common. These fractures are also common in grains without lamellae (Fig. 12A). The lamellae often occur in parallel sets, but they sometimes pinch out in the chalcopyrite (Fig. 12C). Broad lamellae might split up into many thin ones. Commonly, the width of the lamellae varies, ranging from 5 to 50 μm. Often, but with some exceptions, most of the chalcopyrite crystals in one aggregate, or in several aggregates in the same sample, have a similar orientation (Fig. 12A). This can be deduced from the cubanite lamellae and the cleavage fracturing of the chalcopyrite.

Inclusions and exsolution stars of sphalerite are common in the chalcopyrite aggregates (Fig. 12D & E). Mostly they occur in the large aggregates, but some have been found in the smaller ones. They are restricted to the chalcopyrite grains and are normally sparsely distributed. The sphalerite inclusions can either be irregular and jagged or be smooth and rounded. The size is around 50–100 μm in diameter.

Along the cleavage of the chalcopyrite a number of iron-nickel sulphides can be found. The most common is pentlandite, which occurs as fine-grained minor accumulations along the cleavage fractures or in the cubanite lamellae. The grains, 1–5 μm, are either flame-shaped or quadrangular (Figs. 12F & G). Generally, the flame-shaped grains are found in the cubanite lamellae, whereas the quadrangular are mostly found around fractures. There are also accumulations with both types, where the quadrangular are more central than the flame-shaped ones.

Parallel to the cleavage of the chalcopyrite also argentopentlandite occurs. It is not as common as pentlandite but occurs mainly in large chalcopyrite aggregates. The grains are tabular and are situated either alone or together with a number of grains, around 10 μm in width and 50 μm in length (Fig. 12H). Sometimes larger grains or aggregates, around 50–100 μm, of argentopentlandite occur. These are irregular and rounded and not oriented along the cleavage.

The third iron sulphide is mackinawite. It occurs as diffuse grains often situated along fractures and the cleavage of chalcopyrite, however the mackinawite grains are not always oriented. The grains are often irregular and can have various shapes, as rounded, tabular, flame-shaped or somewhat rhombic (Figs. 13A & B). They are 5–100 μm long.

In the aggregates, large grains of sphalerite, 100–500 μm in diameter, are common (Fig. 13C). They are isometric often slightly rounded to polygonal grains, commonly with abundant internal reflections. The sphalerite grains occur mainly in the outer parts of the aggregates. Chalcopyrite emulsion is common, but is not always present. The chalcopyrite emulsions are 1–5 μm and consist of rounded grains oriented in parallel bands in the inner parts of the sphalerite grain (Fig. 13D). Sphalerite grains are often intergrown with pentlandite, coarse-grained, in a myrmekite-like pattern (Fig. 13E). In these intergrowths, other minerals such as galena might occur (Fig. 13 F).

Coarse-grained pentlandite occur also as separate grains in the aggregates. The grains are mostly slightly rounded and irregular, around 50–500 μm in diameter (Fig. 13G). Sometimes a distinct triangular cleavage can be seen in the grains, which in some cases have been filled with magnetite. Coarse-grained pentlandite may occur both in the central and the peripheral parts of the aggregates.

*Fig. 13 A-H (p. 21).* **A.** Bireflectance in mackinawite situated in chalcopyrite (2955 80.70 m). **B.** Mackinawite occuring along fractures in chalcopyrite (DBH2992 100.65 m). **C.** Pentlandite grains between two larger sphalerite grains with abundant orange internal reflections in a chalcopyrite aggregate (DBH2992 94.65). **D.** Large sphalerite grain with chalcopyrite emulsion (DBH 2955 102.60 m). **E.** Myrmektic type of intergrowth of pentlandite and sphalerite in chalcopyrite (DBH2992 100.65 m). **F.** Intergrowth of coarse-grained pentlandite, galena and sphalerite in chalcopyrite and cubanite (DBH2992 80.70 m). **G.** Large grain of coarse-grained pentlandite (white with a pink tint) in a chalcopyrite aggregate (DBH2992 92.74 m). **H**. Magnetite filled fractures along chalcopyrite cleavage with fine-grained pentlandite along the fracture rims (DBH2992 104.69 m).

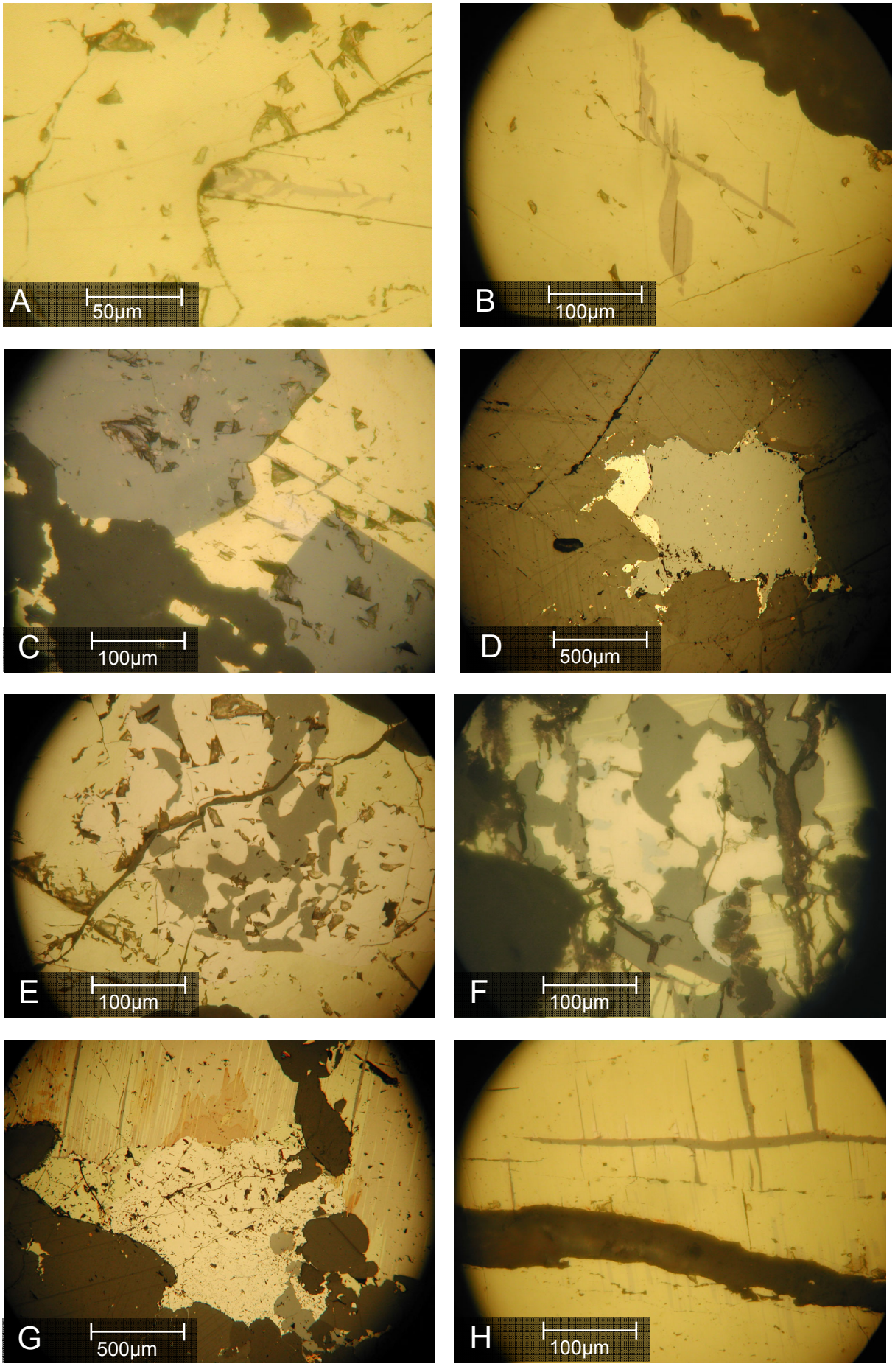
A
50µm
B
100µm
C
100µm
D
500µm
E
100µm
F
100µm
G
500µm
H
100µm

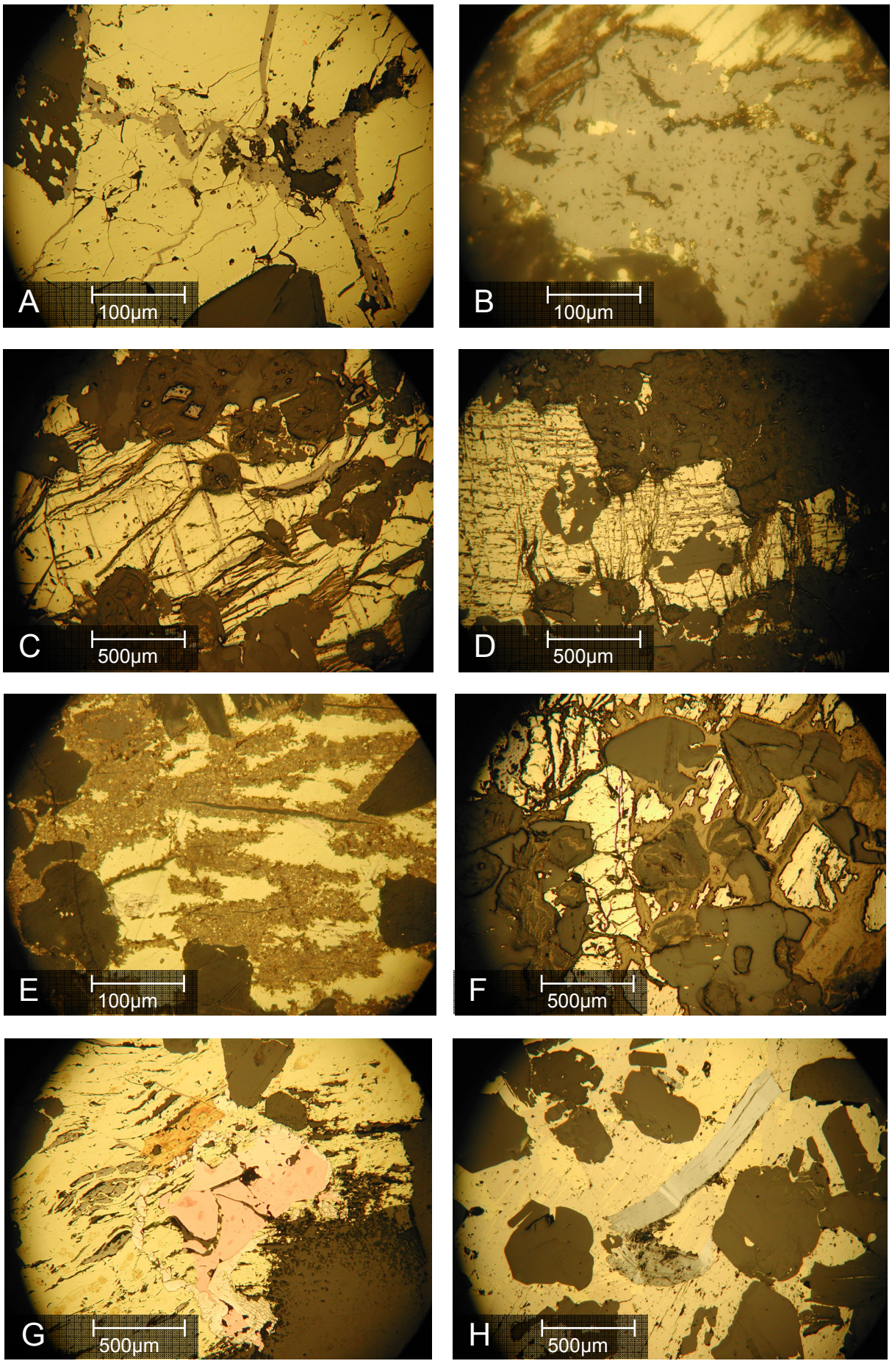
A
100μm
B
100μm
C
500μm
D
500μm
E
100μm
F
500μm
G
500μm
H
500μm

One of the most significant structures in the chalcopyrite aggregates is a frequent fracturing with magnetite filling (Fig. 13H). The fractures are most frequent in chalcopyrite and cubanite but might cut sphalerite, pentlandite grains and sphalerite exsolution stars. Generally, the magnetite-filled fractures are cleavage fractures, which are often sharp with matching fracture sides. The width of the fractures is 10–50 µm. The magnetite fractures often branches into networks with sharp fractures either perpendicular or at a high angle to the cleavage (Fig. 13H). Sometimes the fractures indicate shearing or weak folding (Fig. 14G). The fine-grained pentlandite often borders small magnetite filled fractures (Fig. 12F).

Broader, irregular magnetite filled fractures, which are not oriented along the cleavage of the chalcopyrite are common (Fig. 14A). Rims of magnetite occur around some chalcopyrite aggregates or around grains inside an aggregate. Large rounded and irregular grains or aggregates of magnetite are found either outside or in the outer parts of the chalcopyrite aggregates (Fig. 14B). These range from 100–500 µm and are often granular with rounded gaps of chalcopyrite or the host rock.

Commonly, larger fractures cross the entire aggregates. They can originate from serpentine pseudomorphs located inside the chalcopyrite aggregates (Fig. 14C), or from general fracture directions of the sample (Fig. 14D). Sometimes broader fractures are filled with magnetite, as discussed above, but often they are filled with host rock minerals, such as carbonates. Valleriite is also found as a fracture filling mineral, sometimes together with carbonates. In this case the valleriite occurs as flame like grains. It is common to find valleriite around fractures in the chalcopyrite grains or as larger areas inside the aggregates (Figs. 14E & F).

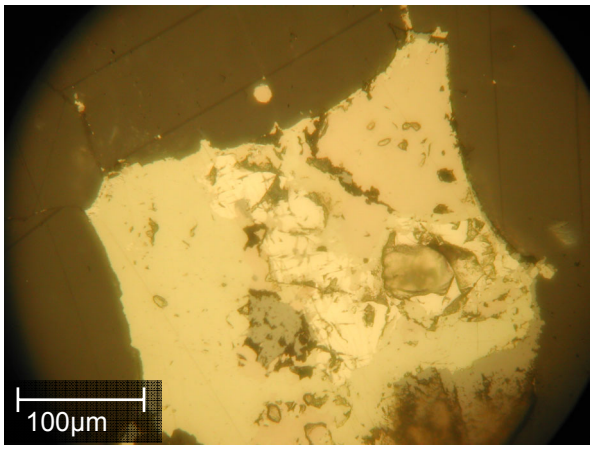


*Fig. 15.* Cubanite dominated grain with pyrrhotite (brown), coarse-grained pentlandite (white) and magnetite (DBH2993 71.90 m).

Other minerals that sometimes occur in the chalcopyrite aggregates are galena, breithauptite and cobaltite. Galena mostly occurs as tiny rounded grains, < 50 µm in diameter, or as thin fracture fillings, but also as larger grains in intergrowths (Fig. 13F). Breithauptite can be found as slightly rounded sharp edged grains, around 100 µm in diameter. These grains are often intergrown with or border on each other, forming accumulations (Fig. 14G). They normally occur in the outer parts of the aggregates. Cobaltite occurs as single hexagonal or octagonal crystals (Fig. 14G). These are mostly around 100 µm but can reach 500 µm in diameter. Occasionally grains of molybdenite (Fig. 14H) and pyrrhotite (Fig. 15) can be found in the chalcopyrite aggregates. It then occurs in small aggregates or larger grains with an intergrowth of several minerals; e.g. cubanite and pentlandite.

### 6.2.2 Sphalerite aggregates

In some samples, aggregates of sphalerite occur in addition to chalcopyrite aggregates. They consist mainly of sphalerite grains, 100–500 µm in diameter, forming narrow often irregular, elongated aggregates. Together with sphalerite often breithauptite, galena, cobaltite, and magnetite are common. The most important difference compared to the chalcopyrite aggregates is the much greater amounts of the latter minerals, whereas copper and iron sulphides are rarer.

Breithauptite occurs as rounded grains, around 100–200 µm in diameter, which often forms groups in the sphalerite aggregates (Fig. 16A). Cobaltite occurs as large often prismatic crystals of varying size, similar to those found in the chalcopyrite aggregates (Fig. 16B). Galena is irregularly shaped and of larger size than in the chalcopyrite aggregates (Fig. 16C). The grains can reach 200 µm in cross section and sometimes the triangular pits characteristic for galena are visible. Magnetite occurs in particular as rims around the minerals in the sphalerite aggregates, especially around the sphalerite grains (Fig. 16C). The rims are often broad and smooth. Chalcopyrite sometimes occurs in the aggregates. Chalcopyrite crystals are around 100 µm in diameter and they can only be found in minor amounts.

*Fig. 14 A-H (p. 22).* **A.** Irregular, coarse magnetite filled fractures in chalcopyrite (DBH2992 106.72 m). **B.** Coarse magnetite aggregate with numerous hollows and chalcopyrite grains (DBH2992 82.60 m). **C.** Chalcopyrite aggregate with parallel magnetite filled fractures and fractures emerging from serpentine pseudomorphs after olivine (DBH2992 80.70 m). **D.** Chalcopyrite aggregate with numerous parallell fractures filled with magnetite and non filled fractures perpendicular to these (DBH2993 94.40 m). **E.** Valleriite replacement along fractures in a chalcopyrite aggregate (DBH2992 82.60 m). **F.** Chalcopyrite aggregate with valleriite replacements in fractures and grains (DBH2992 80.70 m). **G.** Large breithauptite grains surrounded by a ring of cobaltite grains in a chalcopyrite aggregate with folded magnetite filled fractures (DBH2992 98.60 m). **H.** Molybdenite in a chalcopyrite– and cubanite aggregate (DBH2992 102.47 m).

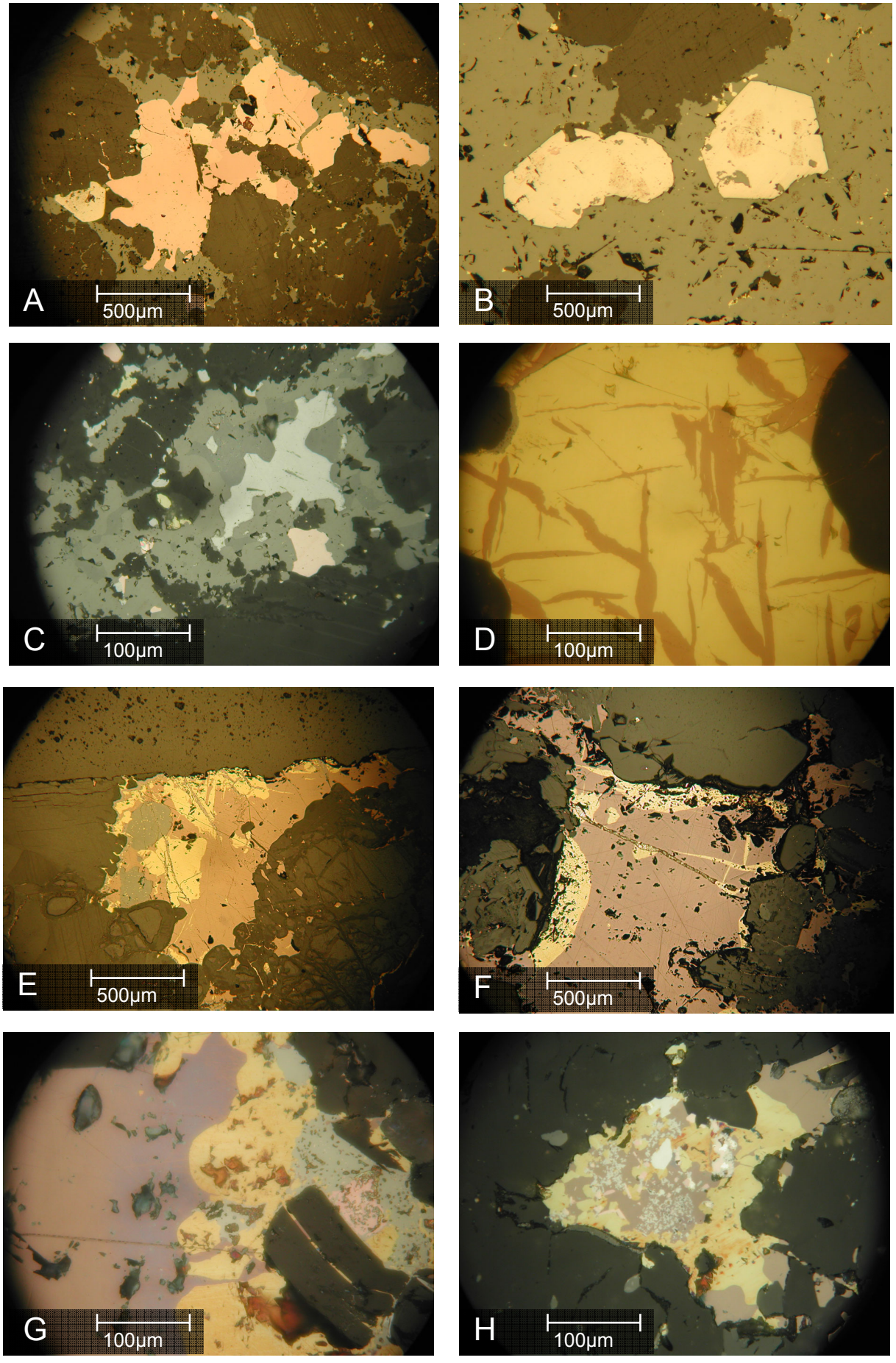
A
500μm
B
500μm
C
100μm
D
100μm
E
500μm
F
500μm
G
100μm
H
100μm

### 6.2.3 Chalcopyrite-bornite aggregates

The chalcopyrite-bornite aggregates are rarer than the sphalerite aggregates. The major difference from chalcopyrite dominated samples, which sometimes have sphalerite aggregates, is that chalcopyrite-bornite aggregates might dominate the thin section. The samples, when it comes to ore minerals, might then exclusively be composed of these aggregates. In those cases, the aggregates are mostly large, around 5–20 mm. However, intergrown grains, 1–5 mm, can also be found in the samples of a more normal mineral composition. The mineralogical composition of the host rock in the samples with high amounts of bornite is rather different from the chalcopyrite dominated samples. Bornite-rich aggregates do not occur in the normal marble but in a host rock that often is rich in biotite and contains diopside. In addition, quartz can be a constituent of this host rock, but carbonates still occur.

In the larger aggregates, chalcopyrite and bornite are the main constituents. These are often intergrown with each other and commonly lamellae of one of the constituents occur in the other (Fig. 16D). Both chalcopyrite dominated aggregates and bornite dominated aggregates are common (Figs. 16E & F). The lamellae are grid-shaped with up to three different directions and are around 10–20 µm wide. Small rounded grains, < 5 µm, of bornite can often be found in the chalcopyrite and vice versa. In the smaller aggregates, chalcopyrite is the dominating mineral and bornite mainly occurs as rounded grains (10–50 µm) intergrown with the chalcopyrite.

Chalcopyrite-bornite aggregates mainly occur in three samples, DBH2992 110.71 m, DBH2955 77.60 m and DBH2993 114.40 m (Tables 2–4). In DBH2992 110.71 m, grains of cobaltite, breithauptite and tetrahedrite occur (Fig. 16G). Sulph-antimonides are common in the sample. Galena and native bismuth occur as small grains in bornite and chalcopyrite grains and as discrete grains close to the aggregates in the host rock. Allargentum can be found as small rounded grains in breithauptite and tetrahedrite grains. In some larger grains, e.g. of bornite, small and sometimes needle shaped grains of gudmundite, costibite, breithauptite, galena and native bismuth occur (Fig. 16H). Galena may occur as small rounded grains in chalcopyrite (Fig. 17). Large grains of bismuth, 20–50 µm in diameter, are found in fractures through a quartzite area in this sample.

In sample DBH2955 77.60, the aggregates commonly have chalcopyrite and bornite lamellae. Sphalerite is also common and occurs as rounded grains, 100–200 µm in diameter. The sphalerite grains normally have chalcopyrite emulsion or inclusions of chalcopyrite.

In DBH2993 114.40 m bornite is the dominating mineral but chalcopyrite is also common. From the largest aggregate, veins or fractures filled with chalcopyrite and bornite emerge. Further away from the largest bornite aggregate chalcopyrite becomes more common. Other minerals that can be found are galena, sphalerite and minor grains of coarse-grained pentlandite. A fracture filled with silver occurs (Fig. 16F). Small amounts of bismuth, probably in the form of parkerite, occur as small grains in the aggregates.

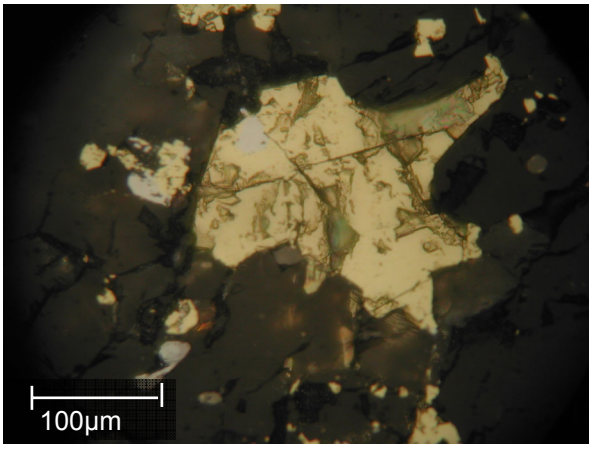


*Fig. 17.* Rounded galena grains in chalcopyrite (DBH2992 110.71 m).

### 6.2.3 Disseminated ore minerals

In the host rock, around the aggregates, there are small grains of varying ore minerals. These are mainly situated at grain boundaries and along cleavages of the host rock minerals and are either composed of separate grains or small grains of different ore minerals intergrown or sharing boundaries with each other (Fig. 18A). Mica has a distinct cleavage, often hosting fine chalcopyrite and breithauptite (Fig. 18B). Very finely grained chalcopyrite can usually be found along the grain boundaries and in the twinning planes of carbonate grains. Along grain boundaries and in fractures of the host rock sphalerite, chalcopyrite and breithauptite occur. Single grains of cobaltite, breithauptite, bornite, galena and chalcopyrite are situated either at grain boundaries or sometimes as inclusions in the silicates or carbonates. Sometimes pyrrhotite occurs in a similar way (Fig. 18C). It is also common to find rounded grains of iron oxide, 50–100 µm in diameter, often agglomerated in the host rock (Fig. 18A). In the host rock, fractures, around 100 µm in width, are sometimes filled with predominantly chalcopyrite. Small

*Fig. 16 A-H (p. 24).* **A.** Breithauptite and cobaltite in a sphalerite aggregate (DBH2992 98.60 m). **B.** Cobaltite grains in sphalerite (DBH2992 98.60 m). **C.** Galena, breithauptite and sphalerite surrounded by magnetite grains in an aggregate (DBH2992 94.65 m). **D.** Chalcopyrite with bornite laths/lamellae (DBH2955 77.60 m). **E.** Bornite and chalcopyrite aggregate with sphalerite grains (DBH2955 77.60 m). **F.** Bornite and Chalcopyrite aggregate with a silver filled fracture (DBH2993 114.40 m). **G.** Tetrahedrite and breithauptite in an oxidised chalcopyrite-bornite aggregate (DBH2992 110.71 m). **H.** Fine-grained intergrowth of galena, costibite, breithauptite, and bismuth in a chalcopyrite-bornite aggregate (DBH2992 110.71 m).

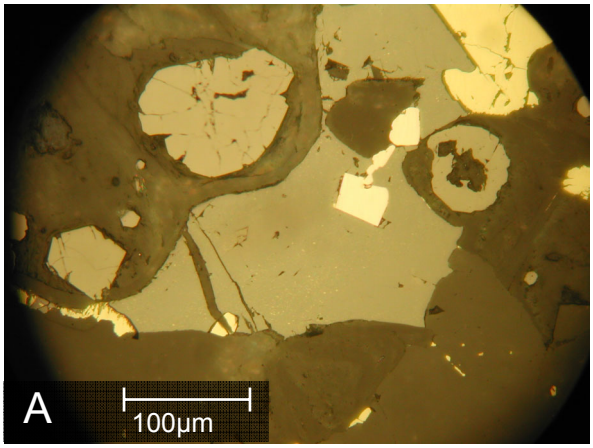
A
100µm

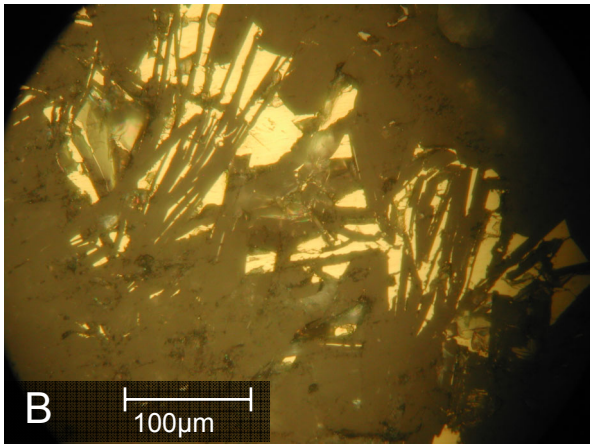
B
100µm

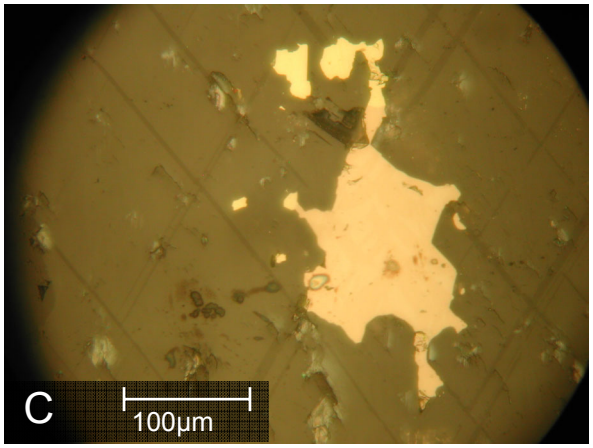
C
100µm

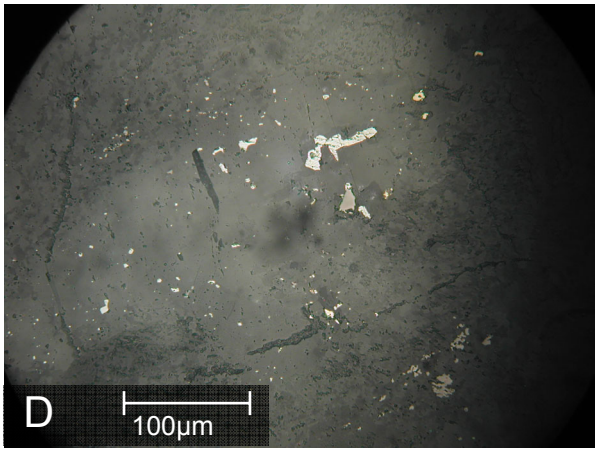
D
100µm

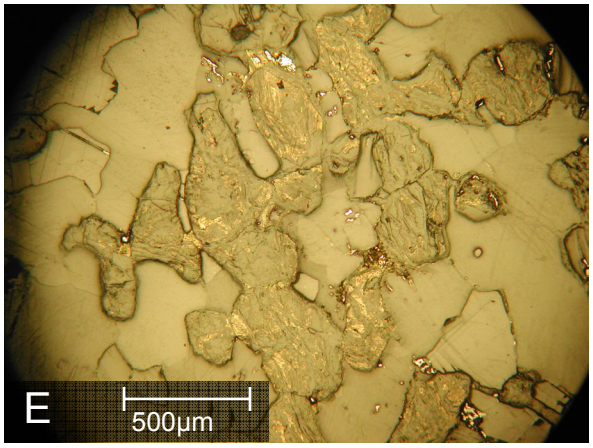
E
500µm

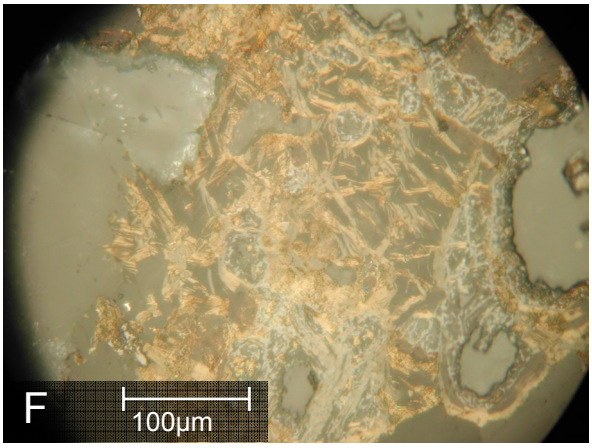
F
100µm

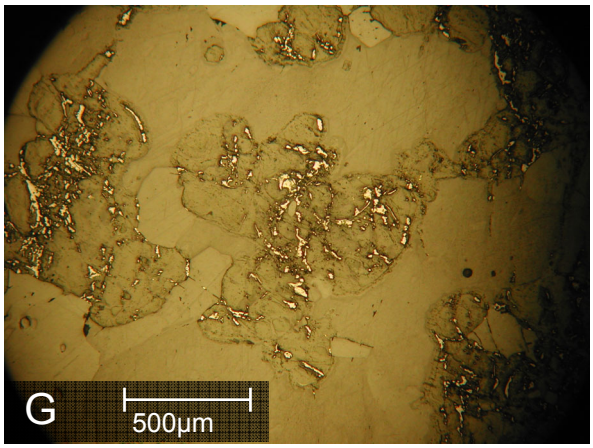
G
500µm

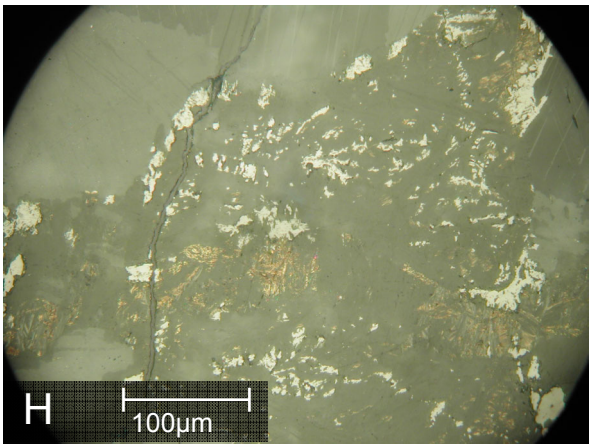
H
100µm

grains, probably of silver, are commonly distributed in the host rock (Fig. 18D). There are also thin fractures, around 10 µm in width, filled with silver or breithauptite.

Almost every sample has serpentine pseudomorphs after olivine, in which ore minerals can be found. Two major minerals occur: valleriite and iron oxide. The iron oxide is probably magnetite; this conclusion is based on the magnetic properties of the serpentine. The size of the grains are though too small for certain identification. Valleriite has a symplectite type of intergrowth with the silicate showing flame– and needle shaped grains of valleriite in the earlier fracture zones of the pseudomorph (Fig. 18E). The flames or needles are very thin, around 1 µm (Fig. 18F). Also the iron oxide has a symplectite type of intergrowth with the serpentine (Fig. 18G). It likewise forms flame- or needle-shaped grains, which are grouped together into feathery or flower-like aggregates (Fig. 18H). Even though these two phases are most common in serpentine pseudomorphs, they sometimes are found also in other minerals of the host rock. Sometimes pleonaste, a spinel, occurs in the samples together with iron oxide (see section 6.1.4).

Small groups of intergrown grains, around 50–100 µm in diameter, of chalcopyrite, other sulphides and arsenic- and antimony containing minerals are frequent (Fig. 19A). Even though they are common, they only occur in small amounts. The most important minerals are cobaltite, breithauptite, gudmundite and nickeline (Figs. 19B, C & D). Safflorite and maucherite have been found in small amounts. The intergrowths are often complex; very small grains of one phase grows in another, causing them to be easily overlooked. However, the chemical analyses and SEM work give evidence of these phases.

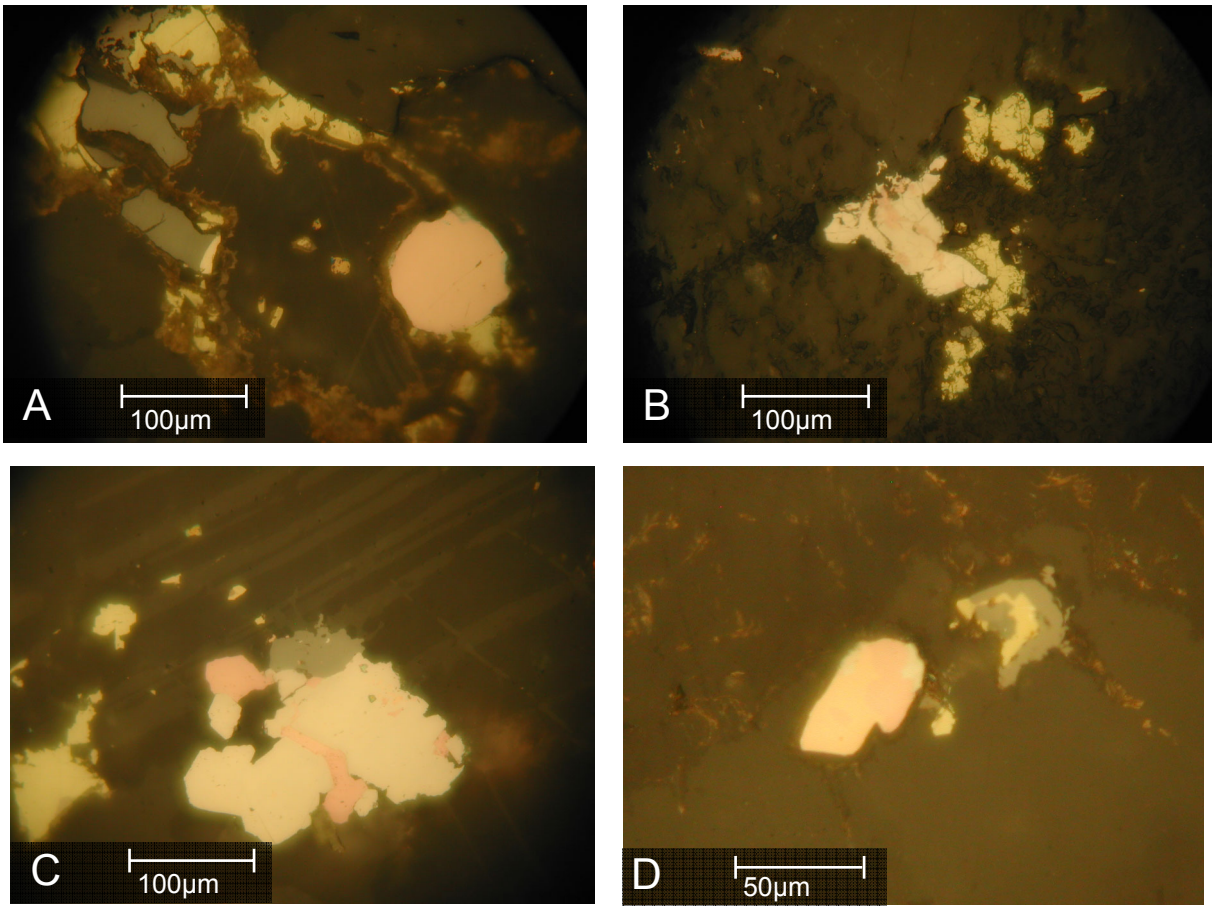


*Fig. 19 A-D (p. 27).* **A.** Round breithauptite grain adjoined to a valleriite-, chalcopyrite- and spahlerite aggregate (DBH2992 78.80 m). **B.** Intergrowth of gudmundite and breithauptite near a small chalcopyrite and sphalerite grain (DBH2992 92.74 m). **C.** Cobaltite grains intergrown with breithauptite (DBH 2992 82.60 m). **D.** Nickeline, breithauptite and probably gudmundite intergrowth (DBH2955 72.60 m).

*Fig. 18 A-H (p. 26).* **A.** Sphalerite with cobaltite inclusions and rounded grains of iron oxide (DBH2992 104.69 m). **B.** Needle shaped grains of chalcopyrite (DBH2955 92.60 m). **C.** Pyrrhotite grain connected to chalcopyrite grains (DBH2993 71.90 m). **D.** Small rounded grains of probably silver in the host rock (DBH2955 67.60 m). **E.** Valleriite in serpentine pseudomorphs after olivine (DBH2992 86.60 m). **F.** Valleriite- and iron oxide symplectites within a silicate grain (DBH2993 71.90 m). **G.** Fine-grained iron oxide symplectites in serpentine pseudomorphs after olivine (DBH2955 102.60 m). **H.** Iron oxide- and valleriite symplectites with silicates (DBH2955 72.60 m).

### 6.2.5 The mineral assemblages in the biotite-rich leptite

In two of the samples, DBH2955 62.60 m (Table 3) and DBH2993 104.40 m (Table 4) the host rock mineralogy is different from the rest of the samples (Appendix 2). There are large amounts of biotite in addition to quartz and microcline. Biotite has a distinct orientation. The composition of the ore minerals differs much from the other samples. The ore minerals found in DBH2955 62.60 m have been determined both optically and chemically, whereas the sample from DBH2993 has a lower amount of ore minerals, which only has been determined optically; hence uncertainties are larger. These two samples show differences as well as similarities in the mineralogy compared to the other samples.

The dominating sulphide minerals in both samples are tetrahedrite and galena. These are often intergrown or occur as separate grains, normally 100–500 µm in cross section (Fig. 20A). Small grains of arsenopyrite in tetrahedrite grains can be found in the samples. Chalcopyrite is very rare and occur solely as small discrete grains. In DBH2993 104.40 m only, bornite occurs as discrete grains roughly 100–500 µm in diameter.

In sample DBH2955 62.60 m, the tetrahedrite and galena occur as large grains or aggregates, around 0.5–2 mm in diameter. Small inclusions of iron rich safflorite are common. They often have a rhombic shape and reach 10 µm (Fig. 20B). It is also common to find grains of chalcocite, around 20 µm, which sometimes have grains of bornite as inclusions, reaching 5 µm (Fig. 20B). The chalcocite grains are often linked to fractures. Near the grain boundaries of the tetrahedrite, grains of arsenopyrite, 20–80 µm in diameter can be found (Fig. 20C). Commonly they are situated next to chalcocite grains, around 20 µm in diameter. Arsenopyrite also occurs as single grains in the host rock. Allargentum and galena filled fractures occur in large tetrahedrite grains (Fig. 20C).

Small intergrown grains of numerous minerals, <100 µm in diameter, occur in the host rock (Fig. 20D). These can be composed of arsenopyrite, safflorite, galena, chalcocite, bornite and tetrahedrite. Often native bismuth and allargentum can be found as small rounded or irregular grains inside the other minerals or in the host rock. Allargentum also occurs as larger grains attached to separate minerals, such as tetrahedrite, in the host rock. Small amounts of gold were also indicated in one of the small aggregates.

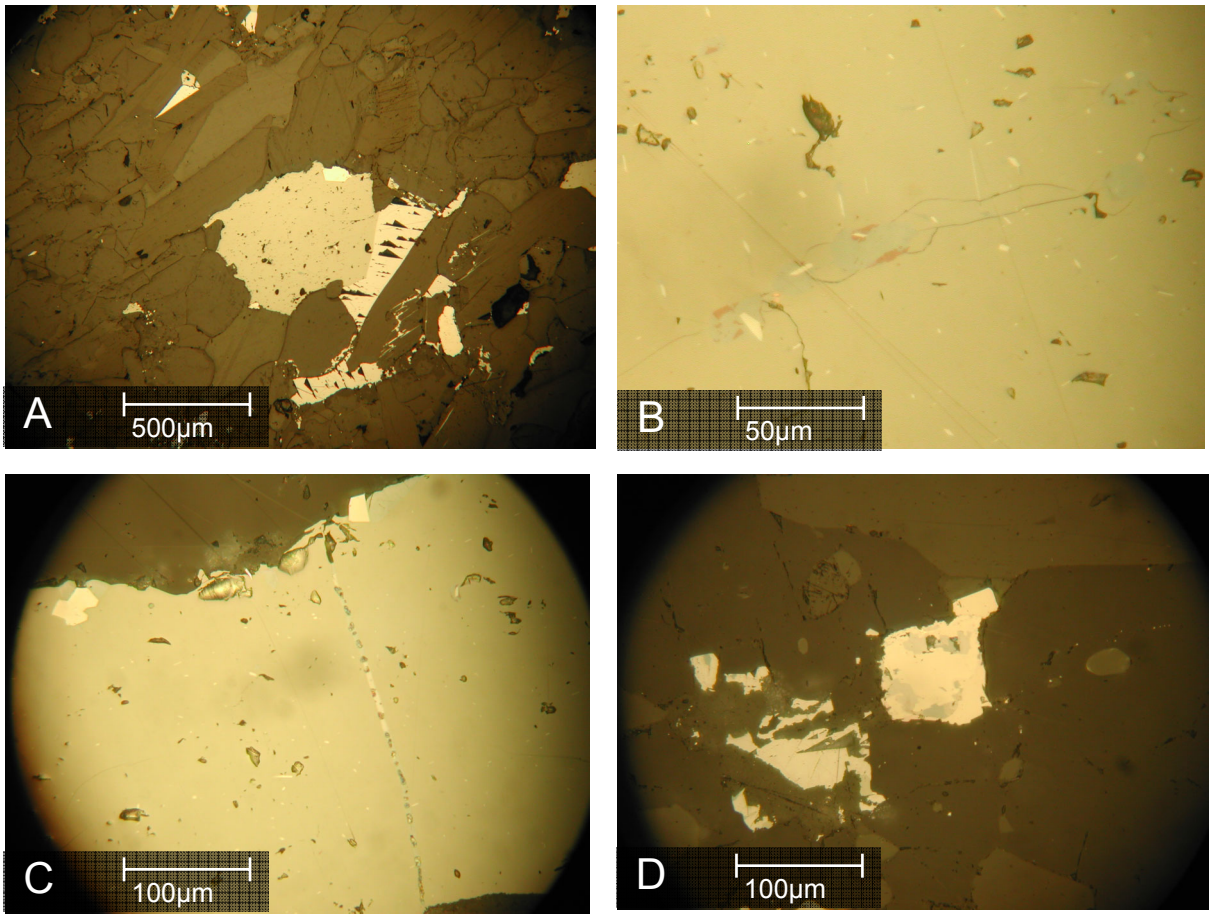


*Fig. 20 A-D.* **A.** Galena and tetrahedrite (DBH2955 62.60 m). **B.** Small sharp inclusions of safflorite (white) in tetrahedrite with rounded grains of chalcocite (grey) and bornite (brown) intergrowth along the fractures of the tetrahedrite (DBH2955 62.60 m). **C.** Tetrahedrite with arsenopyrite grains near boarder and a fracture filled with silver and galena (DBH2955 62.60 m). **D.** Small intergrowth of löllingite, chalcocite, galena and silver (DBH2955 62.60 m).

## 6.3 The distribution of the ore minerals

The main difference between the samples from the richer part of the core compared to the poorer part is amount and size of the chalcopyrite aggregates. In the poor samples, the mineralization is mostly composed of small chalcopyrite aggregates and a high amount of disseminated grains of ore minerals in the host rock. As the samples get richer, the area covered by chalcopyrite aggregates increases and as a consequence the amount of disseminated grains decreases. In the most ore rich parts, almost the entire sample is made up of chalcopyrite aggregates and networks and the host rock only occupies small spaces within the aggregates.

The mineralogical composition is rather constant independently of the distance to the richest parts of the mineralization. Most minerals can be found throughout the cores (Tables 2, 3 and 4). One exception is molybdenite, which has been found solely in either the more ore rich parts or in samples with an uncharacteristic mineralization. Sphalerite aggregates occur in the richer parts of the mineralization, though not in the richest parts (compare Tables 2–4 to Appendix 1). Pyrrhotite mostly occurs in the outer parts of the mineralization, both on the foot wall side and the hanging wall side. However, there are samples with pyrrhotite occurring in the richer parts of the mineralization. Another exception is tetrahedrite, which occurs only in samples of, for the mineralization, abnormal mineral composition (section 6.2.3 and 6.2.5).

The symplectitic growing minerals valleriite and iron oxide occur only when there are serpentine pseudomorphs after olivine (compare Tables 2–4 with Appendix 3). Hence they cannot be found in leptite. They exist independently of the degree of the mineralization. In DBH2992, though, there are no symplectites in the richest parts.

### 6.3.1 The ore minerals in DBH2992

In the reference core, DBH2992, the marble unit occurs throughout the core. The mineralization, which is more or less restricted to a marble host rock, gradually increases toward the richest parts, and then gradually decreases towards the foot wall, as discussed in section 6.1.1. Even though the richness of the mineralization increases, the number of minerals involved is rather constant (compare Appendix 1 with Table 2). However, it is important to note that the general core is very rich in ore minerals compared to the normal content of copper sulphides in the copper mineralization of the Zinkgruvan deposit. The common minerals occur in almost every thin section; but there are thin sections missing one or two of these phases.

The most important differences in mineral composition are found in the outer parts of the analysed area.

*Table 2.* The distribution of the most common ore minerals in DBH2992. For abbreviations of the minerals, see Appendix 3. Agg = major aggregates, > 1 mm, Minerals = minerals occurring in the aggregates and as separate grains, Sympl = symplectites, foremost in serpentine pseudomorphs, Mag(f) = magnetite filled fractures, Mag(g) = larger magnetite or iron oxide grains, Mag= Iron oxide, perhaps magnetite, as symplectite intergrowts, Cpe = coarse-grained pentlandite, Pen = fine-grained pentlandite.

| | Agg | | | Minerals | | | | | | | | | | | | | | | | | | | Sympl | | |
|---|---|---|---|---|---|---|---|---|---|---|---|---|---|---|---|---|---|---|---|---|---|---|---|---|---|
| | Cpy | Sph | Bor | Cpy | Cub | Sph | Cpe | Mag(f) | Pen | Mac | Ape | Val | Pho | Bre | Cob | Gal | Gud | Bor | Mol | The | Mag(g) | Mag | Val | Cpy |
| 72.25 | | | | x | | x | | | | | | | | | x | x | | | | | x | x | x | x |
| 78.80 | x | | | x | x | x | x | x | x | x | x | x | | x | | x | x | x | | | x | | | x |
| 80.70 | x | | | x | x | x | x | x | x | | x | x | | x | x | x | | | | | x | | x | |
| 82.60 | x | | | x | | x | x | x | x | x | x | x | | x | x | x | | x | | | | x | x | x |
| 84.60 | | | | x | x | x | | x | | x | | | | x | x | x | | x | | | x | x | | |
| 86.60 | x | | | x | x | x | x | x | x | x | x | x | | x | x | x | x | x | | | | x | x | |
| 88.78 | x | | | x | x | x | x | x | x | x | | x | x | x | | | x | x | | | x | x | x | x |
| 90.79 | x | | | x | x | x | x | x | | | x | x | | x | x | | x | x | | | x | x | | x |
| 92.74 | x | x | | x | x | x | x | x | x | x | x | | | x | x | | | x | | | x | x | | |
| 94.65 | x | x | | x | x | x | x | x | x | x | x | | | x | x | x | | x | | | | | | |
| 96.50 | x | | | x | x | x | x | x | x | x | x | | | x | x | x | | x | | | | x | | x |
| 98.63 | x | x | | x | x | x | x | x | x | x | x | | | x | x | x | x | x | | | | | | x |
| 100.65 | x | | | x | | x | x | | x | x | x | | | x | x | | | | x | | | | | |
| 102.47 | x | | | x | x | x | x | x | x | | x | | | | | | | | x | | | | | |
| 104.69 | x | | | x | x | x | x | x | x | x | x | | | x | x | | | x | | | x | | x | |
| 106.72 | x | | | x | x | x | | x | x | | | | | x | x | x | | x | | | x | x | x | x |
| 108.73 | x | | | x | | x | x | | x | x | | | | x | x | x | | | | | | | | |
| 110.71 | x | | x | x | | x | | | | | | | | x | x | x | | x | | x | | | | |
| 115.80 | | | | x | | | | | | | | x | | | | | | x | | | | | | |

*Table 3.* The distribution of the most common ore minerals in DBH2955. For abbrevations, see Table 2 and Appendix 3.

| | Agg | | | Minerals | | | | | | | | | | | | | | | | | | | Sympl | | |
|---|---|---|---|---|---|---|---|---|---|---|---|---|---|---|---|---|---|---|---|---|---|---|---|---|---|
| | Cpy | Sph | Bor | Cpy | Cub | Sph | Cpe | Mag(f) | Pen | Mac | Ape | Val | Pho | Bre | Cob | Gal | Gud | Bor | Mol | The | Mag(g) | Mag | Val | Cpy |
| 55.10 | | | | | | | | | | | | X | | | | | | | | | X | X | | |
| 62.60 | | | | X | | | | | | | | | | X | X | | X | X | X | | | | | |
| 67.60 | | | | X | | X | | | | | | | | | X | | | | | | | X | | |
| 72.60 | X | | | X | | X | X | X | X | | | X | | X | X | X | X | | | X | | X | X | |
| 77.60 | X | | X | X | | X | | X | | | | X | | X | X | X | X | X | | | | X | X | |
| 82.60 | X | | | X | | X | X | X | X | X | X | | | X | X | | | | | X | | | X | X |
| 87.60 | X | | | X | | X | X | X | X | | | X | | X | X | | | X | | | | | X | |
| 92.60 | X | | | X | X | X | X | X | X | X | | | | | | X | | | | | X | X | | X |
| 97.60 | X | | | X | X | X | X | X | X | | | | | X | | | | X | | | X | X | | X |
| 102.60 | X | | | X | | X | X | X | X | | | X | | X | X | | X | X | | | X | X | | |
| 107.60 | X | X | | X | X | X | X | X | X | X | | | | X | X | X | | | | | X | X | | X |
| 112.60 | X | X | | X | X | X | X | X | X | X | X | X | | X | X | | | X | | | X | | X | X |
| 117.60 | X | | | X | X | X | X | X | X | X | | X | | X | X | | X | | X | | | X | | X |
| 122.60 | X | | | X | | X | X | X | X | X | | | | X | X | | | | | | X | | | X |
| 130.10 | | | | X | | | | | | | | | X | | X | | | | | | | | | |
| | Cpy | Sph | Bor | Cpy | Cub | Sph | Cpe | Mag(f) | Pen | Mac | Ape | Val | Pho | Bre | Cob | Gal | Gud | Bor | Mol | The | Mag(g) | Mag | Val | Cpy |

Sample 72.25 m mainly consists of small grains of various ore minerals disseminated in the host rock. Fine-grained iron oxide dominates; most of the oxide is found in serpentine pseudomorphs after olivine.

Quartz is not a common mineral in the samples of DBH2992, but in the thin section 110.71 m there is a quartz-rich part, perhaps quartzite (Appendix 2). The skarn part of the thin section is dominated by biotite and diopside. There is a large difference in the mineralogy of the opaque phases depending on the host rock. In the skarn rock, grains and aggregates occur intergrown with bornite and chalcopyrite (section 6.2.4), whereas the quartz-rich rock has a low amount of ore minerals, mainly magnetite, chalcopyrite, galena and bismuth. In sample 115.80 m, which occurs on the foot wall side of the mineralization, the amount of ore minerals is very low and merely a few discrete grains of pyrrhotite, chalcopyrite and bornite occur.

The host rock minerals of sample 108.73 are mainly diopside representing the skarn, but similar to the section 110.71 m there are two parts of the thin section. The other part is dominated by carbonates, the grains of which have an irregular morphology. The ore minerals are mostly located in the skarn dominated part, whereas the carbonate dominated part has only separate grains of chalcopyrite. In the skarn dominated part chalcopyrite dominates and occurs as aggregates and also what resembles cementation of fragmented grains (Fig. 21A). Near the border to the carbonate dominated part the chalcopyrite grains are very rough, which can be seen at smaller scale in other samples with altered minerals. Cubanite lamellae are absent, but in hollows of the chalcopyrite rims, small needles of a mineral similar to cubanite occur (Fig. 21B). The ore minerals occurring in the sample are otherwise similar to the other samples.

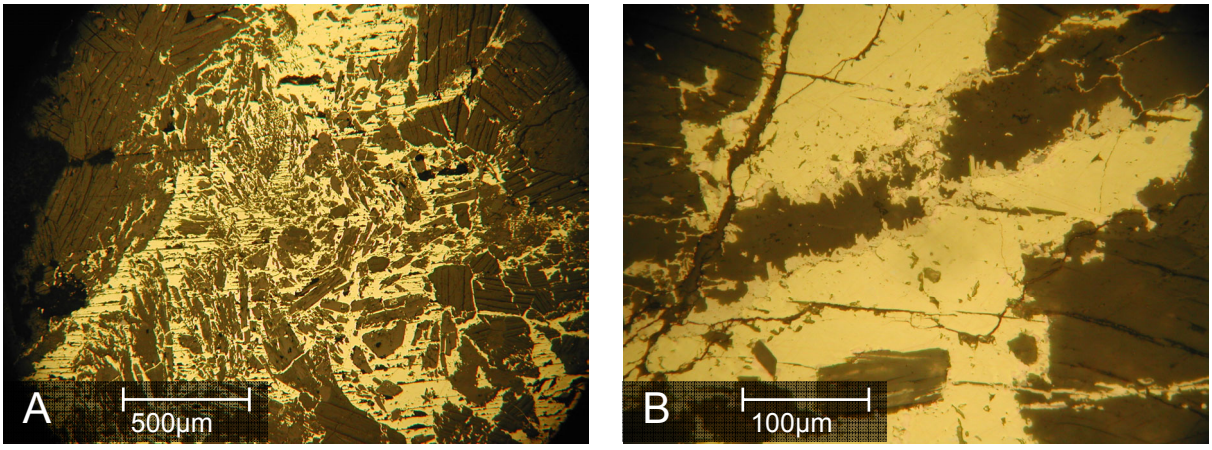


*Fig. 21 A-B.* **A.** Fragmented grains with chalcopyrite cementation. **B.** Chalcopyrite with cubanite(?) rims (DBH2992 108.73 m).

*Table 4.* The distribution of the most common ore minerals in DBH2955. For abbrevations, see Table 2 and Appendix 3.

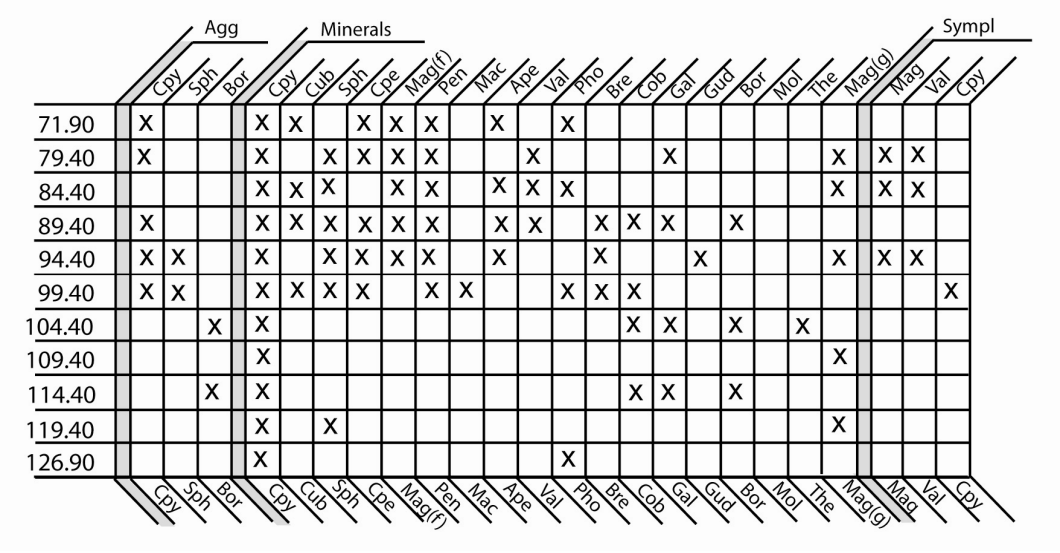


### 6.3.2 The ore minerals in DBH2955

The mineralization in DBH2955 (Table 3) is similar to that in DBH2992, apart from the higher content of ore minerals in the reference core. In the stratigraphical higher parts of the ore zone, to 72.60 m, the mineralization is much weaker and there are only small grains of ore minerals: chalcopyrite, magnetite and pyrrhotite. Sample 62.60 m, with a biotite-rich host rock is situated in dolomite-dominated marble. The sample, which is described in section 6.2.5, differs radically from the rest of the core, with the dominating minerals tetrahedrite and galena. Further, sample 77.60 m has a high content of bornite (section 6.2.3). The section, which this sample represents, has a skarn host rock.

An interval of marble is underlying the skarn section. The degree of mineralization increases but the minerals included are more or less the same. The samples are rich in ore minerals up to the point where the quartz-feldspar leptite unit is reached. Then the ore minerals, such as chalcopyrite, cobaltite and pyrrhotite occur sparsely.

### 6.3.3 The ore minerals in DBH2993

The host rock of DBH2993 is represented by marble in the upper half of the core, whereas in the lower half it is quartz-feldspar leptite (compare Table 4 with Appendix 1). There is a strong correlation between the host rock and the degree of mineralization in the core. The upper half is relatively rich in ore minerals and is similar to the other two cores, except for the pyrrhotite content in three samples. Sphalerite aggregates occur in the richer parts of the core, but there is no molybdenite. The chalcopyrite aggregates, which occur in the upper part of the stratigraphical column are mostly small and reach only 0.5 mm in diameter, which is much smaller than in core DBH2992.

The lower half of the core is very poor. There are no aggregates of chalcopyrite in the lower part of the stratigraphical column but only discrete grains. However, the samples 104.40 m (section 6.2.5) and 114.40 m (section 6.2.3) are rich in bornite.

## 6.4 The composition and optical properties of the opaque minerals

In the following text, the chemical composition and optical properties of the minerals found in the Zinkgruvan copper mineralization are described. For comparison to the general properties of the minerals, see Ramdohr (1980). The generalised stoechiometric chemical formulas can be found in e.g. Anthony et al., (1990) and to a certain extent in Ramdohr (1980). Appendix 3 shows a summary list of the opaque minerals identified during the study.

The opaque minerals are divided into different groups according to the amounts in which they occur in the thin sections. The major ore minerals occur in large quantities in almost every thin sections, the common ore minerals are normally found in all thin sections, minor minerals can be found to a small extent in almost every thin section, whereas the accessory minerals are rare and are sometimes found only in a few thin sections. Statistical errors in the given chemical compositions are normally around 2 relative percent. The relative errors of elements occurring in low amounts are appreciably larger.

### 6.4.1 Major ore minerals

*Chalcopyrite - $CuFeS_2$*

Chalcopyrite is the main mineral of the Zinkgruvan copper mineralization. It occurs as part of different mineral assemblages and in different grain sizes. In reflected light microscopy, it is yellow and has a weak anisotropy. The spot analyses of chalcopyrite grains result in an almost constant composition (Appendix 4, Table 1) close to the stoechiometric composition but

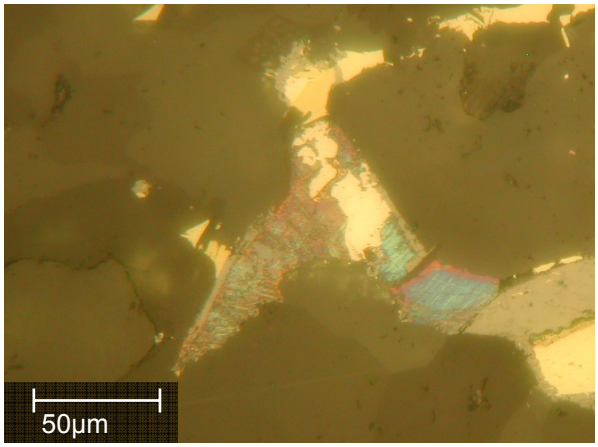


*Fig. 22.* Chalcopyrite grain with severe oxidation from Ag, (DBH2955 117.60 m).

with a slight excess of sulphur. The mean composition is S 50.9 at% , Fe 24.6 at% and Cu 24.5 at%. Due to the constant composition, only twelve representative analyses out of a total of sixty analyses are presented. As the excess sulphur is more or less constant and occurs in most of the sulphur containing minerals, it probably represents a systematic error. This will be discussed later.

In some cases, chalcopyrite has been severely oxidised, resulting in an orange to blue tarnish. Spot analysis has revealed a significant content of silver in some of these grains (Appendix 4, Table 2). The content is low, generally around 0.3 at%, and the silver cannot be optically identified from other than the tarnish. In some chalcopyrite grains, small rounded bright grains, which perhaps could represent the silver anomaly, are visible. However, these grains have not been analysed. During the chemical analysis performed on the tarnished chalcopyrite, there was no visual indication of a separate silver phase. If there is, the grain size is less than the resolution limit of the electron microscope. When silver occurs in higher amounts, up to 7 at%, the tarnish is more extensive (Fig. 22).

### *Cubanite - $CuFe_2S_3$*

Cubanite has a light beige-yellow colour in reflected light microscopy. It shows a distinct bireflectance (Fig. 12B & C), with light beige to a more brownish colour and a distinct anisotropy. The chemical composition of cubanite is close to stoechiometric and is constant (Appendix 4, Table 3). The mean chemical composition is S 51.0 at%, Fe 32.6 at% and Cu 16.5 at%.

### *Bornite - $Cu_5FeS_4$*

Bornite has a pinkish brown colour in reflected light (Fig. 16D-H). It quickly tarnishes to blue and red colours (Fig. 16G), which is a good characteristic during identification. The chemical composition, with the mean values of S 41.1 at%, Fe 9.9 at% and Cu 48.9 at% is almost constant and close to stoechiometric (Appendix 4, Table 4). In some samples silver is detected, similarly to that in chalcopyrite.

## 6.4.2 Common ore minerals

### *Sphalerite - ZnS*

Sphalerite is a dark grey, low reflecting mineral, slightly lighter than the silicates and carbonates, when studied in reflected light microscopy. Abundant yellow to orange internal reflections are common (Fig. 13C). As it is not opaque, it can be identified in transmitted light microscopy. It then appears as dark, reddish brown, semitransparent, isotropic grains.

Zinc in sphalerite can be replaced by iron and manganese, which is very common in the samples (Appendix 4, Table 5). There is a linear relation between the Zn and Fe + Mn content (Fig. 23). Two major groups can be identified. The low-Fe group has a mean composition of S 50.6 at%, Fe 2.3 at% and Zn 46.9 at%, whereas the mean composition of the high-Fe group is S 50.9 at%, Fe 5.8 at% and Zn 42.6 at%. The high-Fe group of sphalerite often has a significant content of Mn but also Cd has been detected. Some analyses also show a low content of Cu, around 1 at%, perhaps originating from the chalcopyrite emulsion also seen in the SEM (Fig. 13D).

### *Magnetite - $Fe_3O_4$*

Magnetite is a low reflecting ore mineral that appears grey with a brownish tint in reflected light. It is slightly lighter and browner than sphalerite. These two minerals are rather similar, but they can be discriminated from each other with the help of the chalcopyrite emulsion in sphalerite. Though, some coarse magnetite grains have chalcopyrite inclusions. Due to the difficulties of determining the oxygen content with the EDS technique (Appendix 4, Table 6), hematite and magnetite cannot be separated with certainty. Thus, the determinations are based on microscopy studies.

The magnetite filled fractures (e.g. fig. 13H) are identified as magnetite from optical data combined with chemical analysis. However, the smaller grains, such as the rounded grains of iron oxide in the host rock (Fig. 18A) and the symplectitic intergrowths with serpentine (Fig. 18H), are more difficult to determine.

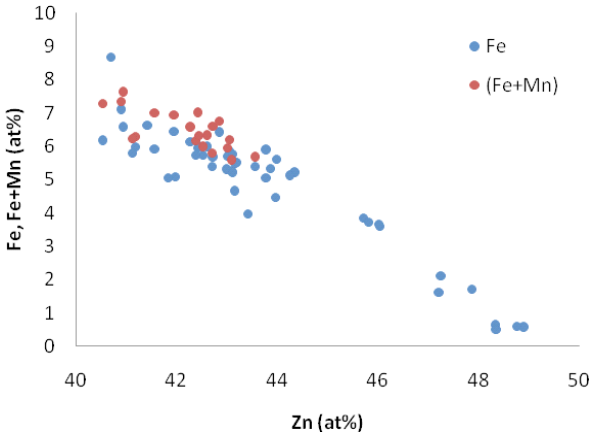


*Fig. 23.* The chemical variations in sphalerite.

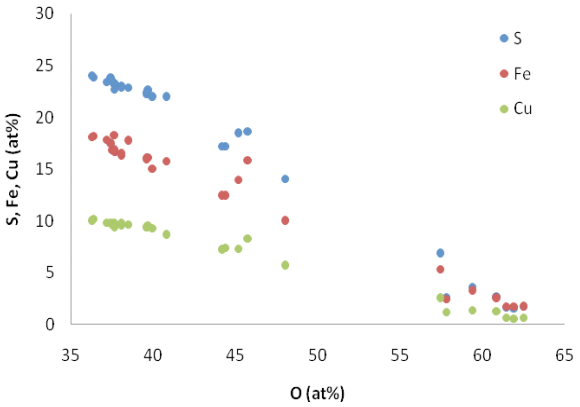


*Fig. 24.* The chemical variations in valleriite.

Thereby the term iron oxide is used. The magnetic properties of the serpentine skarn in the marble indicates that this oxide, with a high probability, is magnetite.

### *Valleriite - $4(Fe,Cu)S{\cdot}3(Mg,Al)(OH)_2$*

Valleriite has a low reflectance. It is bronze yellow to greyish brown and shows distinct bireflectance and anisotropy (Figs. 14E,F, 18E & F). The width of the valleriite flame- and needle-shaped grains is often very small and proper determinations of the chemical composition are difficult. The composition with O, Mg and Al leads to problems during the analyse, especially the oxygen analyses are inferior. Thus, some of the large compositional variation might be an artefact of less reliable analyses (Appendix 4, Table 7). However, there is a linear relationship between the content of S, Fe and Cu and the content of O (Fig. 24) testifying to large real compositional variations.

### *Pentlandite $(Fe,Ni)_9S_8$ - Cobalt pentlandite $Co_9S_8$*

Pentlandite is a nickel containing variety of pyrrhotite; it has nearly equal amounts of Ni and Fe. The pentlandite of Zinkgruvan in addition contains Co. Pentlandite forms a solid solution series with cobalt pentlandite and the ratios of Fe, Ni and Co may vary. In Zinkgruvan two types of pentlandite crystals occur; fine-grained and coarse-grained.

Fine-grained pentlandite occurs as tiny grains, grouped together. These are white with a weak pinkish tint. The reflectivity is slightly higher than that of chalcopyrite and in comparison to chalcopyrite, fine-grained pentlandite sometimes shows a relief. Discrete pentlandite grains can be hard to identify in an optical microscope (Figs. 12F & G), but in the SEM they appear clearly (Fig. 25). The Co content varies between 2.2 and 14.2 at%, the Ni content is from 18.6 to 24.0 at% and the content of Fe ranges from 18.8 to 26.3 at%. The content of S is stable, around 48.0 at% (Appendix 4, Table 8).

Coarse-grained pentlandite occurs as large grains in chalcopyrite aggregates (Figs. 13E-G). The colour is white with a pinkish-brownish tint. It shows no bireflectance or anisotropy. Although it looks homogeneous under the optical microscope, it has a heterogeneous chemical composition, clearly visible in the SEM (Fig. 26). Spot analyses made on a line crossing the light grey – dark grey areas display the variations in chemical composition shown in Fig. 27.

The Fe content of coarse-grained pentlandite varies

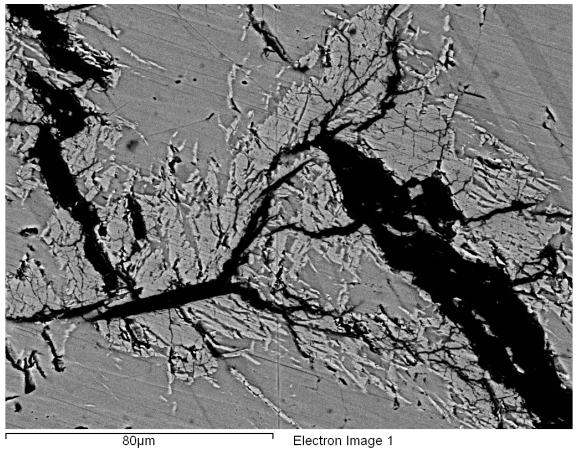


*Fig. 25.* Fine-grained pentlandite, with flame like grains occurring around magnetite filled fractures, BSE image (DBH2992 102.47 m).

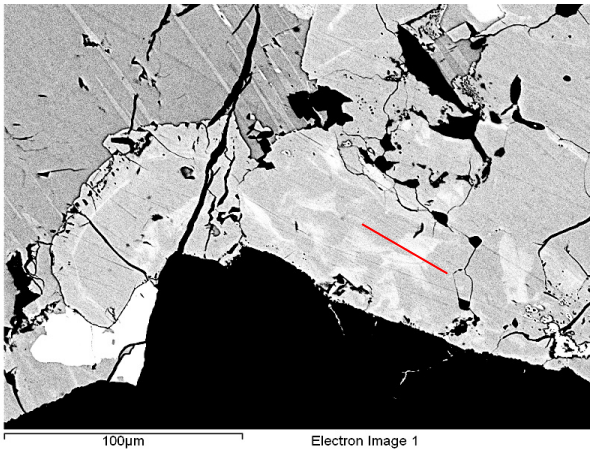


*Fig. 26.* BSE image of heterogeneous coarse-grained pentlandite grain. The red line represents the points of analyse, starting from the left, Fig. 27 (DBH2992 102.47 m).

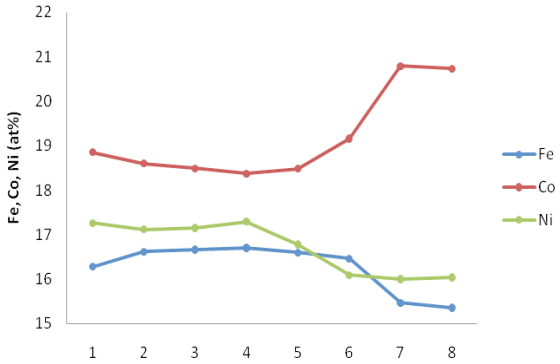


*Fig. 27.* Heterogeneous composition of coarse-grained pentlandite, measurements along the red line in Fig. 26.

from 2.9 to 22.6, the Ni content from 8.2 to 21.1 at% and the Co from 10.7 to 40.8 at% (Appendix 4, Table 9). The content of S is stable, around 47.8 at% .

Both Ni and Fe are replaced by Co (Fig. 28) and there is a strong relation between the cobalt content and the size of the grains. The fine-grained pentlandite has a lower cobalt content than the coarse-grained pentlandite (Fig. 28). However, there are exceptions, such as the extremely cobalt-rich pentlandite in DBH2993 114.40 m (Appendix 4, Table 9), which occurs as small grains. This sample has a high content of bornite. Figure 28 further demonstrates that in Co-rich varieties, the Ni/Fe ratio is increased compared to the ratio at low Co-contents (almost equal to one). This suggests that cobalt replaces iron in preference to nickel.

*Mackinawite - $(Fe,Ni)_9S_8$*

Mackinawite and pentlandite have rather similar chemical compositions. The main difference is that iron clearly exceeds nickel in mackinawite. Mackinawite is easily distinguished in reflected light microscopy due to its characteristically distinct bireflectance and anisotropy. The bireflectance colours vary from white with a grey tint to dark grey. In crossed polars, the variation is even stronger, from black to white. Under the ore microscope, the grains often appear heterogeneous (Figs. 13 A & B). It sometimes has a similar appearance in the SEM.

The mean chemical composition is S 51.1 at%, Fe 43.5 at%, Ni 3.8 at% and Co 1.2 at% (Appendix 4, Table 10), but the amounts of Fe, Ni and Co vary (Fig. 29). Foremost Fe is replaced by Co.

*Argentopentlandite - $Ag(Fe,Ni)_8S_8$*

The colour of argentopentlandite is rather similar to the colour of bornite, but it is lighter and does not have the reddish tone, which bornite often has (Fig. 12H). It shows neither bireflectance nor anisotropy. The chemical composition (Appendix 4, Table 11) shows only a limited variation around the mean composition S 47.8 at%, Fe 31.9 at%, Ni 13.6 at% and Ag 6.3 at%.

### 6.4.3 Minor minerals

*Breithauptite - NiSb*

Breithauptite is characteristically pink in reflected light and shows distinct bireflectance and anisotropy. The chemical composition is mostly close to stoechiometric, but arsenic often occurs in small (0–3.4 at%) amounts. Very small amounts of Fe, up to 1.8 at% have been detected. The mean value is Ni 49.2 at% and Sb 49.4 at% (Appendix 4, Table 12).

*Cobaltite - CoAsS*

Cobaltite is a white mineral with a pinkish tint. It might show bireflectance and is distinctly anisotropic. Due to its high hardness and often euhedral shape it is often easily distinguished. The chemical composition is rather constant in the drill cores, with a mean value of S 33.2 at%, Co 28.3 at%, As 33.9 at%, Ni 3.3 at% and Fe 1.4 at% (Appendix 4, Table 13).

*Galena - PbS*

The colour of galena in reflected light is light grey to white and might sometimes appear slightly bluish, depending on the surrounding minerals. In larger grains, it is possible to see the characteristic triangular pits, but mostly the grains are too small. Galena is a cubic mineral and shows no anisotropy but appears black under crossed polars. Mostly the grains are small and rounded often with an irregular shape.

The chemical composition is close to stoechiometric; S 49.7 at%, Pb 49.5 at%. Often small amounts of Fe (0–4.7 at%) can be found in the galena (Appendix 4, Table 14). The analyses of galena suffers from the lack of suitable standards (see section 5.2.2).

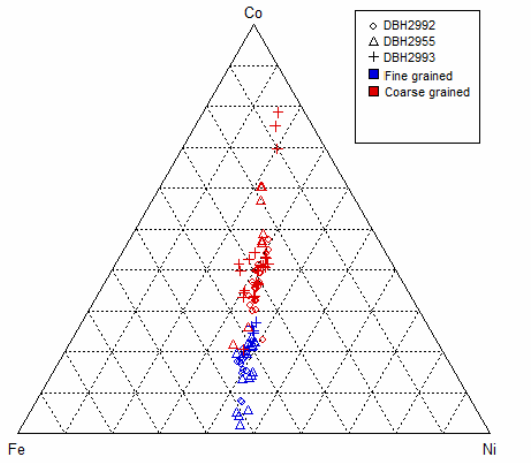


*Fig. 28.* Chemical variation of fine-grained pentlandite (blue) and coarse-grained pentlandite (red).

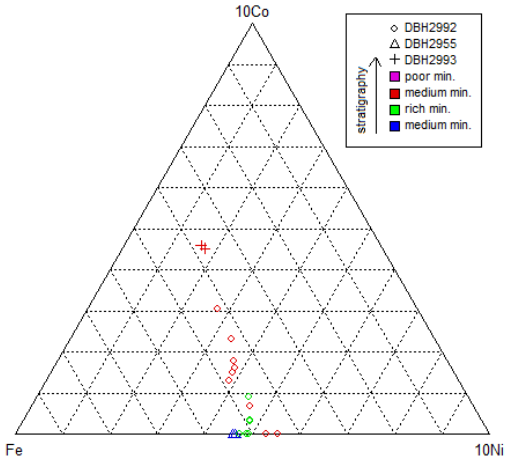


*Fig. 29.* The chemical composition of mackinawite. The amount of Co and Ni is multiplied with 10. Stratigraphy = stratigraphy within the mineralization (see Figs. 34 & 35).

*Pyrrhotite - $Fe_7S_8$*

Pyrrhotite occurs, though to a small extent, as light brown grains in chalcopyrite aggregates. It sometimes shows bireflectance and anisotropy but can be distinguished from cubanite due to its high relief in comparison to the adjoining minerals. The grains are heterogeneous and there is a flame-like structure, which also is visible in the SEM (Fig. 30). The grains are mostly rather large and sometimes have a distinct cleavage.

The amounts of sulphur and iron in the pyrrhotite are almost equal. There are two groups of pyrrhotite. The most common one has S 53.3 at% and Fe 46.6 at%, whereas there is a variety with S 51.2 at% and Fe 48.8 at% (Fig. 31). This variety occurs as flames but is only analysed at one point (Appendix 4, Table 15).

### 6.4.4 Rare minerals

*Molybdenite - $MoS_2$*

The main occurrence of molybdenite is in the richest parts of the mineralization. It forms rectangular grains with a fibrous texture. The colour of molybdenite is white to light grey and it shows a distinct pleochroism to dark grey. It is distinctly anisotropic with black and white interference colours. The chemical formula of molybdenite is $MoS_2$ and the crystals studied were close to stoechiometric (Appendix 4, Table 16).

*Gudmundite - FeSbS*

Gudmundite mostly occurs together with breithauptite. It is white with a weak bluish grey tint and shows bireflectance. Anisotropy is not detected. In gudmundite, S 33.8 at%, Fe 32.0 at% and Sb 33.9 at%, are the major elements. Occasionally, small amounts of As and Ni were detected (Appendix 4, Table 17).

*Nickeline - NiAs*

Nickeline can be found together with breithauptite, cobaltite and bismuth. It occurs as very tiny grains with a peach colour. Compared to breithauptite it has an orange tint, and was found only in the thin sections DBH2992; 82.60, 102.47. Chemically nickeline was difficult to determine due to its small grain size. The grain analysed showed the chemical formula Ni 49.22 at%, As 46.7 at%, Sb 3.6 at% and Fe 0.4 at% (Appendix 4, Table 18).

*Costibite - CoSbS*

Only a few grains of costibite have been identified in one sample (DBH2992 110.71). It occurs as small light bluish grey grains together with other antimony-containing minerals and native bismuth. The chemical composition is S 32.2 at%, Co 29.5 at%, Sb 34.1 at%, Fe 0.7 at% and Ni 3.4 at%. Only a few points have been analysed (Appendix 4, Table 19).

*Maucherite - $Ni_{11}As_8$*

Maucherite has only been detected once (DBH2955 117.60). It is a white mineral which has a low relief in comparison to neighbouring cobaltite. The composition is Ni 53.7 at%, As 40.8 at%, Fe 0.1 at%, Co 3.2 at% and Sb 2.2 at% (Appendix 4, Table 20).

*Tetrahedrite - $(Cu,Fe,Ag,Zn)_{12}Sb_4S_{13}$*

Tetrahedrite only occurs in a few samples, although in rather large amounts. It is grey with a tint of green and shows neither bireflectance nor anisotropy. There are two main chemical varieties (Appendix 4, Table 21), one of which is rich in iron – S 45.3 at%, Fe 5.9 at%, Cu 33.9 at%, Zn 0.9 at% and Sb 13.8 at%, and the other rich in zinc – S 45.3 at%, Fe 1.8 at%, Cu 33.7 at%, Zn 5.2 at%, Sb 14.0 at%. In the Fe-rich variety, it is common to find arsenic (0.2–0.5 at%). Silver (around 0.3 at%) can sometimes be found in both varieties.

*Safflorite - $(Co,Fe)As_2$*

There are two types of safflorite found in the samples (Appendix 4, Table 22 and 23). A Fe-rich, Co-poor variety with Fe 25.3 at%, Co 0–7.0 at%, Ni 0–6.2 at%, As 65.7 at% and S 1.7 at% occurs as small rhombic inclusions in tetrahedrite in DBH2955 62.60. It is white and appears milky. It also occurs intergrown with for example arsenopyrite, galena and chalcocite. There is a Fe-poor, Co-rich variety with Co 20.79 at%,

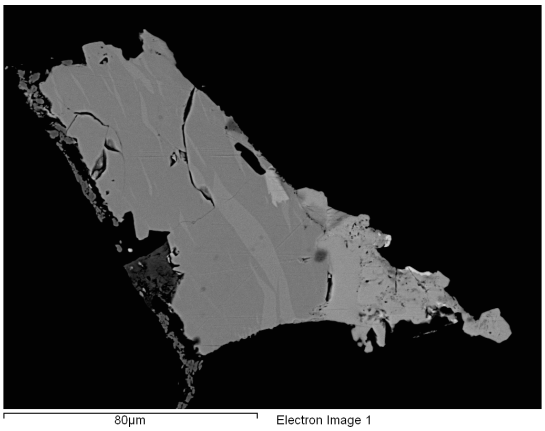


*Fig. 30.* BSE image of flame-like textures in pyrrhotite. Lighter areas are of cubanite and pentlandite (DBH2993 71.90 m).

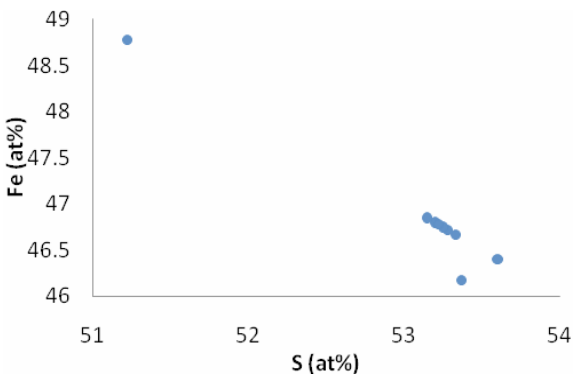


*Fig. 31.* The chemical variations in pyrrhotite.

Fe 8.4 at%, Ni 3.5 at%, As 64.1 at%, S 2.0 at% and Sb 1.2 at%, which occurs as grain intergrown with cobaltite and breithauptite in DBH2955 117.60 m. It is white with a light greyish blue tint.

### *Arsenopyrite - FeAsS*

Arsenopyrite has only been identified with certainty in one sample, DBH2955 62.60 m, where it occurs together with tetrahedrite and galena. It might also occur in another sample, DBH2993 104.40 m, which has a similar mineral composition. The grains are often small and subhedral to euhedral, but not as euhedral as the cobaltite grains found in other samples. The crystals can also be larger and occur as single grains in the host rock. It has a white colour with a very weak creamy pink tint and shows a weak anisotropy.

In the arsenopyrite, it is common to find low amounts of Co 0–3.1 at% and Ni 0–2.6 at%. Otherwise the mean composition is S 32.0 at%, Fe 30.0 at% and As 36.0 at% (Appendix 4, Table 24).

### *Chalcocite - $Cu_2S$*

Chalcocite has only been found in DBH2955 62.60. It is grey with a bluish tint and only occurs as small grains, <20 mm, intergrown with other minerals. The chemical composition is S 34.7 at%, Cu 64.5 at%, Fe 0–2.2 at% (Appendix 4, Table 25). The contents of Cu and S are rather stable whereas the Fe-content varies.

### *Silver - Ag*

Silver can mainly be found as fracture fillings and small grains in the host rock. In one sample, silver occurring as fracture fillings in a chalcopyrite-bornite aggregate has been found (DBH2993 114.40 m). Silver is rather easily distinguished, since oxides easily form on the surface, creating a heterogeneous white colour and oxidised texture. When freshly polished, the colour is brilliant white and the grains have high reflectivity. In a few cases, silver has been detected in chalcopyrite, but only in EDS analyses. Optically an oxidised surface of the chalcopyrite is the most common indication of a silver content. The silver is often pure but in some cases a mercury alloy has formed, 3.5–5.2 at% (Appendix 4, Table 26). There are also traces of S and Fe, however this might be due to disturbances from the surrounding crystals.

### *Allargentum - ($Ag_{1-x}Sb_x$)*

Allargentum occurs as small grains in for example tetrahedrite, both as small rounded included grains and in fractures. It is brilliant white but can be difficult to see due to its small grain size. The chemical composition varies, where Ag 80.8–91.2 at% and Sb 8.4–19.2 at% are the most extreme values (Appendix 4, Table 27). Small amounts of S have been detected rarely.

### *Bismuth - Bi*

Native bismuth mostly occurs as small rounded grains in the host rock or in other ore minerals such as coarse-grained pentlandite (DBH2992 92.74 m) but might also occur as larger grains or intergrowths (Fig. 32). It has a bright white colour with a slight peach tint, visible when the grains are coarse. The reflectivity is high. Bismuth is hard to identify under the optical microscope, due to the small sizes of the grains and the white colour. Mostly it is pure, 100 at% Bi (Appendix 4, Table 28).

### *Parkerite - $Ni_3(Bi,Pb)_2S_2$*

Parkerite has occasionally been detected with EDS analysis. It is light grey and often very fine-grained. The chemical composition is around S 28 at%, Ni 42 at%, Bi 28 at% with a low Fe content around 0.9–2.5 at% (Appendix 4, Table 29).

### *Graphite - C*

Graphite occurs as small rounded grains grouped together in some samples. Possibly, small amounts of graphite occur in the serpentine pseudomorphs after olivine. The graphite is dark grey with a tint of brown and show pleochroism from light to dark grey. In the graphite, small rounded grains of an unidentified high-

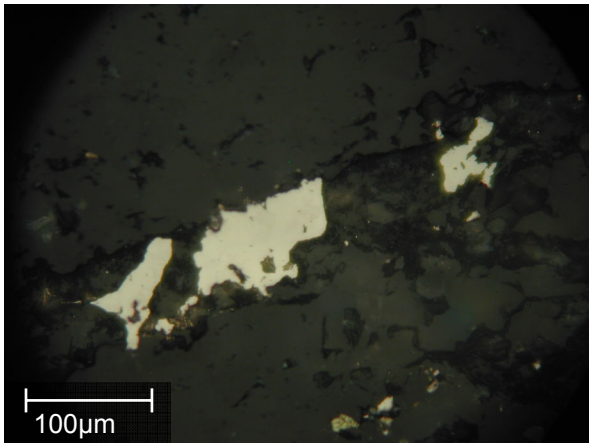


*Fig. 32.* Bismuth grains situated in a sulphide filled fracture (DBH2992 110.71 m).

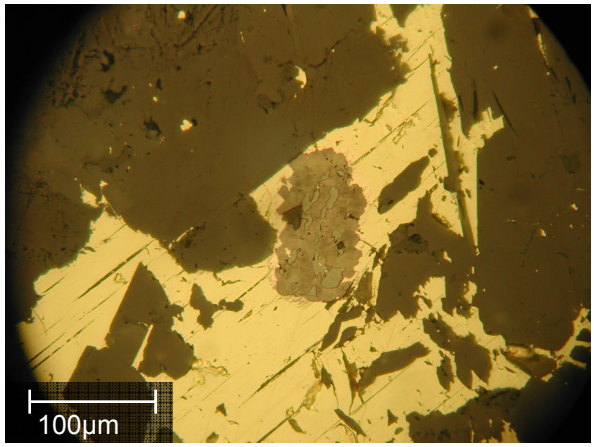


*Fig. 33.* Rounded Ag, Pb, U containing grains, inside graphite surrounded by pentlandite grains in a chalcopyrite aggregate (DBH2992 108.74 m).

relief, grey opaque mineral is found (Fig. 33 and Appendix 4, Table 30).

As the graphite consists of carbon (C) it is difficult to analyse with the EDS technique, especially when the samples are carbon coated. The presence of a high C-peak together with the absence of other elements is the main indicator of graphite.

## 6.5 Chemical variations

Most minerals found in the three drill cores have a rather constant chemical composition, both regarding the possible variations within a drill core and among the different cores. However, pentlandite varies in chemical composition (Fig. 34). There is no distinct systematic difference other than a restriction of the most extreme values to the foot wall side of the mineralization. The chemical composition of sphalerite varies. Generally, the Fe content is higher in parts with richer mineralization than in poorer parts on the stratigraphical foot wall side. However, on the stratigraphical hanging wall side, the Fe-content is the highest in poorer mineralization (Fig. 35).

Chemical analyses on the bulk of the ore has been made for Zinkgruvan AB (see section 5.1.2) in all three cores (Fig. 36 A-F). The whole rock chemistry correlates rather well with the results obtained from the microscopic studies (compare Fig. 36 with Appendix 1). The analytical results show an undulating content of Cu and Fe throughout the mineralization. The contents increase in the zones rich in ore minerals. In DBH2992 the rise is much quicker and more distinct than in DBH2955, where the increase is more gradual. Overall, the Cu- and Fe contents vary much in both the rich and poor sections. The content of Zn shows peaks in the richest zones of the mineralization.

The contents of Ni and Co correlate rather well with the mineralization in all three cores. As the content of Fe and Cu increases, so do the contents of the other elements (Co, Ni and Sb). However, the Co-content in DBH2992 has a very strong peak in the stratigraphical lower part of the core, approximately where sample 108.73 m is located. That sample was situated in a skarn section.

There is a peak in Sb in the stratigraphical lowest part of core DBH2992 (Fig. 36 B), which can be correlated with sample 110.71 m, a biotite and diopside rich sample in which minerals such as bornite, tetrahedrite and costibite occur. Distinct Sb peaks are also located in sample DBH2955 (Fig. 36 D), one which correlates with sample 77.60 m. This thin section is dominated by bornite-chalcopyrite aggregates in a skarn host rock. The large peak in Sb in DBH2993 (Fig. 36 F) is correlated with the biotite leptite section in which tetrahedrite and bornite were found.

# 7 Discussion

## 7.1 Is the study representative?

Three drill cores have been chosen from the richest part of a mineralization, which extends more than 1000 m vertically and is 30 m wide. The mineralization is patchy and uneven, which might result in samples that are not representative in spite of short sampling intervals. Consequently, the restricted sampling area raises questions whether the results of this study can be generalised. Only future studies can answer this question.

Some phases occur in very limited amounts. Small discrete grains found far away from chalcopyrite or sphalerite aggregates during optical microscopy are difficult to relocate in the SEM. Very few chemical analyses exist of such crystals. These phases are difficult to identify optically and if not relocated in the SEM, their identification is tentative. Some of these crystals are also close to the lower size limit for EDS analyses.

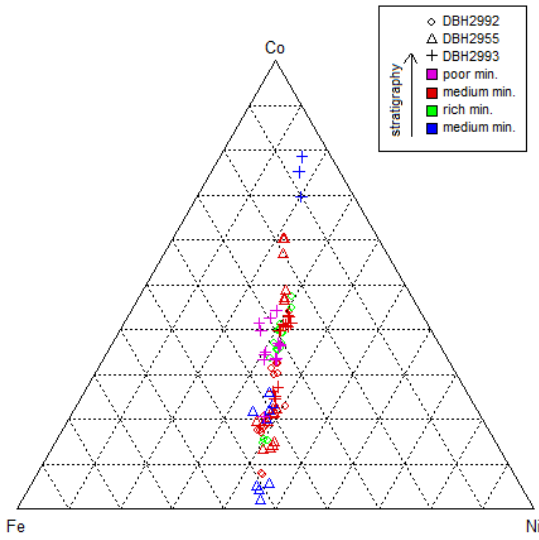


*Fig. 34.* Chemical variation of fine- and coarse-grained pentlandite, depending on location of the sample.

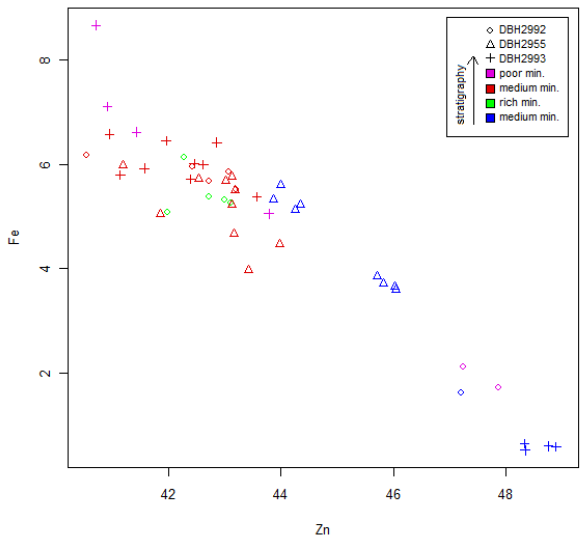


*Fig. 35.* The chemical composition of sphalerite depending on the location of the sample.

The points chosen for EDS analyses are biased due to the nature and irregularity of the mineralization. Prerequisites for good analyses are smooth surfaces and sufficiently large and homogeneous grains (minimum 5 µm in diameter).

Indications of tightly intergrown phases exist for the As- and Sb bearing minerals. The chemical composition of these minerals seems to vary. Besides a real variation in chemical composition, non-resolvable phase intergrowths might be responsible for some of this variation.

When the atomic percentage does not sum to 100, small amounts of elements, which should not occur in the analysed minerals have been excluded from the analysis. The most common of these elements are Cu, Zn, Fe and Ni. Most probably they occur in fracture filling minerals or in neighbouring grains. Grains smaller than five micrometres, or with analyses which lie outside 97–103 wt%, have generally been sorted out. Sometimes poor data has been kept due to too small amounts of data left.

Standards measured in this instrument do not exist for all elements occurring in the minerals identified. Default data from the INCA program has been used, creating a source of error. Some of the existing standards, notably Ag and S, have proven somewhat unre-

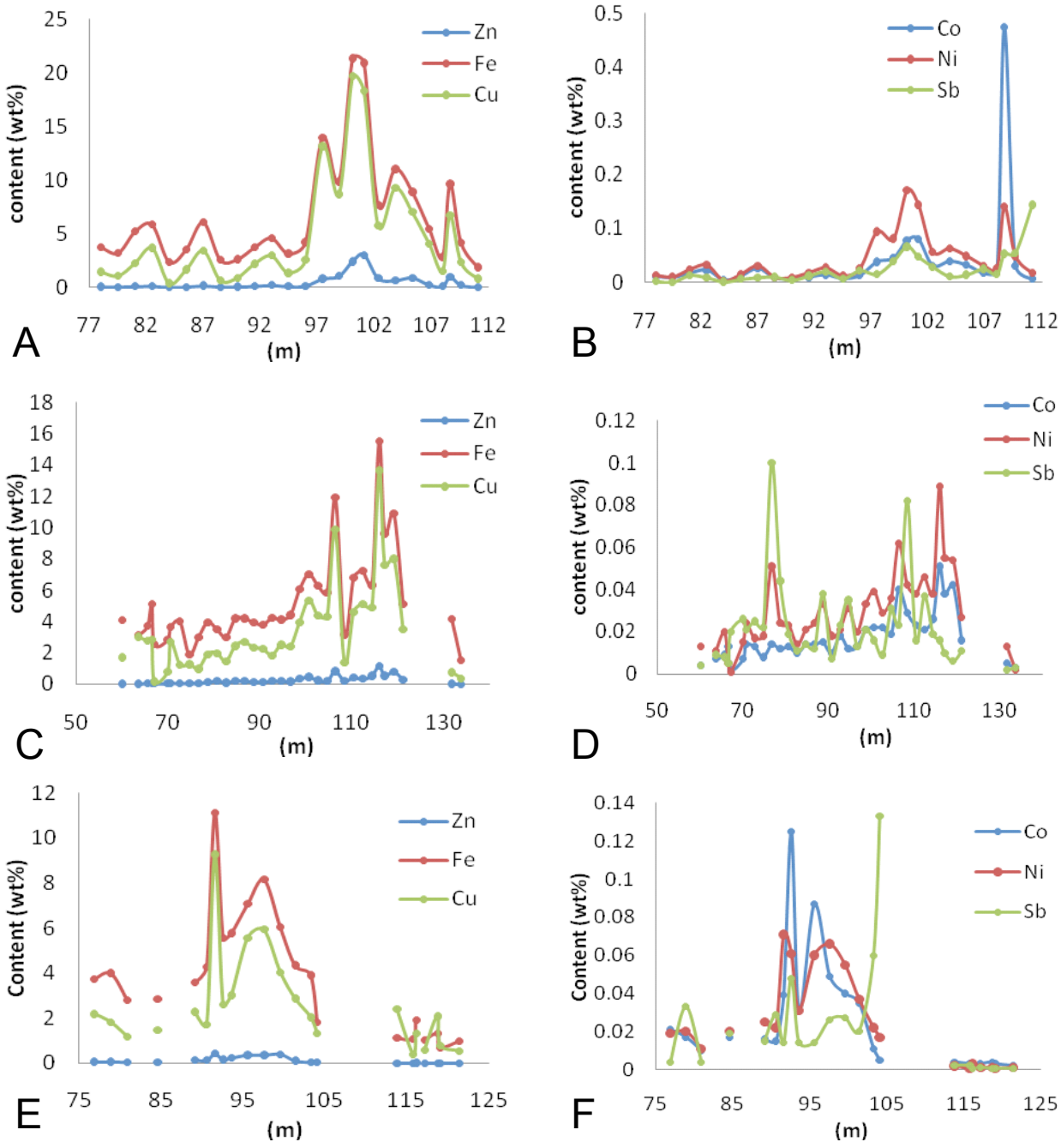


*Fig. 36 A-F.* The chemical variations in Zn, Fe, Cu (left side) and Co,Ni,Sb (right side). **A-B.** DBH2992. **C-D.** DBH2955. **E-F.** DBH2993.

liable during the analyses. Most sulphides show an excess of sulphur around one atomic percent unit. This is probably a standard-related problem generated either from errors during the standard measurements or errors within the standard compound. The analyses of silver and allargentum have wt% sums beyond the accepted range. The reason might be that the standard was a sulphide, whereas the silver analysed is metallic, meaning that a small error in the standard is multiplied due to the higher content of the element in the mineral.

Many of the phases studied chemically showed small oxygen peaks, even where oxygen was unlikely to occur. For this reason much data has been sorted out. The oxidation of sulphides is slow and should not be the problem. Spectra of bornite, which shows a rapid and extensive oxidation, did not contain any abnormal oxygen peaks. The occurrence of the peak might be due to the programming; it might be a sulphur escape peak, the size of which was not properly recognized by the program. The software company have been notified, but no answer has been obtained.

The purpose of this study was to deliver a general description of the mineralization. The qualitative nature of some of the data should thus not be very problematic.

## 7.2 The mineralization

The data from the logging and the microscopy studies independently show that the mineralization mostly occurs as aggregates and networks and to a less extent as separate grains of ore minerals. The gradual increase in mineralization degree from the stratigraphical hanging wall towards the richest part and a decrease towards the foot wall can be seen in all three cores. It is most pronounced in DBH2992. However, the gradual increase is rather patchy with large aggregates occurring both near the part that is richest in ore and in more distal areas. This correlates well with the chemical analyses of the bulk of the ore, where the content of Fe and Cu increase in an undulating way.

The degree of mineralization is different in the three cores. The main core (DBH2992) is the richest one; the overlying core (DBH2993) is poorest, whereas the underlying core (DBH2955) is intermediate. Marble dominates the DBH2992 whereas half of DBH2993 was dominated by marble, and the other half with quartz-feldspar leptite.

Generally the samples studied are similar. However, the host rock influences the mineralization. If the host rock has a high amount of biotite or diopside, the bornite and chalcopyrite dominate among the ore minerals. Bornite is rare in the marble dominated host rocks. In the quartz-feldspar leptite, the mineralization is sparse. In leptite with higher biotite contents, ore minerals occur to a greater extent, but, e.g., tetrahedrite occurs in large amounts. Tetrahedrite is rare in other host rocks.

Differences in the ore mineral content are mostly related to the degree of mineralization and to the host rock. It is necessary to study more cores at different locations in the mineralization to test whether other parameters influence the ore-mineral assemblages.

## 7.3 The ore minerals and their distribution

All samples, rich or poor in ore minerals, contain chalcopyrite. Chalcopyrite is the main sulphide mineral in most samples, followed by cubanite. These two minerals mostly occur in aggregates. Sphalerite is common. Cubanite and sphalerite are commonly, and independently, intergrown with chalcopyrite. The textures observed could have formed from the unmixing of excess FeS or Zn in high temperature chalcopyrite (Ramdohr 1980). The matter of exsolution has long been debated and the textures could though have another origin.

Fe-Ni-Co minerals are commonly found in the sulphide aggregates. During logging of the cores, pyrrhotite was often identified. Pyrrhotite was probably mistaken for coarse-grained pentlandite. Pyrrhotite occurs mostly in the outer parts of the mineralization. It often has a flame texture, which might indicate formation at high temperatures (Ramdohr 1980). Further, according to Ramdohr (1980), pentlandite is often found as flames in pyrrhotite indicating a close relation between the two phases.

During the microscopical study, bornite was found together with chalcopyrite in a few samples. Macroscopically, the bornite content of the two reference cores was interpreted to be much higher than it really is. The explanation probably lies in a misidentification of oxidised chalcopyrite for bornite. Despite the fact that bornite occurs to a restricted extent in the thin sections, bornite could be an important ore mineral in the mineralization. This is based on the fact that e.g. samples DBH2955 77.60 m and DBH2993 114.40 m are rich in both chalcopyrite and bornite.

Valleriite, which is an alteration product of chalcopyrite (Hedin & Jansson 2007) often occurs in the aggregates. Valleriite contains Cu and it might be considered an ore mineral of importance. However, the amounts of Cu are much below the chalcopyrite content and are varying.

Some chalcopyrite grains, independently on location, are severely tarnished. The tarnish can be correlated with a content of silver. Chen et al. (1980) showed that chalcopyrite grains, which were in direct contact with silver tarnished quickly, leading to the formation of $Ag_2S$ on the surface of the grain.

The ore minerals are distributed in a rather constant way in the cores, even if the amounts vary. The common minerals are found in more or less all samples in a similar way. The rarer minerals mostly occur in the host rock. They generally vary more in distribution than the more common ore minerals. From the samples collected no strong zonation of the mineral distribution can be demonstrated. Mostly, the chalcopyrite varies in amounts. In the richest samples the high content of chalcopyrite result in other ore minerals appearing to

occur to a smaller extent, which probably is not correct. Due to the irregularity of the mineralization, no point-counting have been performed and thereby the ratios between different minerals are hard to estimate. Exceptions are sphalerite and molybdenite, which occur to a greater extent in the richer parts of the ore. It would be interesting to look into the way the distribution of all ore minerals changes over greater distances; at greater depths and in poorer mineralisation.

The minerals found during this study, the distribution, the chemical composition and variations are similar to those found in the Tunaberg Cu-Co mineralization (Dobbe 1994). Tunaberg is located in the southeastern parts of Bergslagen. The host rock of the mineralization is similar to that in Zinkgruvan and so are the ore minerals. In contrast to the Zinkgruvan deposit, the Cu-Co sulphide sequence of Tunaberg is situated stratigraphically above the Zn-Pb horizon. The number of different minerals found in the Cu-Co mineralization clearly exceeds that found in Zinkgruvan.

In this study, the number of ore minerals found, especially As- and Sb containing phases, increased steadily with time. The diversity was high in comparison to the restricted amount of samples. Further studies should probably result in even more minerals being identified. Nevertheless, the main minerals identified during the study are predictable in their distribution and should not vary very much, at least not in the richest parts of the mineralization.

## 7.4 Penalty elements

One purpose of the study is to investigate the whereabouts of the penalty giving elements As, Sb, Bi and Hg. The study shows that these elements mainly occur in minor and rare minerals. These minerals can, though, be situated inside chalcopyrite aggregates.

Arsenic mostly occurs in cobaltite. Cobaltite is found in almost every sample as grains situated either in the chalcopyrite aggregates or more commonly in the host rock. Other arsenic-containing minerals are arsenopyrite, safflorite and nickeline. Small amounts can be found in antimony-containing minerals. Most of the arsenic-containing minerals, excluding cobaltite, are mainly distributed as grains in the host rock and are not included in the chalcopyrite aggregates.

Most of the antimony occurs in breithauptite, which is found in almost every sample. In sphalerite-rich samples, the content of breithauptite is often increased. Commonly, breithauptite occurs as grains in the host rock but it also occur in the chalcopyrite aggregates. Gudmundite and costibite, which occur to a small extent, contain antimony. In addition, antimony is a major element in tetrahedrite, which occurs in the outer part of the ore zone. Small amounts of antimony occur in arsenide and sulph-arsenide minerals.

Due to the frequent small grain size, bismuth has been hard to identify during the microscopy study. Studies in the electron microscope show that metallic bismuth occurs as small grains in the host rock, in chalcopyrite, bornite and tetrahedrite. Though, the limits of the applied methods do not allow a complete exploration of the bismuth speciation. Large grains of metallic bismuth occur in one sample. Grains of parkerite, in which Bi is a constituent, have been found in samples having a rather high copper content. The grains are small and rare.

Small amounts of mercury are detected in silver filled fractures in the host rock and in bornite. The amounts are low, the fractures are rare and silver does not always contain mercury. The partly overlapping X-ray peaks of Ag and Hg lead to uncertainties, which hamper the analyses.

Uranium is included in an opaque phase occurring in the richest zone of the main core. Grains have been analysed in two samples and show different composition. The grains are possibly made up of several phases. The analyses are uncertain due to the closeness of the peaks of U and Ag. Large amounts of radiation-damaged biotite occur in the outer part of the reference core. The mineral inclusions in the biotite, probably zircon, are transparent and have a high relief.

## 7.5 Variations in chemical composition

The chemical composition of most minerals is rather constant. In the rare phases. this is, however, more uncertain. The Fe-Ni-Co-sulphides show the largest variation. Especially the ratios among Fe, Ni and Co vary and the elements replace each other due to their similar atomic size and outer electron configuration. In coarse-grained pentlandite, a chemical variation is indicated both within single grains and among the samples. This means that the reported compositions depend on which point in the grain that has been analysed. There is no clear stratigraphical zonation obtained from the spot analyses; more detailed studies including larger parts of the mineralization are needed for a conclusive answer to this question. However, there is a strong relation between grain size and cobalt content of pentlandite.

The composition of sphalerite and tetrahedrite varies, with Fe-rich and Fe-poor varieties. The Fe-poor varieties of sphalerite were mostly located in the outer parts of the mineralization, especially at the foot wall side. Sphalerite from the hanging wall side of the mineralization can be both Fe-poor and Fe-rich.

Tetrahedrite is only analysed from two samples and the number of analyses are thus limited. The tetrahedrite from the hanging wall is richer in Fe than the tetrahedrite of the foot wall side of the mineralization. Due to the limited amount of analyses, this observation should not be generalised. The samples, in which the tetrahedrite is found, are abnormal in their mineral composition. Further, the sample, in which the Fe-rich tetrahedrite is found is characterised by high Fe and low Co contents of the minerals. Instead of cobaltite, arsenopyrite is found and the safflorite is rich in Fe, compared to the Co-rich safflorite in another sample.

# 8 Conclusions

- Aggregates of mainly chalcopyrite in a marble host rock are characteristic for the mineralization of the Zinkgruvan Deposit. Discrete grains and disseminated ore minerals are common, but are of less importance.
- The degree of the mineralization increases from the stratigraphical hanging wall side of the mineralization, toward the richest parts, and then decreases toward the foot wall side.
- With increasing degree of mineralization, the volume of aggregates increases, leading to a decrease in the amount of discrete ore mineral grains.
- The increase in aggregate volume is gradual, but not even; large aggregates occur in samples both poor and rich in ore minerals.
- The main ore minerals are chalcopyrite and cubanite. Valleriite is generally located around these minerals and could be considered to belong to this group.
- Other common minerals are sphalerite, magnetite, coarse-grained pentlandite, fine-grained pentlandite, argentopentlandite and mackinawite. These minerals occur mainly in chalcopyrite aggregates.
- In the aggregates, sometimes cobaltite, breithauptite and galena occur.
- In the biotite and diopside rich host rock, bornite occurring together with chalcopyrite is an important ore mineral. Thus, relations exist between the host rock and the ore minerals found therein.
- Most ore minerals, except for Fe-Co-Ni sulphides can be found as discrete grains in the host rock. Intergrowths of As- and Sb-minerals also occur outside the aggregates.
- Minerals containing As and Sb are frequently found, Bi phases are commonly found and possibly occur to a greater extent than the analyses of the study have shown. Hg can be found in small amounts in silver filled fractures.
- The distribution of the minerals found in the mineralization is rather constant, independent of stratigraphic or altitude-related location. The increase in degree of mineralization is not accompanied by any change in the number of different minerals. The increase in grade is related to size and abundance of aggregates.
- Most minerals have a more or less constant chemical composition. The main exceptions are valleriite, sphalerite, cobalt containing pentlandite and tetrahedrite.

# 9 Acknowledgements

This study has been a great experience and has given me new knowledge in ore geology and I want to thank everyone who have helped me to reach my goals. Special thanks goes to my supervisor Anders Lindh for discussions, reviewing and technical support. Your commitment to the study has been inspiring and made the project even more interesting. Thanks goes also to Lars Malmström, my supervisor at Zinkgruvan, for the opportunity to work with this project. I also want to thank Stefan Sandberg, Sven-Olof Niklasson and Anja Hagerud at Zinkgruvan for support during sample collection, for providing me with illustrations, information and for discussions. In the initial stages of the study I was challenged by learning ore microscopy and I thank Per Nysten and Magnus Ripa at SGU, Uppsala, for providing the opportunity and essential instructions.

# 10 References

Allen, R.L., Lundström, I., Ripa, M., Simeonov, A. & Christofferson, H., 1996: Facies analysis of a 1.9 Ga, continental margin, back-arc, felsic caldera province with diverse Zn-Pb-Ag-(Cu-Au) sulfide and Fe oxide deposits, Bergslagen Region, Sweden. *Economic Geology 91*, 979–1008.

Anthony, J.W., Bideaux, R.A., Bladh, K.W. & Nichols, M.C., 1990: *Handbook of mineralogy. Vol.1, Elements, sulfides, sulfosalts.* Mineral Data Publishing, Tucson. 588 pp.

Bogdanova, S.V., Bibikova, E.V., 1993: The "Saamian" of the Belomorian Mobile Belt: new geochronological constraints. *Precambrian Research 64*, 131–152.

Chen, T.T., Dutrizac, J.E., Owens, D.R. & Laflamme, J.H.G., 1980: Accelerated tarnishing of some chalcopyrite and tennantite specimens. *The Canadian Mineralogist 18*, 173–180.

Dobbe, R., 1994: *The Geology and mineralizations of the Tunaberg area, se Bergslagen, Sweden*. Ph.D. Thesis, Vrije University of Amsterdam, Amsterdam, The Netherlands. 184 pp.

Evans, A.M., 1993: *Ore geology and industrial minerals: an introduction.* Blackwell Scientific Publications, Oxford. 389 pp.

Frietsch, R., 1982a: A model for the formation of the iron, manganese and sulphide ores of central Sweden. *Geologische Rundschau 71*, 206–212.

Frietsch, R., 1982b: Alkali metasomatism in the ore-bearing metavolcanics of central Sweden. *Sveriges Geologiska Undersökning, Serie C, Avhandlingar och Uppsatser 791*, 1–54.

Gaál, G & Gorbatschev, R., 1987: An outline of the Precambrian evolution of the Baltic Shield. *Precambrian Research 35*, 15–52.

Geijer, P., 1964: On the origin of the Falun type of sulfide mineralization. *Geologiska Föreningens i Stockholm Förhandlingar 86,* 3–27.

Gunnarsson, E. & Gunnarsson, M., 2007: *Zinkgruvan*

*Mining 1857-2007*, Zinkgruvan Mining AB and Bild & Kultur AB, Skyllberg. 197 pp.

Hedin, L-H. & Jansson, M., 2007: *Mineral i Sverige: en fälthandbok*. Förlags AB Björnen, Borlänge. 224 pp.

Hedström, P., Simeonov, A. & Malmström, L., 1989: The Zinkgruvan ore deposit, south-central Sweden; a Proterozoic, proximal Zn-Pb-Ag deposit in distal volcanic facies. *Economic Geology 84*, 1235–1261.

Hellingwerf, R.H., 1996: Regional and local hydrothermal alteration of Proterozoic metavolcanic footwall rocks of the Zinkgruvan Zn-Pb-Ag ore deposit, Central Sweden. *Neues Jahrbuch für Mineralogie. Monatshefte 11*, 491–518.

Henriques, Å., 1964: *Geology and ores of the Åmmeberg district (Zinkgruvan), Sweden.* Ph.D. Thesis, University of Stockholm, Stockholm, Sweden. 246 pp.

Hietanen, A., 1975: Generation of potassium-poor magmas in the northern Sierra Nevada and the Svecofennian of Finland. *Journal of Research of the U. S. Geological Survey 3*, 631–645.

Karis, L. & Wikström, A., 1991: *Beskrivning till kartblad Finspång NO,SO,NV,SV Af 165*, Sveriges geologiska undersökning. 216 pp

Kumpulainen, R.A., Mansfeld, J., Sundblad, K., Neymark, L. & Bergman, T., 1996: Stratigraphy, age, and Sm-Nd isotope systematics of the country rocks to Zn-Pb sulphide deposits, Åmmeberg District, Sweden. *Economic Geology 91*, 1009–1021.

Lahtinen, R., Korja, A. & Nironen, M., 2005: Paleoproterozoic tectonic evolution. *In* Lahtinen, M., Nurmi, P.A., Rämö, O.T. (eds), *Precambrian geology of Finland; key to the evolution of the Fennoscandian Shield*, 481–532. Elsevier B.V., Amsterdam.

Lundin Mining: March 2009 technical report, Zinkgruvan. http://www.lundinmining.com (090521).

Lundqvist, T., 1979: The Precambrian of Sweden. *Sveriges Geologiska Undersökning, Serie C, Avhandlingar och Uppsatser 768*, 1–87.

Lundström, I., 1987: Lateral variations in supracrustal geology within the Swedish part of the southern Svecokarelian volcanic belt. *Precambrian Research 35*, 353–365.

Magnusson, N.H., 1953: *Malmgeologi*. Jernkontoret, Stockholm, 439 pp.

Magnusson, N.H., Grip, E. & Frietsch, R., 1973: *Malm i Sverige. 1, Mellersta och södra Sverige*. Almqvist & Wiksell Förlag AB, Stockholm, 320 pp.

Nironen, M., 1997: The Svecofennian Orogen: A tectonic model. *Precambrian Research 86*, 21–44.

Oen, I.S., Helmers, H., Verschure, R.H. & Wiklander, U., 1982: Ore deposition in a Proterozoic incipient rift zone environment; a tentative model for the Filipstad-Grythyttan-Hjulsjoe region, Bergslagen, Sweden. *Geologische Rundschau 71*, 182–194.

Pirajno, F. & Bagas, L., 2008: A review of Australia's proterozoic mineral systems and genetic models. *Precambrian Research 166*, 54–80.

Plimer, I.R., 1986: Sediment-hosted exhalative Pb-Zn deposits; products of contrasting ensialic rifting. *Transactions of the Geological Society of South Africa 89*, 57–73.

Ramdohr, P., 1980: *The ore minerals and their intergrowths*. 2 ed. Pergamon press, Oxford. 1205 pp.

Sundblad, K., 1994: A genetic reinterpretation of the Falun and Åmmeberg ore types, Bergslagen, Sweden. *Mineralium Deposita 29*, 170–179.

Törnebohm, A.E., 1881: *Geologisk öfversigtskarta öfver mellersta Sveriges Bergslag 7*, Jernkontoret.

Walters, S.G., 1998: Broken hill-type deposits. *AGSO Journal of Australian Geology and Geophysics 17*, 229–237.

Wenk, H-R. & Bulakh, A.G., 2004: *Minerals: their constitution and origin*. Cambridge University Press, Cambridge, 646 pp.

Welin, E., Kähr, A.M. & Lundegårdh, P.H., 1980: Rb-Sr isotope systematic at amphibolites facies conditions, Uppsala Region, Eastern Sweden. *Precambrian Research 13*, 87–101.

Åberg, G. & Strömberg, A.G.B., 1984: Radiometric dating of Svecokarelian metarhyolites and prekinematic granitoids from Bergslagen, south central Sweden. *Geologiska Föreningens i Stockholm Förhandlingar 106*, 209–213.

## Appendix 1 - drill core mapping

Drill core logs of DBH2992 (A), DBH2955 (B) and DBH2993 (C) with an associative legend.

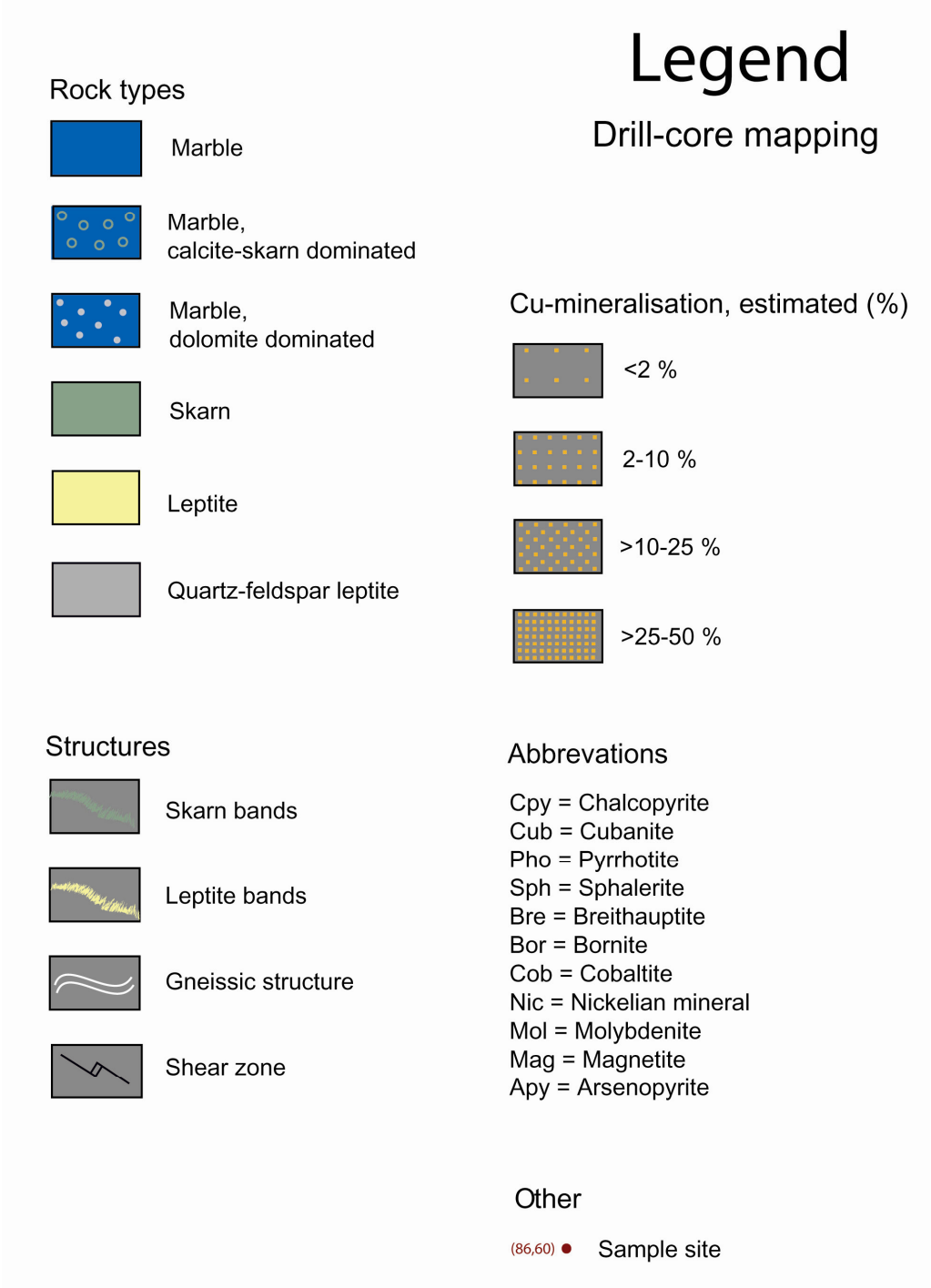

A

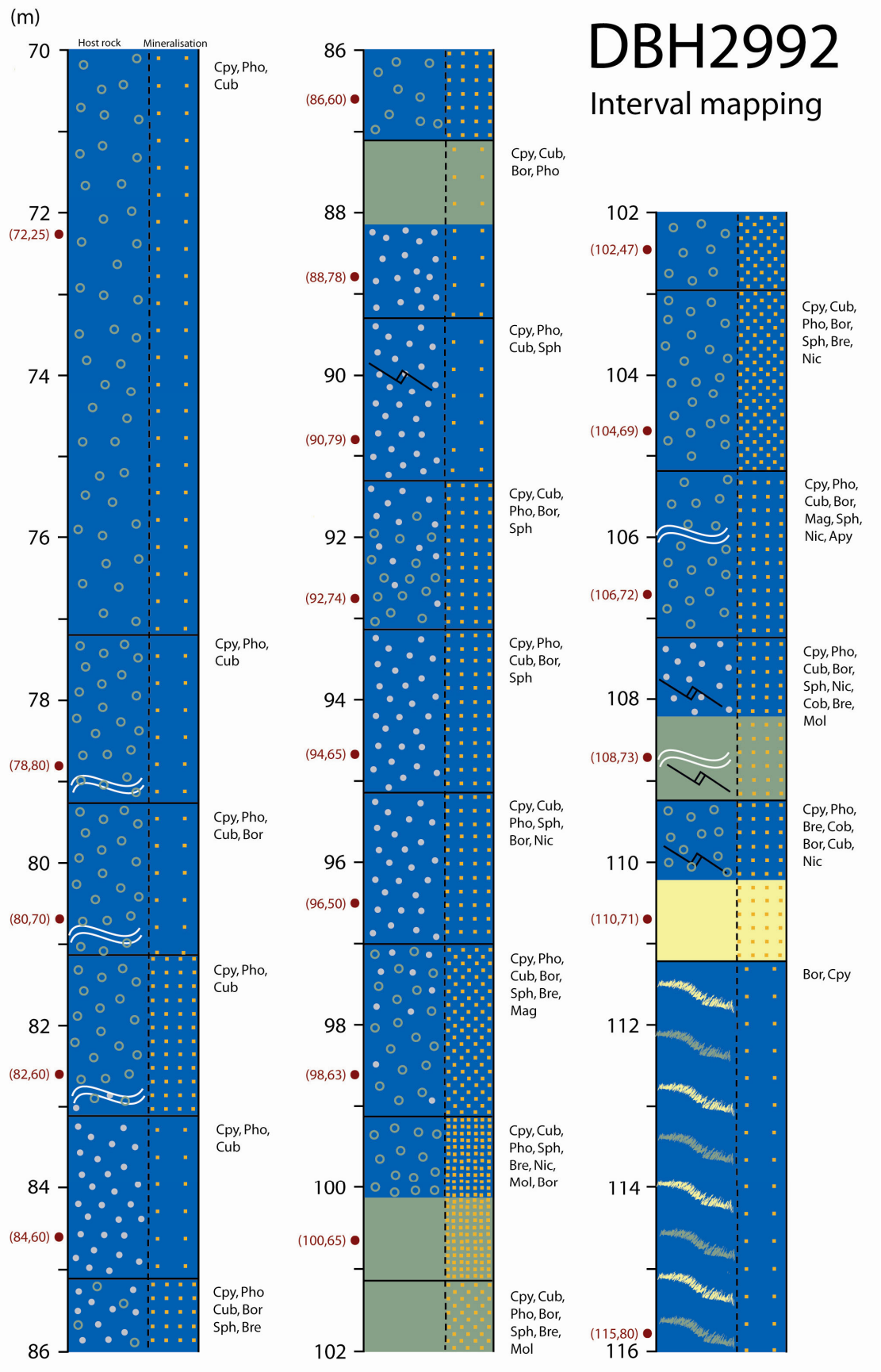
(m)
Host rock
Mineralisation
DBH2992
Interval mapping
70
72
74
76
78
80
82
84
86
(72,25)
(78,80)
(80,70)
(82,60)
(84,60)
Cpy, Pho, Cub
Cpy, Pho, Cub
Cpy, Pho, Cub, Bor
Cpy, Pho, Cub
Cpy, Pho, Cub
Cpy, Pho Cub, Bor Sph, Bre
86
88
90
92
94
96
98
100
102
(86,60)
(88,78)
(90,79)
(92,74)
(94,65)
(96,50)
(98,63)
(100,65)
Cpy, Cub, Bor, Pho
Cpy, Pho, Cub, Sph
Cpy, Cub, Pho, Bor, Sph
Cpy, Pho, Cub, Bor, Sph
Cpy, Cub, Pho, Sph, Bor, Nic
Cpy, Pho, Cub, Bor, Sph, Bre, Mag
Cpy, Cub, Pho, Sph, Bre, Nic, Mol, Bor
Cpy, Cub, Pho, Bor, Sph, Bre, Mol
102
104
106
108
110
112
114
116
(102,47)
(104,69)
(106,72)
(108,73)
(110,71)
(115,80)
Cpy, Cub, Pho, Bor, Sph, Bre, Nic
Cpy, Pho, Cub, Bor, Mag, Sph, Nic, Apy
Cpy, Pho, Cub, Bor, Sph, Nic, Cob, Bre, Mol
Cpy, Pho, Bre, Cob, Bor, Cub, Nic
Bor, Cpy

**B**

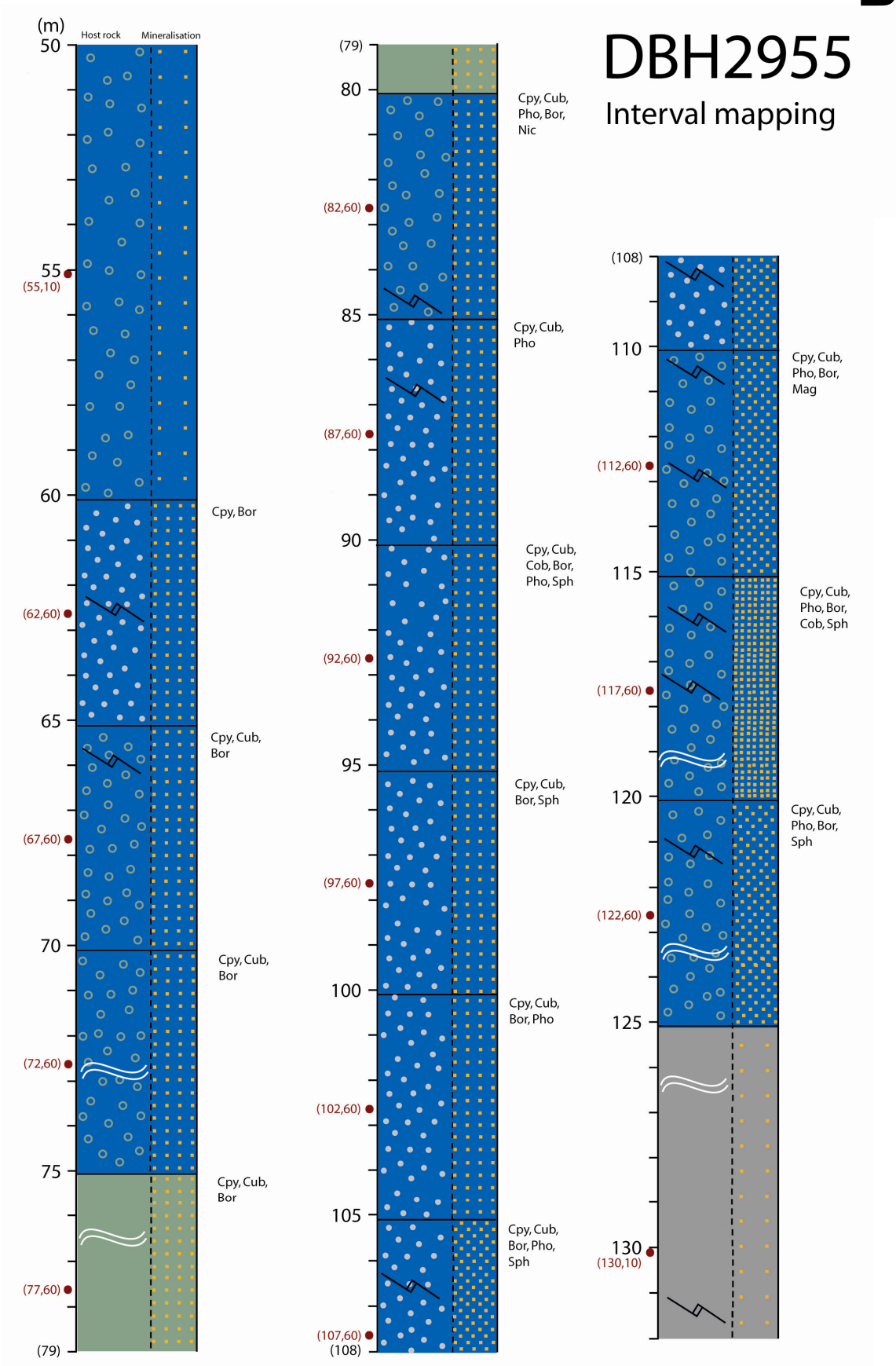
DBH2955
Interval mapping
(m)
Host rock
Mineralisation
50
55
(55,10)
60
(62,60)
65
(67,60)
70
(72,60)
75
(77,60)
(79)
Cpy, Bor
Cpy, Cub, Bor
Cpy, Cub, Bor
Cpy, Cub, Bor
(79)
80
(82,60)
85
(87,60)
90
(92,60)
95
(97,60)
100
(102,60)
105
(107,60)
(108)
Cpy, Cub, Pho, Bor, Nic
Cpy, Cub, Pho
Cpy, Cub, Cob, Bor, Pho, Sph
Cpy, Cub, Bor, Sph
Cpy, Cub, Bor, Pho
Cpy, Cub, Bor, Pho, Sph
(108)
110
(112,60)
115
(117,60)
120
(122,60)
125
130
(130,10)
Cpy, Cub, Pho, Bor, Mag
Cpy, Cub, Pho, Bor, Cob, Sph
Cpy, Cub, Pho, Bor, Sph

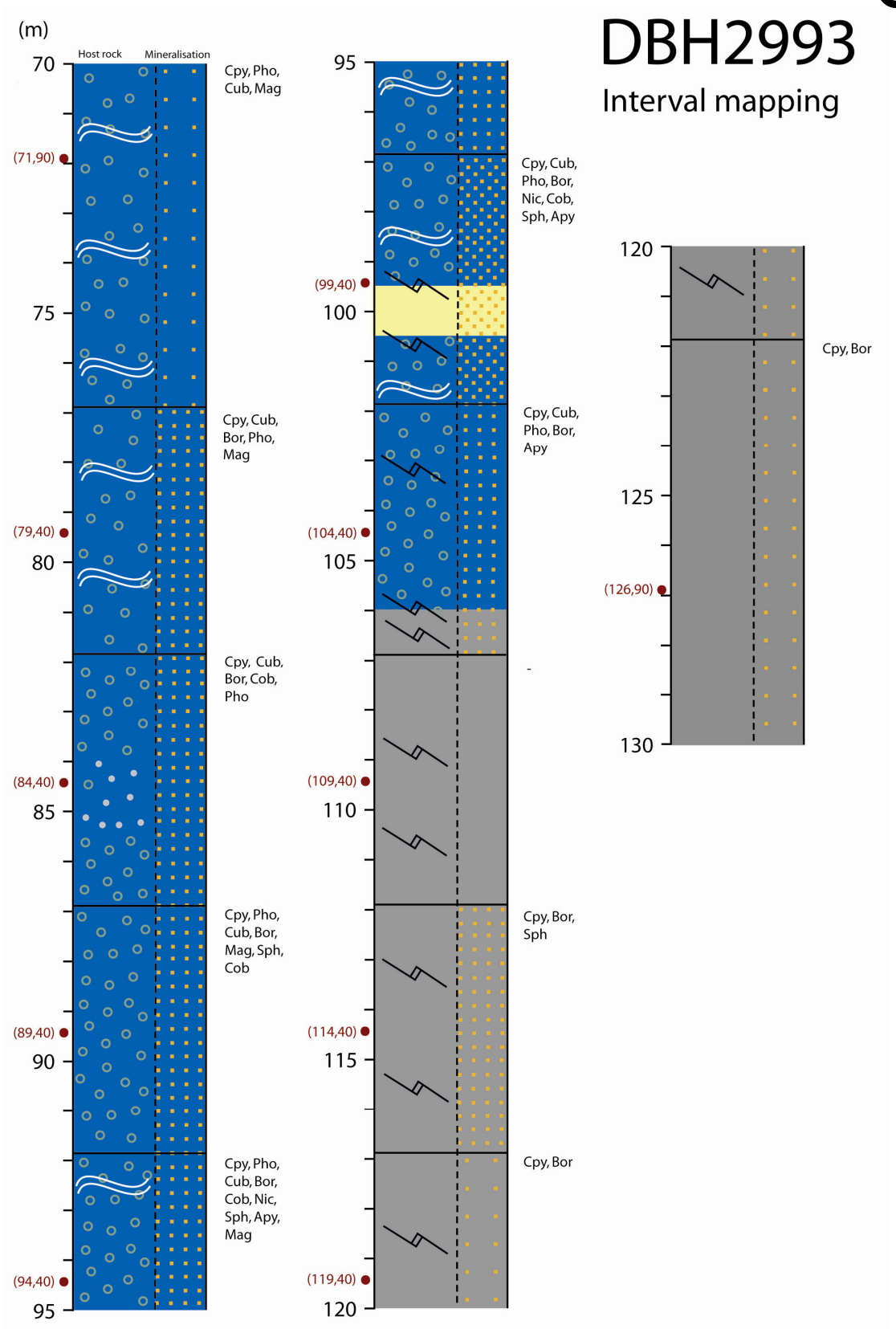
C
DBH2993
Interval mapping
(m)
Host rock
Mineralisation
70
(71,90)
75
(79,40)
80
(84,40)
85
(89,40)
90
(94,40)
95
Cpy, Pho, Cub, Mag
Cpy, Cub, Bor, Pho, Mag
Cpy, Cub, Bor, Cob, Pho
Cpy, Pho, Cub, Bor, Mag, Sph, Cob
Cpy, Pho, Cub, Bor, Cob, Nic, Sph, Apy, Mag
95
(99,40)
100
(104,40)
105
(109,40)
110
(114,40)
115
(119,40)
120
Cpy, Cub, Pho, Bor, Nic, Cob, Sph, Apy
Cpy, Cub, Pho, Bor, Apy
Cpy, Bor, Sph
Cpy, Bor
120
125
(126,90)
130
Cpy, Bor

# Appendix 2 – Table of the host rock minerals

*Table 1.* Non-opaque minerals observed during petrological microscopy. Carb= carbonates, Mica= light mica, Chl= chlorite, Serp= serpentine, Oliv= olivine, Diop= diopside, Qtz=quartz, Mcl= mircocline, Bio= biotite, Tita= titanite, Spin= spinel (pleonast).

| Core | Sample | Carb. | Mica | Chl. | Serp. | Oliv | Diop. | Qts | Mcl | Bio | Tita | Spin |
|---|---|---|---|---|---|---|---|---|---|---|---|---|
| DBH2992 | 72.25 | x | x | x | x | x | | | | | | |
| DBH2992 | 78.80 | x | x | x | x | x | | | | | | |
| DBH2992 | 80.70 | x | x | x | x | | | | | | | |
| DBH2992 | 82.60 | x | x | x | x | | | x | | | | |
| DBH2992 | 84.60 | x | x | x | x | | | | | | | x |
| DBH2992 | 86.80 | x | x | x | x | | | | | | | |
| DBH2992 | 88.78 | x | x | x | x | x | | | | | | x |
| DBH2992 | 90.79 | x | x | x | x | | | | | | | |
| DBH2992 | 92.74 | x | x | x | x | | | | | | | |
| DBH2992 | 94.65 | x | x | x | x | | | | | | | x |
| DBH2992 | 96.50 | x | x | x | x | | | | | | | |
| DBH2992 | 98.60 | x | x | x | x | | | | | | | |
| DBH2992 | 100.65 | x | x | x | x | | | | | | | |
| DBH2992 | 102.47 | x | x | x | | | x | | | x | | |
| DBH2992 | 104.69 | x | x | x | x | | | | | | | x |
| DBH2992 | 106.72 | x | x | x | x | | | | | | | x |
| DBH2992 | 108.73 | x | x | x | | | x | | | | | |
| DBH2992 | 110.71 | x | x | | | | x | x | | x | | |
| DBH2992 | 115.80 | x | x | | x | | x | | | | | |
| DBH2955 | 55.10 | x | x | | x | x | | | | | | x |
| DBH2955 | 62.60 | x | x | | | | x | x | x | x | | |
| DBH2955 | 67.60 | x | x | | x | x | x | x | | | | |
| DBH2955 | 72.60 | x | x | x | x | | | | | | | |
| DBH2955 | 77.60 | x | x | | x | x | x | | | | | |
| DBH2955 | 82.60 | x | x | x | x | | | | | | | x |
| DBH2955 | 87.60 | x | x | x | x | | | | | | | x |
| DBH2955 | 92.60 | x | x | x | x | | x | | | | | x |
| DBH2955 | 97.60 | x | x | x | x | x | | | | | | x |
| DBH2955 | 102.60 | x | x | x | x | | | | | | | x |
| DBH2955 | 107.60 | x | x | x | x | x | | | | | | |
| DBH2955 | 112.60 | x | x | x | x | x | | | | | | |
| DBH2955 | 117.60 | x | x | x | x | x | x | | | | | |
| DBH2955 | 122.60 | x | x | x | x | x | | | | | | |
| DBH2955 | 130.10 | | | | | x | | x | x | x | x | |
| DBH2993 | 71.90 | x | x | x | x | | | | | | | x |
| DBH2993 | 79.40 | x | x | x | x | | | | | | | |
| DBH2993 | 84.40 | x | x | x | x | x | | | | | | |
| DBH2993 | 89.40 | x | x | x | x | | | | | | | |
| DBH2993 | 94.40 | x | x | x | x | x | | | | | | |
| DBH2993 | 99.40 | x | x | x | x | | | | | | | |
| DBH2993 | 104.40 | x | | | | | x | x | x | x | | |
| DBH2993 | 109.40 | | | | | | x | x | x | x | x | |
| DBH2993 | 114.40 | | x | | | | x | x | x | x | x | |
| DBH2993 | 119.40 | | | | | | | x | x | x | x | |
| DBH2993 | 126.90 | | x | | | | | x | x | x | x | |

# Appendix 3 – Summary table of the opaque minerals

Summary of the opaque phases found during the study, further divided into general mineral groups.

| Name | Generalised stoechiometric formula | | Abbrevation |
|---|---|---|---|
| *Native elements* | | | |
| Bismuth | Bi | | Bis |
| Graphite | C | | Gra |
| Silver | Ag | | Sil |
| *Alloys* | | | |
| Allargentum | $(Ag_{1-x}Sb_x)$ | (x=0.09-0.16) | All |
| *Fe- and (Fe,Ni,Co)-Sulphides* | | | |
| Argentopentlandite | $Ag(Fe,Ni)_8S_8$ | | Ape |
| Cobalt-Pentlandite | $Co_9S_8$ | | C-pe |
| Pentlandite | $(Fe,Ni)_9S_8$ | (Fe≈Ni) | Pen |
| Pyrrhotite | $Fe_7S_8$ | | Pho |
| Mackinawite | $(Fe,Ni)_9S_8$ | (Fe>Ni) | Mac |
| *Cu-Sulphides* | | | |
| Bornite | $Cu_5FeS_4$ | | Bor |
| Chalcopyrite | $CuFeS_2$ | | Cpy |
| Chalcocite | $Cu_2S$ | | Cci |
| Cubanite | $CuFe_2S_3$ | | Cub |
| *Other sulphides* | | | |
| Galena | PbS | | Gal |
| Molybdenite | $MoS_2$ | | Mol |
| Sphalerite | (Zn,Fe)S | | Sph |
| Parkerite | $Ni_3(Bi,Pb)_2S_2$ | | Par |
| *Sulphantimonides* | | | |
| Costibite | CoSbS | | Cos |
| Gudmundite | FeSbS | | Gud |
| Tetrahedrite | $(Cu,Fe,Ag,Zn)_{12}Sb_4S_{13}$ | | The |
| *Sulpharsenides* | | | |
| Arsenopyrite | FeAsS – $(Fe_{0.90}Co_{0.10})AsS$ | | Apy |
| Cobaltite | CoAsS | | Cob |

| | | |
|---|---|---|
| *Antimonides* | | |
| Breithauptite | NiSb | Bre |
| *Arsenides* | | |
| Safflorite | $(Co,Fe, Ni)As_2$ | Saf |
| Maucherite | $Ni_{11}As_8$ | Mau |
| Nickeline | NiAs | Nic |
| *Oxides* | | |
| Magnetite | $Fe_3O_4$ | Mag |
| Valleriite | $4(Fe,Cu)S{\cdot}3(Mg,Al)(OH)_2$ | Val |

# Appendix 4 – Tables of the chemical composition of the ore minerals

Tables 1-30 show the chemical composition of the opaque phases, where the values of each element is in at%. ∑(at%) 99.9-100.1 = 100 %. When there is a lower value, there are small amounts of other elements, which are not normally part of the minerals. The limits of the total wt% of each analyse are 97-103 %. Analyses that do not reach these values are marked grey and should be regarded with caution.

*Table 1.* The chemical composition (at%) of chalcopyrite

| core | sample | S | Fe | Cu | ∑(at%) | ∑(wt%) |
|---|---|---|---|---|---|---|
| DBH2992 | 72,25:2:4 | 50.84 | 24.67 | 24.49 | 100.00 | 100.57 |
| DBH2992 | 80.70:1:1 | 50.42 | 25.15 | 24.43 | 100.00 | 98.28 |
| DBH2992 | 82.60:2 | 50.92 | 24.46 | 24.62 | 100.00 | 98.81 |
| DBH2992 | 92.74:1:4 | 51.27 | 24.38 | 24.35 | 100.00 | 99.79 |
| DBH2992 | 102.47:2 | 50.69 | 24.79 | 24.52 | 100.00 | 102.02 |
| DBH2992 | 108.73:1 | 50.66 | 24.71 | 24.63 | 100.00 | 98.44 |
| DBH2992 | 110.71:1 | 50.70 | 24.50 | 24.80 | 100.00 | 99.59 |
| DBH2955 | 92.60:2 | 51.33 | 24.00 | 24.67 | 100.00 | 97.42 |
| DBH2955 | 117.60:3 | 50.75 | 24.72 | 24.53 | 100.00 | 99.92 |
| DBH2993 | 71.90:4 | 51.18 | 24.39 | 24.43 | 100.00 | 97.59 |
| DBH2993 | 94.40:2 | 50.89 | 24.64 | 24.47 | 100.00 | 100.03 |
| DBH2993 | 114.40:1 | 51.05 | 24.36 | 24.59 | 100.00 | 97.52 |
| mean value (at%) | | 50.89 | 24.56 | 24.54 | | |
| minimum (at%) | | 50.42 | 24.00 | 24.35 | | |
| maximum (at%) | | 51.33 | 25.15 | 24.80 | | |
| Weight% sigma (±) | | 0.19 | 0.26 | 0.41 | | |

*Table 2*. The chemical composition (at%) of chalcopyrite with silver

| core | sample | S | Fe | Cu | Ag | ∑(at%) | ∑(wt%) |
|---|---|---|---|---|---|---|---|
| DBH2992 | 110.71:11 | 50.88 | 24.40 | 24.39 | 0.33 | 100.00 | 99.61 |
| DBH2955 | 117.60:3 | 50.49 | 24.67 | 24.55 | 0.29 | 100.00 | 95.09 |
| DBH2955 | 117.60:3 | 50.29 | 24.85 | 24.54 | 0.33 | 100.01 | 95.55 |
| DBH2955 | 117.60:3 | 50.77 | 24.40 | 24.53 | 0.29 | 99.99 | 100.36 |
| DBH2955 | 117.60:5 | 51.00 | 24.26 | 24.42 | 0.32 | 100.00 | 100.56 |
| DBH2955 | 117.60:5 | 50.68 | 24.49 | 24.51 | 0.33 | 100.01 | 99.73 |
| DBH2955 | 117.60:5 | 45.88 | 23.84 | 22.99 | 7.28 | 99.99 | 93.99 |
| DBH2955 | 117.60:5 | 50.06 | 23.82 | 23.35 | 2.77 | 100.00 | 99.02 |
| DBH2955 | 117.60:7 | 49.74 | 24.85 | 23.93 | 1.48 | 100.00 | 100.53 |
| DBH2955 | 117.60:7 | 49.70 | 24.28 | 23.16 | 2.86 | 100.00 | 97.90 |
| DBH2955 | 117.60:7 | 49.86 | 24.14 | 23.49 | 2.52 | 100.01 | 98.77 |
| mean value (at%) | | 49.94 | 24.36 | 23.99 | 1.71 | | |
| minimum (at%) | | 51.00 | 24.14 | 22.99 | 0.29 | | |
| maximum (at%) | | 50.06 | 24.85 | 24.55 | 7.28 | | |
| Weight% sigma (±) | | 0.19 | 0.27 | 0.42 | 0.15 | | |

*Table 3.* The chemical composition (at%) of cubanite

| core | sample | S | Fe | Cu | ∑(at%) | ∑(wt%) |
|---|---|---|---|---|---|---|
| DBH2992 | 92.74:2:1 | 50.85 | 32.63 | 16.53 | 100.01 | 98.81 |
| DBH2992 | 102.47:2 | 50.82 | 32.98 | 16.20 | 100.00 | 100.96 |
| DBH2992 | 102.47:5 | 50.77 | 32.53 | 16.70 | 100.00 | 100.89 |
| DBH2992 | 102.47:7 | 50.81 | 32.85 | 16.34 | 100.00 | 99.89 |
| DBH2955 | 92.60:5 | 50.78 | 32.53 | 16.69 | 100.00 | 99.20 |
| DBH2955 | 92.60:7 | 51.35 | 32.23 | 16.42 | 100.00 | 98.72 |

| | | | | | | |
|---|---|---|---|---|---|---|
| DBH2993 | 71.90:3 | 51.11 | 32.57 | 16.32 | 100.00 | 97.25 |
| DBH2993 | 71.90:7 | 50.89 | 32.49 | 16.62 | 100.00 | 98.42 |
| DBH2993 | 71.90:8 | 50.96 | 32.64 | 16.40 | 100.00 | 97.92 |
| DBH2993 | 71.90:8 | 51.38 | 32.35 | 16.27 | 100.00 | 98.76 |
| DBH2993 | 71.90:9 | 51.04 | 32.52 | 16.44 | 100.00 | 97.70 |
| mean value (at%) | | 50.98 | 32.57 | 16.45 | | |
| minimum (at%) | | 50.77 | 32.23 | 16.20 | | |
| maximum (at%) | | 51.38 | 32.98 | 16.70 | | |
| Weight% sigma (±) | | 0.19 | 0.31 | 0.36 | | |

*Table 4.* The chemical composition (at%) of bornite

| core | Sample | S | Fe | Cu | ∑(at%) | ∑(wt%) |
|---|---|---|---|---|---|---|
| DBH2992 | 110.71:1 | 41.20 | 9.98 | 48.82 | 100.00 | 99.65 |
| DBH2992 | 110.71:1 | 40.60 | 10.08 | 49.32 | 100.00 | 97.96 |
| DBH2992 | 110.71:5 | 40.82 | 10.16 | 48.25 | 99.23 | 100.40 |
| DBH2992 | 110.71:7 | 41.11 | 9.56 | 48.69 | 99.36 | 99.52 |
| DBH2992 | 110.71:8 | 41.75 | 10.11 | 48.14 | 100.00 | 100.52 |
| DBH2992 | 110.71:11 | 40.85 | 9.95 | 49.20 | 100.00 | 100.01 |
| DBH2955 | 62.60:8 | 41.56 | 9.07 | 49.37 | 100.00 | 97.87 |
| DBH2993 | 114.40:1 | 40.77 | 9.89 | 49.34 | 100.00 | 99.02 |
| DBH2993 | 114.40:1 | 40.93 | 10.13 | 48.65 | 99.71 | 98.76 |
| DBH2993 | 114.40:3 | 41.11 | 9.98 | 48.91 | 100.00 | 98.75 |
| DBH2993 | 114.40:3 | 40.70 | 9.98 | 49.32 | 100.00 | 97.41 |
| DBH2993 | 114.40:4 | 41.39 | 9.58 | 49.03 | 100.00 | 99.63 |
| DBH2993 | 114.40:4 | 41.25 | 9.78 | 48.97 | 100.00 | 98.90 |
| DBH2993 | 114.40:6 | 41.27 | 10.33 | 48.40 | 100.00 | 99.90 |
| mean value (at%) | | 41.09 | 9.90 | 48.89 | | |
| minimum (at%) | | 40.60 | 9.07 | 48.14 | | |
| maximum (at%) | | 41.75 | 10.33 | 49.37 | | |
| Weight% sigma (±) | | 0.17 | 0.18 | 0.53 | | |

*Table 5*. The chemical composition (at%) of sphalerite

| core | sample | S | Zn | Fe | Mn | ∑(at%) | ∑(wt%) |
|---|---|---|---|---|---|---|---|
| DBH2992 | 72.25:3 | 50.70 | 46.36 | 2.95 | 0.00 | 100.01 | 101.40 |
| DBH2992 | 72.25:3 | 50.42 | 47.87 | 1.71 | 0.00 | 100.00 | 99.08 |
| DBH2992 | 72.25:4 | 50.64 | 47.25 | 2.11 | 0.00 | 100.00 | 101.72 |
| DBH2992 | 80.70:1:5 | 50.58 | 42.42 | 5.95 | 1.06 | 100.01 | 97.02 |
| DBH2992 | 80.70:1:7 | 50.69 | 42.72 | 5.68 | 0.91 | 100.00 | 98.21 |
| DBH2992 | 80.70:3:7 | 51.30 | 40.54 | 6.18 | 1.09 | 99.11 | 99.66 |
| DBH2992 | 82.60:5 | 50.75 | 43.06 | 5.85 | 0.35 | 100.01 | 98.74 |
| DBH2992 | 92.74:3 | 51.28 | 43.20 | 5.52 | 0.00 | 100.00 | 97.61 |
| DBH2992 | 102.47:4 | 50.60 | 42.71 | 5.38 | 0.42 | 99.11 | 101.03 |
| DBH2992 | 102.47:4 | 50.47 | 43.10 | 5.25 | 0.34 | 99.16 | 99.31 |
| DBH2992 | 102.47:5 | 50.76 | 42.27 | 6.13 | 0.45 | 99.61 | 100.27 |
| DBH2992 | 102.47:9 | 50.07 | 43.00 | 5.31 | 0.00 | 98.38 | 101.65 |
| DBH2992 | 108.73:6 | 51.03 | 41.98 | 5.08 | 0.00 | 98.09 | 97.05 |
| DBH2992 | 110.71:8 | 51.17 | 47.21 | 1.62 | 0.00 | 100.00 | 102.35 |
| DBH2955 | 92.60:2 | 51.55 | 43.97 | 4.47 | 0.00 | 99.99 | 98.11 |
| DBH2955 | 92.60:2 | 50.96 | 43.42 | 3.96 | 0.00 | 98.34 | 99.22 |
| DBH2955 | 92.60:3 | 51.53 | 41.84 | 5.04 | 0.00 | 98.41 | 99.14 |
| DBH2955 | 92.60:3 | 51.05 | 41.18 | 5.98 | 0.31 | 98.52 | 100.33 |
| DBH2955 | 92.60:3 | 51.39 | 43.16 | 4.66 | 0.00 | 99.21 | 100.85 |
| DBH2955 | 92.60:4 | 49.39 | 43.78 | 5.90 | 0.00 | 99.07 | 98.46 |
| DBH2955 | 92.60:4 | 50.57 | 43.12 | 5.22 | 0.00 | 98.91 | 99.88 |
| DBH2955 | 92.60:8 | 51.04 | 43.01 | 5.69 | 0.26 | 100.00 | 99.94 |

| | | | | | | | |
|---|---|---|---|---|---|---|---|
| DBH2955 | 92.60:8 | 51.12 | 43.12 | 5.76 | 0.00 | 100.00 | 100.18 |
| DBH2955 | 92.60:8 | 51.32 | 43.17 | 5.50 | 0.00 | 99.99 | 99.87 |
| DBH2955 | 92.60:8 | 51.48 | 42.53 | 5.72 | 0.27 | 100.00 | 100.95 |
| DBH2955 | 117.60:6 | 50.45 | 45.72 | 3.84 | 0.00 | 100.01 | 100.96 |
| DBH2955 | 117.60:6 | 50.48 | 45.82 | 3.71 | 0.00 | 100.01 | 101.19 |
| DBH2955 | 117.60:6 | 50.37 | 46.05 | 3.59 | 0.00 | 100.01 | 101.00 |
| DBH2955 | 117.60:6 | 50.31 | 46.03 | 3.66 | 0.00 | 100.00 | 101.36 |
| DBH2955 | 117.60:9 | 50.43 | 44.35 | 5.22 | 0.00 | 100.00 | 101.86 |
| DBH2955 | 117.60:9 | 50.62 | 44.25 | 5.13 | 0.00 | 100.00 | 102.18 |
| DBH2955 | 117.60:9 | 50.80 | 43.87 | 5.32 | 0.00 | 99.99 | 100.54 |
| DBH2955 | 117.60:9 | 50.41 | 43.99 | 5.60 | 0.00 | 100.00 | 100.91 |
| DBH2993 | 71.90:3 | 51.42 | 40.90 | 7.11 | 0.23 | 99.66 | 99.09 |
| DBH2993 | 71.90:4 | 51.58 | 41.42 | 6.62 | 0.00 | 99.62 | 98.55 |
| DBH2993 | 71.90:5 | 50.64 | 40.70 | 8.67 | 0.00 | 100.01 | 98.73 |
| DBH2993 | 71.90:5 | 51.17 | 43.78 | 5.05 | 0.00 | 100.00 | 97.75 |
| DBH2993 | 94.40:1 | 50.75 | 41.13 | 5.80 | 0.43 | 98.11 | 98.21 |
| DBH2993 | 94.40:1 | 50.53 | 42.39 | 5.72 | 0.45 | 99.09 | 99.23 |
| DBH2993 | 94.40:3 | 51.27 | 41.56 | 5.92 | 1.07 | 99.82 | 99.30 |
| DBH2993 | 94.40:3 | 50.74 | 40.94 | 6.58 | 1.05 | 99.31 | 100.14 |
| DBH2993 | 94.40:4 | 51.12 | 41.95 | 6.45 | 0.48 | 100.00 | 99.15 |
| DBH2993 | 94.40:6 | 51.07 | 42.61 | 5.99 | 0.34 | 100.01 | 100.75 |
| DBH2993 | 94.40:6 | 50.76 | 43.57 | 5.38 | 0.30 | 100.01 | 100.50 |
| DBH2993 | 94.40:6 | 51.23 | 42.45 | 6.01 | 0.30 | 99.99 | 100.55 |
| DBH2993 | 94.40:6 | 50.40 | 42.85 | 6.42 | 0.33 | 100.00 | 101.55 |
| DBH2993 | 114.40:3 | 50.84 | 48.34 | 0.64 | 0.00 | 99.82 | 99.51 |
| DBH2993 | 114.40:3 | 50.82 | 48.35 | 0.51 | 0.00 | 99.68 | 99.66 |
| DBH2993 | 114.40:3 | 50.53 | 48.90 | 0.58 | 0.00 | 100.01 | 100.07 |
| DBH2993 | 114.40:3 | 50.41 | 48.77 | 0.59 | 0.00 | 99.77 | 99.69 |
| mean Fe-low (at%) | | 50.62 | 46.93 | 2.27 | 0.00 | | |
| mean Fe-high (at%) | | 50.89 | 42.61 | 5.76 | 0.28 | | |
| minimum (at%) | | 49.39 | 40.54 | 0.51 | 0.00 | | |
| maximum (at%) | | 51.58 | 48.90 | 8.67 | 1.09 | | |
| Weight% sigma (±) | | 0.19 | 0.15 | 0.59 | 0.09 | | |

*Table 6.* The chemical composition (at%) of iron oxide

| core | sample | O | Fe | ∑(at%) | ∑(wt%) |
|---|---|---|---|---|---|
| DBH2992 | 80.70:1:1 | 58.25 | 41.75 | 100.00 | 98.00 |
| DBH2992 | 80.70:1:1 | 58.62 | 41.38 | 100.00 | 99.36 |
| DBH2992 | 80.70:1:7 | 59.47 | 40.53 | 100.00 | 99.16 |
| DBH2992 | 80.70:3:4 | 62.40 | 37.60 | 100.00 | 102.46 |
| DBH2992 | 80.70:3:6 | 57.76 | 42.24 | 100.00 | 97.71 |
| DBH2992 | 82.60:3 | 59.75 | 40.25 | 100.00 | 99.45 |
| DBH2992 | 82.60:3 | 60.06 | 39.94 | 100.00 | 101.75 |
| DBH2992 | 82.60:3 | 59.07 | 40.93 | 100.00 | 100.36 |
| DBH2992 | 82.60:6 | 59.05 | 40.95 | 100.00 | 99.26 |
| DBH2993 | 71.90:6 | 60.43 | 39.57 | 100.00 | 99.33 |
| DBH2993 | 71.90:7 | 59.85 | 40.15 | 100.00 | 99.39 |
| mean value (at%) | | 59.52 | 40.48 | | |
| minimum (at%) | | 57.76 | 37.60 | | |
| maximum (at%) | | 62.40 | 42.24 | | |
| Weight% sigma (±) | | 0.28 | 0.41 | | |

*Table 7.* The chemical composition (at%) of valleriite

| Core | Sample | O | Mg | Al | Si | S | Fe | Cu | Mn | ∑(at%) | ∑(wt%) |
|---|---|---|---|---|---|---|---|---|---|---|---|
| DBH2992 | 72.25:2:2 | 45.72 | 9.93 | 0.00 | 1.59 | 18.64 | 15.85 | 8.28 | 0.00 | 100.01 | 98.22 |
| DBH2992 | 72.25:2:2 | 45.17 | 12.40 | 0.00 | 2.40 | 18.52 | 13.94 | 7.30 | 0.27 | 100.00 | 99.95 |
| DBH2992 | 75.25:2:4 | 39.66 | 11.82 | 0.00 | 0.00 | 22.63 | 16.11 | 9.54 | 0.23 | 99.99 | 103.11 |
| DBH2992 | 80.70:1:9 | 59.38 | 19.58 | 0.00 | 12.37 | 3.63 | 3.33 | 1.40 | 0.11 | 99.80 | 85.32 |
| DBH2992 | 80.70:1:9 | 61.90 | 20.56 | 0.00 | 13.35 | 1.56 | 1.73 | 0.60 | 0.09 | 99.79 | 88.47 |
| DBH2992 | 80.70:1:9 | 48.00 | 15.99 | 0.00 | 6.18 | 14.03 | 10.05 | 5.75 | 0.00 | 100.00 | 90.77 |
| DBH2992 | 80.70:1:9 | 62.49 | 20.19 | 0.00 | 12.94 | 1.76 | 1.79 | 0.69 | 0.00 | 99.86 | 87.91 |
| DBH2992 | 80.70:1:9 | 61.44 | 20.86 | 0.00 | 13.59 | 1.63 | 1.73 | 0.66 | 0.00 | 99.91 | 89.05 |
| DBH2992 | 80.70:1:9 | 57.43 | 18.66 | 0.00 | 8.79 | 6.91 | 5.33 | 2.60 | 0.12 | 99.84 | 103.41 |
| DBH2992 | 80.70:1:9 | 44.38 | 15.04 | 0.00 | 3.47 | 17.21 | 12.47 | 7.43 | 0.00 | 100.00 | 94.24 |
| DBH2992 | 80.70:1:8 | 44.15 | 15.18 | 0.00 | 3.70 | 17.22 | 12.47 | 7.27 | 0.00 | 99.99 | 89.50 |
| DBH2992 | 80.70:1:8 | 57.82 | 21.56 | 0.00 | 14.30 | 2.62 | 2.48 | 1.22 | 0.00 | 100.00 | 85.37 |
| DBH2992 | 80.70:1:8 | 60.84 | 20.07 | 0.00 | 12.38 | 2.69 | 2.59 | 1.29 | 0.00 | 99.86 | 93.23 |
| DBH2992 | 82.60:2 | 37.39 | 10.89 | 0.07 | 0.00 | 23.81 | 17.52 | 9.81 | 0.51 | 100.00 | 98.71 |
| DBH2992 | 82.60:2 | 36.35 | 10.68 | 0.09 | 0.12 | 23.84 | 18.18 | 10.19 | 0.56 | 100.01 | 97.49 |
| DBH2992 | 82.60:2 | 36.26 | 10.81 | 0.15 | 0.00 | 24.02 | 18.09 | 10.05 | 0.63 | 100.01 | 98.75 |
| DBH2992 | 82.60:2 | 37.61 | 10.23 | 0.05 | 0.00 | 23.28 | 18.31 | 9.86 | 0.66 | 100.00 | 99.42 |
| DBH2992 | 82.60:2 | 37.15 | 11.07 | 0.09 | 0.00 | 23.38 | 17.82 | 9.85 | 0.64 | 100.00 | 98.66 |
| DBH2992 | 82.60:4 | 37.66 | 12.16 | 0.19 | 0.00 | 23.23 | 16.67 | 9.63 | 0.46 | 100.00 | 99.49 |
| DBH2992 | 82.60:4 | 37.46 | 11.87 | 0.11 | 0.00 | 23.61 | 16.83 | 9.71 | 0.40 | 99.99 | 97.99 |
| DBH2992 | 82.60:4 | 38.04 | 12.36 | 0.18 | 0.00 | 23.06 | 16.35 | 9.60 | 0.41 | 100.00 | 100.64 |
| DBH2992 | 82.60:6 | 39.58 | 12.79 | 0.00 | 0.00 | 22.21 | 15.99 | 9.43 | 0.00 | 100.00 | 100.63 |
| DBH2992 | 82.60:6 | 38.06 | 12.74 | 0.00 | 0.00 | 22.91 | 16.52 | 9.78 | 0.00 | 100.01 | 98.58 |
| DBH2992 | 82.60:6 | 39.57 | 12.54 | 0.00 | 0.00 | 22.44 | 16.07 | 9.38 | 0.00 | 100.00 | 100.34 |
| DBH2992 | 82.60:6 | 40.80 | 12.73 | 0.00 | 0.00 | 22.01 | 15.75 | 8.71 | 0.00 | 100.00 | 102.75 |
| DBH2992 | 82.60:6 | 37.63 | 12.84 | 0.15 | 0.39 | 22.67 | 16.89 | 9.42 | 0.00 | 99.99 | 98.51 |
| DBH2993 | 71.90:4 | 38.48 | 10.01 | 0.87 | 0.12 | 22.84 | 17.79 | 9.65 | 0.26 | 100.02 | 97.88 |
| DBH2993 | 71.90:4 | 39.93 | 10.67 | 2.42 | 0.63 | 22.02 | 15.03 | 9.30 | 0.00 | 100.00 | 98.66 |
| mean S low (at%) | | 60.19 | 20.21 | 0.00 | 12.53 | 2.97 | 2.71 | 1.21 | 0.05 | | |
| mean S high (at%) | | 39.95 | 12.13 | 0.21 | 0.89 | 21.60 | 15.94 | 9.04 | 0.24 | | |
| minimum (at%) | | 36.26 | 9.93 | 0.00 | 0.00 | 1.56 | 1.73 | 0.60 | 0.00 | | |
| maximum (at%) | | 62.49 | 21.56 | 2.42 | 14.30 | 24.02 | 18.31 | 10.19 | 0.66 | | |
| Weight% sigma (±) | | 0.33 | 0.14 | 0.06 | - | 0.17 | 0.10 | 0.29 | 0.35 | | |

*Table 8.* The chemical composition (at%) of fine-grained pentlandite

| Core | Sample | S | Fe | Co | Ni | ∑(at%) | ∑(wt%) |
|---|---|---|---|---|---|---|---|
| DBH2992 | 80.70:1:1 | 47.76 | 24.49 | 4.07 | 21.73 | 98.05 | 98.92 |
| DBH2992 | 80.70:1:1 | 47.32 | 24.96 | 3.95 | 22.43 | 98.66 | 99.96 |
| DBH2992 | 92.74:4 | 48.35 | 21.60 | 10.62 | 19.43 | 100.00 | 100.26 |
| DBH2992 | 92.74:4 | 48.43 | 22.39 | 9.51 | 19.68 | 100.01 | 99.47 |
| DBH2992 | 92.74:4 | 48.36 | 21.82 | 10.09 | 19.73 | 100.00 | 99.60 |
| DBH2992 | 92.74:2:5 | 48.33 | 22.51 | 9.16 | 20.00 | 100.00 | 99.67 |
| DBH2992 | 92.74:2:5 | 48.40 | 21.81 | 9.72 | 20.07 | 100.00 | 98.83 |
| DBH2992 | 92.74:2:5 | 48.11 | 21.49 | 10.36 | 20.05 | 100.01 | 98.31 |
| DBH2992 | 92.74:2:6 | 48.27 | 22.88 | 9.06 | 19.79 | 100.00 | 97.61 |
| DBH2992 | 92.74:2:7 | 48.28 | 22.98 | 9.04 | 19.45 | 99.75 | 97.45 |
| DBH2992 | 92.74:2:7 | 47.84 | 22.73 | 8.83 | 19.99 | 99.39 | 98.16 |
| DBH2992 | 92.74:2:7 | 47.98 | 22.33 | 9.37 | 19.96 | 99.64 | 97.73 |
| DBH2992 | 92.74:2:7 | 48.27 | 22.59 | 9.06 | 19.60 | 99.52 | 97.76 |
| DBH2992 | 102.47:8 | 47.87 | 22.79 | 7.98 | 21.36 | 100.00 | 100.97 |
| DBH2992 | 102.47:8 | 47.74 | 23.56 | 7.77 | 20.93 | 100.00 | 101.44 |
| DBH2992 | 102.47:8 | 47.45 | 23.24 | 8.26 | 21.04 | 99.99 | 101.73 |
| DBH2955 | 92.60:5 | 48.00 | 20.54 | 11.08 | 20.38 | 100.00 | 99.79 |
| DBH2955 | 92.60:5 | 48.01 | 20.15 | 11.55 | 20.29 | 100.00 | 99.53 |

| | | | | | | | |
|---|---|---|---|---|---|---|---|
| DBH2955 | 92.60:5 | 48.32 | 21.66 | 9.96 | 20.05 | 99.99 | 97.71 |
| DBH2955 | 92.60:5 | 48.55 | 20.27 | 11.40 | 19.78 | 100.00 | 97.43 |
| DBH2955 | 92.60:5 | 48.18 | 22.19 | 9.74 | 18.58 | 98.69 | 99.54 |
| DBH2955 | 92.60:5 | 48.27 | 20.37 | 10.72 | 19.86 | 99.22 | 99.43 |
| DBH2955 | 92.60:6 | 47.55 | 22.51 | 7.72 | 22.22 | 100.00 | 101.44 |
| DBH2955 | 92.60:6 | 47.69 | 22.78 | 7.37 | 22.15 | 99.99 | 100.55 |
| DBH2955 | 92.60:6 | 48.17 | 23.19 | 6.65 | 20.65 | 98.66 | 101.64 |
| DBH2955 | 92.60:6 | 47.74 | 22.95 | 6.98 | 21.90 | 99.57 | 101.17 |
| DBH2955 | 117.60:5 | 48.62 | 26.34 | 2.53 | 22.50 | 99.99 | 99.66 |
| DBH2955 | 117.60:5 | 48.37 | 26.34 | 2.18 | 23.11 | 100.00 | 98.87 |
| DBH2955 | 117.60:5 | 47.79 | 25.33 | 2.88 | 24.00 | 100.00 | 101.02 |
| DBH2955 | 117.60:9 | 47.91 | 20.20 | 12.09 | 19.79 | 99.99 | 100.37 |
| DBH2955 | 117.60:9 | 48.33 | 21.61 | 10.29 | 19.77 | 100.00 | 99.13 |
| DBH2955 | 117.60:9 | 47.79 | 21.06 | 11.38 | 19.78 | 100.01 | 99.85 |
| DBH2993 | 94.40:5 | 47.72 | 18.76 | 14.23 | 19.28 | 99.99 | 100.20 |
| DBH2993 | 94.40:5 | 47.74 | 19.60 | 13.23 | 19.43 | 100.00 | 98.62 |
| DBH2993 | 94.40:5 | 47.49 | 19.81 | 12.99 | 19.71 | 100.00 | 99.23 |
| DBH2993 | 94.40:5 | 48.06 | 19.43 | 13.65 | 18.86 | 100.00 | 100.87 |
| mean value (at%) | | 48.03 | 22.20 | 9.04 | 20.48 | | |
| minimum (at%) | | 47.32 | 18.76 | 2.18 | 18.58 | | |
| maximum (at%) | | 48.62 | 26.34 | 14.23 | 24.00 | | |
| Weight% sigma (±) | | 0.20 | 0.28 | 0.26 | 0.36 | | |

*Table 9*. The chemical composition (at%) of coarse-grained pentlandite

| Core | Sample | S | Fe | Co | Ni | ∑(at%) | ∑(wt%) |
|---|---|---|---|---|---|---|---|
| DBH2992 | 80.70:1:5 | 47.70 | 19.16 | 12.04 | 21.09 | 99.99 | 97.22 |
| DBH2992 | 80.70:1:5 | 47.57 | 13.30 | 23.05 | 16.07 | 99.99 | 97.10 |
| DBH2992 | 92.74:1:3 | 48.14 | 14.92 | 20.40 | 16.54 | 100.00 | 98.34 |
| DBH2992 | 92.74:1:3 | 47.74 | 17.46 | 16.99 | 17.74 | 99.93 | 97.21 |
| DBH2992 | 92.74:1:6 | 48.13 | 17.31 | 16.87 | 17.69 | 100.00 | 98.04 |
| DBH2992 | 92.74:1:6 | 48.46 | 18.03 | 16.10 | 17.40 | 99.99 | 97.82 |
| DBH2992 | 92.74:2:1 | 48.12 | 17.87 | 15.62 | 18.39 | 100.00 | 99.70 |
| DBH2992 | 92.74:2:1 | 47.86 | 18.19 | 15.48 | 17.84 | 99.37 | 99.60 |
| DBH2992 | 102,47:2 | 47.64 | 14.85 | 21.66 | 15.85 | 100.00 | 102.52 |
| DBH2992 | 102,47:2 | 48.05 | 17.71 | 17.53 | 16.71 | 100.00 | 100.35 |
| DBH2992 | 102.47:3 | 47.62 | 16.28 | 18.85 | 17.26 | 100.01 | 102.96 |
| DBH2992 | 102.47:3 | 47.67 | 16.62 | 18.60 | 17.12 | 100.01 | 102.39 |
| DBH2992 | 102.47:3 | 47.70 | 16.66 | 18.49 | 17.15 | 100.00 | 102.58 |
| DBH2992 | 102.47:3 | 48.14 | 16.60 | 18.48 | 16.78 | 100.00 | 101.65 |
| DBH2992 | 102.47:3 | 48.30 | 16.46 | 19.16 | 16.09 | 100.01 | 100.69 |
| DBH2992 | 102.47:3 | 47.75 | 15.47 | 20.79 | 16.00 | 100.01 | 102.90 |
| DBH2992 | 102.47:3 | 47.88 | 15.36 | 20.73 | 16.04 | 100.01 | 102.93 |
| DBH2992 | 102.47:5 | 47.79 | 15.15 | 20.51 | 16.54 | 99.99 | 100.11 |
| DBH2992 | 108.73:2 | 47.72 | 15.13 | 20.55 | 16.60 | 100.00 | 99.14 |
| DBH2992 | 108.73:8 | 48.11 | 15.67 | 19.20 | 17.02 | 100.00 | 99.06 |
| DBH2992 | 108.73:8 | 48.25 | 11.97 | 24.56 | 15.21 | 99.99 | 97.81 |
| DBH2992 | 108.73:8 | 48.15 | 12.59 | 23.26 | 16.00 | 100.00 | 97.38 |
| DBH2955 | 92.60:3 | 47.79 | 9.46 | 31.44 | 11.31 | 100.00 | 100.98 |
| DBH2955 | 92.60:3 | 48.08 | 10.44 | 29.50 | 11.99 | 100.01 | 100.38 |
| DBH2955 | 92.60:3 | 47.87 | 9.60 | 31.36 | 11.17 | 100.00 | 100.24 |
| DBH2955 | 92.60:7 | 47.50 | 12.99 | 24.71 | 14.79 | 99.99 | 98.91 |
| DBH2955 | 92.60:7 | 47.95 | 13.08 | 24.21 | 14.76 | 100.00 | 99.56 |
| DBH2955 | 92.60:7 | 48.23 | 12.25 | 25.24 | 14.29 | 100.01 | 98.74 |
| DBH2955 | 117.60:7 | 47.59 | 20.16 | 13.47 | 18.79 | 100.01 | 100.63 |
| DBH2955 | 117.60:7 | 48.10 | 22.62 | 11.22 | 18.06 | 100.00 | 98.10 |
| DBH2993 | 71.90:2 | 48.05 | 16.67 | 21.37 | 13.38 | 99.47 | 98.33 |
| DBH2993 | 71.90:2 | 47.84 | 16.89 | 20.47 | 13.98 | 99.18 | 97.55 |

| | | | | | | | |
|---|---|---|---|---|---|---|---|
| DBH2993 | 71.90:3 | 47.85 | 15.27 | 21.92 | 14.20 | 99.24 | 98.77 |
| DBH2993 | 71.90:3 | 47.76 | 14.25 | 22.72 | 14.39 | 99.12 | 98.15 |
| DBH2993 | 71.90:7 | 47.97 | 17.21 | 17.42 | 17.39 | 99.99 | 98.77 |
| DBH2993 | 71.90:7 | 47.43 | 17.45 | 17.48 | 17.34 | 99.70 | 98.01 |
| DBH2993 | 71.90:7 | 48.14 | 21.78 | 10.67 | 19.41 | 100.00 | 97.44 |
| DBH2993 | 71.90:8 | 47.65 | 16.03 | 19.23 | 17.09 | 100.00 | 100.05 |
| DBH2993 | 71.90:8 | 47.63 | 16.24 | 19.02 | 17.11 | 100.00 | 100.36 |
| DBH2993 | 71.90:8 | 47.74 | 16.23 | 19.29 | 16.74 | 100.00 | 100.04 |
| DBH2993 | 71.90:10 | 48.11 | 17.85 | 18.16 | 15.87 | 99.99 | 99.25 |
| DBH2993 | 71.90:10 | 48.39 | 18.36 | 17.25 | 16.00 | 100.00 | 99.06 |
| DBH2993 | 71.90:10 | 47.70 | 18.28 | 18.01 | 16.01 | 100.00 | 100.25 |
| DBH2993 | 94.40:1 | 47.56 | 13.75 | 21.69 | 16.91 | 99.91 | 100.72 |
| DBH2993 | 94.40:1 | 47.63 | 14.08 | 21.70 | 16.59 | 100.00 | 100.39 |
| DBH2993 | 94.40:3 | 47.82 | 15.10 | 20.58 | 16.04 | 99.54 | 100.95 |
| DBH2993 | 94.40:3 | 47.37 | 14.64 | 21.55 | 16.19 | 99.75 | 100.16 |
| DBH2993 | 94.40:3 | 47.32 | 13.62 | 22.81 | 16.25 | 100.00 | 101.42 |
| DBH2993 | 94.40:4 | 47.82 | 14.29 | 21.44 | 16.45 | 100.00 | 100.29 |
| DBH2993 | 94.40:4 | 47.64 | 14.67 | 19.90 | 15.33 | 97.54 | 101.28 |
| DBH2993 | 94.40:4 | 47.60 | 14.34 | 21.29 | 16.77 | 100.00 | 101.97 |
| DBH2993 | 94.40:4 | 47.74 | 13.56 | 22.41 | 16.30 | 100.01 | 101.18 |
| DBH2993 | 114.40:4 | 48.23 | 5.26 | 36.07 | 10.43 | 99.99 | 99.92 |
| DBH2993 | 114.40:4 | 48.16 | 2.92 | 40.75 | 8.17 | 100.00 | 99.07 |
| DBH2993 | 114.40:4 | 48.22 | 4.07 | 38.94 | 8.77 | 100.00 | 98.75 |
| mean value (at%) | | 47.87 | 15.02 | 21.13 | 15.84 | | |
| minimum (at%) | | 47.32 | 2.92 | 10.67 | 8.17 | | |
| maximum (at%) | | 48.46 | 22.62 | 40.75 | 21.09 | | |
| Weight% sigma (±) | | 0.18 | 0.23 | 0.31 | 0.32 | | |

*Table 10.* The chemical composition (at%) of mackinawite

| Core | Sample | S | Fe | Co | Ni | ∑(at%) | ∑(wt%) |
|---|---|---|---|---|---|---|---|
| DBH2992 | 82.60:2 | 51.41 | 43.66 | 0.00 | 4.93 | 100.00 | 97.74 |
| DBH2992 | 82.60:2 | 51.43 | 42.49 | 0.00 | 5.29 | 99.21 | 98.42 |
| DBH2992 | 92.74:5 | 51.41 | 43.90 | 1.20 | 3.50 | 100.01 | 97.21 |
| DBH2992 | 92.74:5 | 51.29 | 42.98 | 2.32 | 3.42 | 100.01 | 98.01 |
| DBH2992 | 92.74:5 | 51.15 | 43.89 | 0.64 | 4.32 | 100.00 | 98.11 |
| DBH2992 | 92.74:2:1 | 51.20 | 42.90 | 3.11 | 2.78 | 99.99 | 98.49 |
| DBH2992 | 92.74:2:8 | 50.90 | 43.29 | 1.55 | 3.63 | 99.37 | 100.28 |
| DBH2992 | 92.74:2:8 | 50.74 | 43.56 | 1.74 | 3.60 | 99.64 | 100.08 |
| DBH2992 | 92.74:2:8 | 51.08 | 43.41 | 1.40 | 3.57 | 99.46 | 99.07 |
| DBH2992 | 102.47:2 | 51.17 | 42.83 | 0.00 | 4.08 | 98.08 | 100.36 |
| DBH2992 | 102.47:9 | 51.23 | 44.18 | 0.00 | 3.95 | 99.36 | 99.09 |
| DBH2992 | 102.47:9 | 51.02 | 44.38 | 0.00 | 4.31 | 99.71 | 98.07 |
| DBH2992 | 102.47:13 | 50.76 | 44.11 | 0.29 | 4.32 | 99.48 | 100.68 |
| DBH2992 | 102.47:13 | 51.05 | 43.82 | 0.87 | 4.26 | 100.00 | 99.49 |
| DBH2992 | 102.47:13 | 51.08 | 43.88 | 0.31 | 4.28 | 99.55 | 100.22 |
| DBH2955 | 117.60:3 | 51.02 | 45.07 | 0.00 | 3.91 | 100.00 | 98.77 |
| DBH2955 | 117.60:3 | 51.38 | 44.71 | 0.00 | 3.79 | 99.88 | 100.03 |
| DBH2993 | 71.90:10 | 50.92 | 42.15 | 5.13 | 1.80 | 100.00 | 98.13 |
| DBH2993 | 71.90:10 | 51.23 | 41.77 | 5.06 | 1.94 | 100.00 | 98.28 |
| mean value (at%) | | 51.13 | 43.53 | 1.24 | 3.77 | | |
| minimum (at%) | | 50.74 | 41.77 | 0.00 | 1.80 | | |
| maximum (at%) | | 51.43 | 45.07 | 5.13 | 5.29 | | |
| Weight% sigma (±) | | 0.19 | 0.36 | 0.18 | 0.20 | | |

*Table 11.* The chemical composition (at%) of argentopentlandite

| Core | Sample | S | Fe | Ni | Ag | ∑(at%) | ∑(wt%) |
|---|---|---|---|---|---|---|---|
| DBH2992 | 92.74:3 | 48.04 | 31.44 | 13.82 | 6.69 | 99.99 | 97.01 |
| DBH2992 | 92.74:6 | 48.01 | 32.40 | 13.09 | 6.50 | 100.00 | 98.37 |
| DBH2992 | 92.74:6 | 47.98 | 32.19 | 13.15 | 6.59 | 99.91 | 98.43 |
| DBH2992 | 92.74:2:1 | 47.80 | 31.95 | 13.70 | 6.54 | 99.99 | 100.62 |
| DBH2992 | 92.74:2:1 | 47.79 | 32.30 | 13.56 | 6.36 | 100.01 | 99.17 |
| DBH2992 | 92.74:2:1 | 47.70 | 32.20 | 13.59 | 6.51 | 100.00 | 99.92 |
| DBH2992 | 102.47:2 | 47.54 | 31.87 | 14.29 | 6.30 | 100.00 | 102.06 |
| DBH2992 | 102.47:2 | 47.93 | 32.67 | 13.05 | 6.35 | 100.00 | 102.12 |
| DBH2992 | 102.47:2 | 47.52 | 32.20 | 13.89 | 6.39 | 100.00 | 101.58 |
| DBH2992 | 102.47:4 | 47.67 | 32.66 | 13.25 | 6.19 | 99.77 | 99.71 |
| DBH2992 | 102.47:4 | 47.70 | 31.68 | 14.17 | 6.45 | 100.00 | 100.17 |
| DBH2992 | 102.47:4 | 47.82 | 32.32 | 13.51 | 6.35 | 100.00 | 100.93 |
| DBH2992 | 102.47:4 | 47.42 | 32.12 | 13.49 | 6.25 | 99.28 | 101.88 |
| DBH2992 | 102.47:4 | 47.48 | 31.83 | 13.02 | 6.21 | 98.54 | 102.28 |
| DBH2992 | 102.47:10 | 47.70 | 31.68 | 14.17 | 6.45 | 100.00 | 100.17 |
| DBH2992 | 102.47:10 | 47.82 | 32.32 | 13.51 | 6.35 | 100.00 | 100.93 |
| DBH2955 | 117.60:3 | 47.53 | 33.05 | 13.09 | 6.33 | 100.00 | 99.71 |
| DBH2955 | 117.60:3 | 47.85 | 32.88 | 13.00 | 6.27 | 100.00 | 98.77 |
| DBH2993 | 71.90:7 | 47.45 | 31.79 | 14.14 | 5.90 | 99.28 | 99.35 |
| DBH2993 | 71.90:7 | 49.06 | 30.58 | 13.55 | 5.18 | 98.37 | 97.96 |
| DBH2993 | 71.90:9 | 49.42 | 30.66 | 12.25 | 5.16 | 97.49 | 97.61 |
| DBH2993 | 94.40:2 | 47.53 | 30.80 | 14.53 | 6.27 | 99.13 | 102.38 |
| DBH2993 | 94.40:7 | 47.44 | 31.06 | 14.43 | 6.26 | 99.19 | 102.76 |
| DBH2993 | 94.40:7 | 47.43 | 30.83 | 14.75 | 6.18 | 99.19 | 102.78 |
| mean value (at%) | | 47.82 | 31.90 | 13.63 | 6.25 | | |
| minimum (at%) | | 47.42 | 30.58 | 12.25 | 5.16 | | |
| maximum (at%) | | 49.42 | 33.05 | 14.75 | 6.69 | | |
| Weight% sigma (±) | | 0.18 | 0.31 | 0.28 | 0.27 | | |

*Table 12.* The chemical composition (at%) of breithauptite

| Core | Sample | Ni | Sb | As | Fe | ∑(at%) | ∑(wt%) |
|---|---|---|---|---|---|---|---|
| DBH2992 | 80.70:3:3 | 48.99 | 51.01 | 0.00 | 0.00 | 100.00 | 98.68 |
| DBH2992 | 80.70:3:7 | 49.66 | 50.34 | 0.00 | 0.00 | 100.00 | 99.21 |
| DBH2992 | 82.60:1 | 48.38 | 48.21 | 1.89 | 0.00 | 98.48 | 97.85 |
| DBH2992 | 82.60:1 | 49.30 | 49.44 | 1.27 | 0.00 | 100.01 | 101.39 |
| DBH2992 | 102.47:6 | 48.81 | 49.82 | 0.00 | 1.37 | 100.00 | 100.37 |
| DBH2992 | 102.47:12 | 49.57 | 48.00 | 2.43 | 0.00 | 100.00 | 100.63 |
| DBH2992 | 102.47:12 | 49.89 | 46.57 | 3.36 | 0.17 | 99.99 | 101.46 |
| DBH2992 | 108.73:2 | 49.47 | 48.89 | 1.64 | 0.00 | 100.00 | 100.15 |
| DBH2992 | 110.71:3 | 48.38 | 51.62 | 0.00 | 0.00 | 100.00 | 99.76 |
| DBH2992 | 110.71:3 | 48.57 | 51.43 | 0.00 | 0.00 | 100.00 | 99.78 |
| DBH2992 | 110.71:6 | 48.03 | 50.19 | 0.00 | 1.78 | 100.00 | 100.83 |
| DBH2992 | 110.71:6 | 48.29 | 50.07 | 0.00 | 1.64 | 100.00 | 102.17 |
| DBH2992 | 110.71:8 | 49.67 | 50.33 | 0.00 | 0.00 | 100.00 | 100.23 |
| DBH2992 | 110.71:8 | 49.48 | 49.59 | 0.93 | 0.00 | 100.00 | 101.53 |
| DBH2992 | 110.71:9 | 49.83 | 48.13 | 2.04 | 0.00 | 100.00 | 102.48 |
| DBH2992 | 110.71:9 | 49.53 | 49.69 | 0.79 | 0.00 | 100.01 | 102.33 |
| DBH2992 | 110.71:11 | 49.83 | 48.13 | 2.04 | 0.00 | 100.00 | 102.48 |
| DBH2992 | 110.71:11 | 48.96 | 51.04 | 0.00 | 0.00 | 100.00 | 99.35 |
| DBH2955 | 92.60:2 | 49.35 | 48.44 | 2.21 | 0.00 | 100.00 | 100.39 |
| DBH2955 | 92.60:2 | 49.45 | 48.58 | 1.97 | 0.00 | 100.00 | 99.70 |
| DBH2955 | 92.60:2 | 49.36 | 48.53 | 2.11 | 0.00 | 100.00 | 99.30 |
| DBH2955 | 117.60:5 | 49.06 | 49.71 | 0.82 | 0.41 | 100.00 | 102.26 |
| DBH2955 | 117.60:5 | 49.25 | 48.92 | 1.83 | 0.00 | 100.00 | 102.17 |

| | | | | | |
|---|---|---|---|---|---|
| mean value (at%) | 49.18 | 49.42 | - | - | |
| minimum (at%) | 48.03 | 46.57 | 0.00 | 0.00 | |
| maximum (at%) | 49.89 | 51.62 | 3.36 | 1.78 | |
| Weight% sigma (±) | 0.35 | 0.40 | - | . | |

*Table 13*. The chemical composition (at%) of cobaltite

| Core | Sample | S | Fe | Co | Ni | As | ∑(at%) | ∑(wt%) |
|---|---|---|---|---|---|---|---|---|
| DBH2992 | 80.70:1:7 | 33.35 | 1.97 | 25.56 | 5.92 | 33.21 | 100.01 | 100.83 |
| DBH2992 | 80.70:1:7 | 33.42 | 1.56 | 27.55 | 4.17 | 33.30 | 100.00 | 102.63 |
| DBH2992 | 82.60:1 | 32.35 | 0.70 | 30.21 | 2.53 | 34.20 | 99.99 | 102.83 |
| DBH2992 | 82.60:1 | 32.15 | 0.85 | 28.12 | 4.43 | 34.45 | 100.00 | 101.16 |
| DBH2992 | 108.73:7 | 33.41 | 0.28 | 31.34 | 0.95 | 34.03 | 100.01 | 101.68 |
| DBH2992 | 108.73:7 | 33.40 | 1.74 | 27.19 | 3.78 | 33.89 | 100.00 | 101.97 |
| DBH2992 | 108.73:7 | 33.08 | 1.53 | 28.40 | 3.12 | 33.86 | 99.99 | 99.55 |
| DBH2992 | 108.73:10 | 33.28 | 0.60 | 31.33 | 1.37 | 33.43 | 100.01 | 99.72 |
| DBH2992 | 108.73:10 | 33.35 | 1.30 | 26.98 | 4.61 | 33.75 | 99.99 | 100.90 |
| DBH2992 | 108.73:10 | 33.70 | 1.25 | 28.29 | 3.00 | 33.76 | 100.00 | 98.36 |
| DBH2992 | 110.71:1 | 33.15 | 2.52 | 25.72 | 4.42 | 34.19 | 100.00 | 103.11 |
| DBH2992 | 110.71:8 | 33.32 | 0.38 | 29.68 | 2.89 | 33.73 | 100.00 | 103.47 |
| DBH2992 | 110.71:8 | 32.41 | 2.52 | 26.26 | 4.61 | 34.20 | 100.00 | 104.14 |
| DBH2955 | 117.60:4 | 33.53 | 0.35 | 30.64 | 1.71 | 33.77 | 100.00 | 105.18 |
| DBH2955 | 117.60:4 | 33.07 | 0.32 | 30.73 | 2.02 | 33.85 | 99.99 | 105.84 |
| DBH2955 | 117.60:4 | 33.30 | 0.45 | 29.93 | 2.51 | 33.81 | 100.00 | 105.23 |
| DBH2993 | 71.90:6 | 32.99 | 2.33 | 27.09 | 3.24 | 34.36 | 100.01 | 102.24 |
| DBH2993 | 71.90:6 | 33.22 | 2.53 | 26.23 | 3.66 | 34.36 | 100.00 | 101.67 |
| DBH2993 | 71.90:6 | 33.31 | 2.85 | 26.28 | 3.75 | 33.80 | 99.99 | 101.96 |
| mean value (at%) | | 33.15 | 1.37 | 28.29 | 3.30 | 33.89 | | |
| minimum (at%) | | 32.15 | 0.28 | 25.56 | 0.95 | 33.21 | | |
| maximum (at%) | | 33.70 | 2.85 | 31.34 | 5.92 | 34.45 | | |
| Weight% sigma (±) | | 0.16 | 0.12 | 0.31 | 0.22 | 0.34 | | |

*Table 14.* The chemical composition (at%) of galena

| core | sample | S | Pb | Fe | ∑(at%) | ∑(wt%) |
|---|---|---|---|---|---|---|
| DBH2992 | 80.70:1:5 | 50.17 | 49.83 | 0.00 | 100.00 | 93.69 |
| DBH2992 | 108.73:5 | 49.19 | 46.16 | 4.65 | 100.00 | 93.84 |
| DBH2992 | 108.73:9 | 49.10 | 49.60 | 1.31 | 100.01 | 94.45 |
| DBH2992 | 110.71:4 | 49.69 | 50.31 | 0.00 | 100.00 | 95.51 |
| DBH2955 | 62.60:2 | 50.21 | 49.79 | 0.00 | 100.00 | 93.46 |
| DBH2955 | 62.60:2 | 50.19 | 49.81 | 0.00 | 100.00 | 92.58 |
| DBH2955 | 62.60:2 | 50.00 | 50.00 | 0.00 | 100.00 | 91.37 |
| DBH2955 | 62.60:6 | 49.32 | 49.50 | 1.18 | 100.00 | 94.91 |
| DBH2955 | 62.60:7 | 50.20 | 48.77 | 1.03 | 100.00 | 93.70 |
| DBH2955 | 62.60:10 | 49.07 | 49.63 | 1.35 | 100.05 | 93.56 |
| DBH2955 | 62.60:12 | 49.48 | 50.52 | 0.00 | 100.00 | 95.40 |
| DBH2955 | 62.60:12 | 50.01 | 49.99 | 0.00 | 100.00 | 94.63 |
| DBH2955 | 62,60.13 | 50.14 | 49.86 | 0.00 | 100.00 | 94.34 |
| DBH2955 | 62.60.19 | 49.68 | 49.39 | 0.92 | 99.99 | 93.99 |
| DBH2955 | 62.60.19 | 50.19 | 49.81 | 0.00 | 100.00 | 87.30 |
| DBH2955 | 62.60.19 | 49.85 | 50.15 | 0.00 | 100.00 | 93.88 |
| DBH2955 | 117.60:8 | 48.61 | 47.59 | 3.80 | 100.00 | 98.84 |
| mean value (at%) | | 49.71 | 49.45 | - | | |
| minimum (at%) | | 48.61 | 46.16 | 0.00 | | |
| maximum (at%) | | 50.21 | 50.52 | 4.65 | | |
| Weight% sigma (±) | | 0.19 | 0.66 | - | | |

*Table 15.* The chemical composition (at%) of pyrrhotite

| core | sample | S | Fe | ∑(at%) | ∑(wt%) |
|---|---|---|---|---|---|
| DBH2993 | 71,90:2 | 53.37 | 46.17 | 99.54 | 97.12 |
| DBH2993 | 71,90:7 | 53.20 | 46.80 | 100.00 | 97.68 |
| DBH2993 | 71,90:7 | 53.33 | 46.67 | 100.00 | 98.01 |
| DBH2993 | 71,90:8 | 53.28 | 46.72 | 100.00 | 98.97 |
| DBH2993 | 71,90:8 | 53.25 | 46.75 | 100.00 | 98.91 |
| DBH2993 | 71,90:9 | 53.15 | 46.85 | 100.00 | 97.78 |
| DBH2993 | 71,90:9 | 51.22 | 48.78 | 100.00 | 97.98 |
| DBH2993 | 71,90:9 | 53.22 | 46.78 | 100.00 | 97.76 |
| DBH2993 | 71,90:10 | 53.60 | 46.40 | 100.00 | 98.44 |
| mean value (at%) | | 53.30 | 46.64 | | |
| fe-low (at%) | | 51.22 | 48.78 | | |
| minimum (at%) | | 51.22 | 46.17 | | |
| maximum (at%) | | 53.60 | 48.78 | | |
| Weight% sigma (±) | | 0.20 | 0.39 | | |

*Table 16.* The chemical composition (at%) of molybdenite

| core | sample | S | Mo | ∑(at%) | ∑(wt%) |
|---|---|---|---|---|---|
| DBH2992 | 102.47:7 | 66.50 | 33.50 | 100.00 | 101.42 |
| DBH2992 | 102.47:7 | 66.97 | 33.03 | 100.00 | 105.79 |
| DBH2992 | 102.47:11 | 65.86 | 34.14 | 100.00 | 101.05 |
| DBH2992 | 102.47:11 | 65.97 | 34.03 | 100.00 | 104.92 |
| DBH2992 | 102.47:11 | 66.93 | 33.07 | 100.00 | 104.35 |
| DBH2992 | 102.47:11 | 66.09 | 33.91 | 100.00 | 104.10 |
| DBH2992 | 102.47:11 | 66.31 | 33.69 | 100.00 | 102.83 |
| DBH2992 | 102.47:11 | 65.67 | 34.33 | 100.00 | 105.64 |
| DBH2992 | 102.47:11 | 65.39 | 34.61 | 100.00 | 103.28 |
| mean value (at%) | | 66.19 | 33.81 | | |
| minimum (at%) | | 66.97 | 33.03 | | |
| maximum (at%) | | 65.39 | 34.61 | | |
| Weight% sigma (±) | | 0.40 | 1.13 | | |

*Table 17.* The chemical composition (at%) of gudmundite

| core | sample | S | Fe | Sb | ∑(at%) | ∑(wt%) |
|---|---|---|---|---|---|---|
| DBH2992 | 72,25:2:4 | 33.46 | 32.55 | 33.50 | 99.51 | 101.95 |
| DBH2992 | 92,74:2:3 | 34.28 | 31.76 | 33.95 | 99.99 | 100.22 |
| DBH2992 | 92,74:2:3 | 34.07 | 31.36 | 34.57 | 100.00 | 100.34 |
| DBH2992 | 92,74:2:3 | 34.22 | 31.73 | 34.05 | 100.00 | 100.73 |
| DBH2992 | 92,74:2:3 | 33.68 | 32.27 | 34.04 | 99.99 | 99.42 |
| DBH2992 | 92,74:2:4 | 33.67 | 31.69 | 33.83 | 99.19 | 100.93 |
| DBH2992 | 92,74:2:4 | 33.61 | 32.12 | 34.27 | 100.00 | 100.06 |
| DBH2992 | 110,71:6 | 33.77 | 32.21 | 34.02 | 100.00 | 100.80 |
| DBH2992 | 110,71:6 | 33.53 | 32.52 | 33.94 | 99.99 | 100.41 |
| DBH2992 | 110,71:7 | 33.53 | 31.79 | 32.65 | 97.97 | 100.03 |
| mean value (at%) | | 33.78 | 32.00 | 33.88 | | |
| minimum (at%) | | 33.46 | 31.36 | 32.65 | | |
| maximum (at%) | | 34.28 | 32.55 | 34.57 | | |
| Weight% sigma (±) | | 0.13 | 0.27 | 0.38 | | |

*Table 18.* The chemical composition (at%) of nickeline

| core | sample | Fe | Ni | As | Sb | ∑(at%) | ∑(wt%) |
|---|---|---|---|---|---|---|---|
| DBH2992 | 102,47:12 | 0.40 | 49.22 | 46.73 | 3.64 | 99.99 | 105.69 |
| Weight% sigma (±) | | 0.09 | 0.38 | 0.38 | 0.19 | | |

*Table 19*. The chemical composition (at%) of costibite

| core | sample | S | Fe | Co | Ni | Sb | ∑(at%) | ∑(wt%) |
|---|---|---|---|---|---|---|---|---|
| DBH2992 | 110,71:6 | 32.19 | 0.74 | 29.50 | 3.44 | 34.14 | 100.01 | 98.98 |
| Weight% sigma (±) | | 0.13 | 0.11 | 0.29 | 0.20 | 0.37 | | |

*Table 20*. The chemical composition (at%) of maucherite

| core | sample | Fe | Co | Ni | As | Sb | ∑(at%) | ∑(wt%) |
|---|---|---|---|---|---|---|---|---|
| DBH2955 | 117.60:4 | 0.00 | 2.99 | 54.23 | 40.54 | 2.24 | 100.00 | 105.97 |
| DBH2955 | 117.60:4 | 0.00 | 3.10 | 54.01 | 40.58 | 2.30 | 99.99 | 106.10 |
| DBH2955 | 117.60:4 | 0.33 | 3.42 | 52.96 | 41.25 | 2.05 | 100.01 | 106.86 |
| mean value (at%) | | - | 3.17 | 53.73 | 40.79 | 2.20 | | |
| minimum (at%) | | 0.00 | 2.99 | 52.96 | 40.54 | 2.05 | | |
| maximum (at%) | | 0.33 | 3.42 | 54.23 | 41.25 | 2.24 | | |
| Weight% sigma (±) | | - | 0.15 | 0.41 | 0.38 | 0.17 | | |

*Table 21*. The chemical composition (at%) of tetrahedrite

| core | sample | S | Fe | Cu | Zn | Ag | As | Sb | ∑(at%) | ∑(wt%) |
|---|---|---|---|---|---|---|---|---|---|---|
| DBH2992 | 110.71:2 | 45.32 | 1.70 | 33.63 | 5.01 | 0.29 | 0.00 | 14.05 | 100.00 | 101.57 |
| DBH2992 | 110.71:4 | 45.00 | 1.92 | 33.84 | 5.28 | 0.00 | 0.00 | 13.96 | 100.00 | 101.51 |
| DBH2992 | 110.71:5 | 45.42 | 1.83 | 33.70 | 5.19 | 0.00 | 0.00 | 13.86 | 100.00 | 101.27 |
| DBH2955 | 62.60:3 | 44.73 | 5.98 | 34.06 | 1.38 | 0.00 | 0.00 | 13.85 | 100.00 | 99.48 |
| DBH2955 | 62.60:6 | 45.63 | 5.68 | 34.75 | 0.00 | 0.00 | 0.00 | 13.94 | 100.00 | 97.09 |
| DBH2955 | 62.60:7 | 45.29 | 5.55 | 34.48 | 0.81 | 0.00 | 0.00 | 13.87 | 100.00 | 98.05 |
| DBH2955 | 62.60:7 | 45.16 | 6.28 | 33.82 | 0.78 | 0.00 | 0.00 | 13.96 | 100.00 | 98.06 |
| DBH2955 | 62.60:8 | 45.23 | 5.95 | 33.94 | 0.87 | 0.00 | 0.36 | 13.65 | 100.00 | 97.68 |
| DBH2955 | 62.60:9 | 45.25 | 5.87 | 33.50 | 1.30 | 0.00 | 0.26 | 13.82 | 100.00 | 98.22 |
| DBH2955 | 62.60:10 | 45.54 | 5.93 | 33.58 | 0.95 | 0.00 | 0.24 | 13.76 | 100.00 | 98.60 |
| DBH2955 | 62.60:12 | 45.51 | 5.92 | 33.34 | 1.05 | 0.37 | 0.26 | 13.55 | 100.00 | 99.19 |
| DBH2955 | 62.60:12 | 44.85 | 5.84 | 33.95 | 1.06 | 0.35 | 0.00 | 13.95 | 100.00 | 99.30 |
| DBH2955 | 62.60:14 | 45.66 | 5.62 | 34.54 | 0.00 | 0.00 | 0.40 | 13.78 | 100.00 | 99.35 |
| DBH2955 | 62.60:15 | 45.75 | 5.78 | 34.33 | 0.00 | 0.00 | 0.46 | 13.69 | 100.01 | 98.28 |
| DBH2955 | 62.60:17 | 45.63 | 6.39 | 33.03 | 0.89 | 0.00 | 0.42 | 13.65 | 100.01 | 99.76 |
| DBH2955 | 62.60:17 | 44.58 | 6.62 | 33.49 | 1.23 | 0.00 | 0.32 | 13.77 | 100.01 | 100.57 |
| DBH2955 | 62.60:18 | 45.57 | 5.44 | 33.66 | 1.57 | 0.00 | 0.00 | 13.75 | 99.99 | 98.72 |
| DBH2955 | 62.60:18 | 45.32 | 5.45 | 33.69 | 1.60 | 0.00 | 0.00 | 13.94 | 100.00 | 99.25 |
| mean value (at%) | | 45.30 | 5.21 | 33.85 | 1.61 | - | - | 13.82 | | |
| mean Fe-low (at%) | | 45.25 | 1.82 | 33.72 | 5.16 | - | - | 13.96 | | |
| mean Fe-high (at%) | | 45.31 | 5.89 | 33.88 | 0.90 | - | - | 13.80 | | |
| minimum (at%) | | 44.58 | 1.70 | 33.03 | 0.00 | 0.00 | 0.00 | 13.55 | | |
| maximum (at%) | | 45.75 | 6.62 | 34.75 | 5.28 | 0.37 | 0.46 | 13.96 | | |
| Weight% sigma (±) | | 0.17 | 0.15 | 0.43 | 0.23 | - | - | 0.29 | | |

*Table 22*. The chemical composition (at%) of Fe-safflorite

| core | sample | S | Fe | Co | Ni | As | ∑(at%) | ∑(wt%) |
|---|---|---|---|---|---|---|---|---|
| DBH2955 | 62.60:2 | 2.47 | 21.26 | 6.22 | 5.54 | 64.51 | 100.00 | 101.83 |
| DBH2955 | 62.60:2 | 2.35 | 20.99 | 5.41 | 5.89 | 65.36 | 100.00 | 100.30 |
| DBH2955 | 62.60:6 | 1.13 | 32.29 | 0.00 | 0.00 | 66.58 | 100.00 | 101.52 |
| DBH2955 | 62.60:6 | 0.62 | 32.40 | 0.00 | 0.00 | 66.98 | 100.00 | 99.07 |
| DBH2955 | 62.60:18 | 1.93 | 19.53 | 7.04 | 6.24 | 65.25 | 99.99 | 102.28 |
| mean value (at%) | | 1.70 | 25.29 | - | - | 65.74 | | |
| minimum (at%) | | 0.62 | 19.53 | 0.00 | 0.00 | 64.51 | | |
| maximum (at%) | | 2.47 | 32.40 | 7.04 | 6.24 | 66.98 | | |
| Weight% sigma (±) | | 0.07 | 0.23 | 0.19 | 0.20 | 0.39 | | |

*Table 23*. The chemical composition (at%) of Co-safflorite

| core | sample | S | Fe | Co | Ni | As | Sb | ∑(at%) | ∑(wt%) |
|---|---|---|---|---|---|---|---|---|---|
| DBH2955 | 117.60:2 | 2.05 | 8.63 | 20.87 | 3.09 | 64.26 | 1.09 | 99.99 | 109.65 |
| DBH2955 | 117.60:2 | 1.97 | 8.21 | 20.67 | 3.61 | 64.24 | 1.30 | 100.00 | 109.09 |
| DBH2955 | 117.60:2 | 2.10 | 8.20 | 20.83 | 3.88 | 63.82 | 1.16 | 99.99 | 110.75 |
| mean value (at%) | | 2.04 | 8.35 | 20.79 | 3.53 | 64.11 | 1.18 | | |
| minimum (at%) | | 1.97 | 8.20 | 20.67 | 3.09 | 63.82 | 1.09 | | |
| maximum (at%) | | 2.10 | 8.63 | 20.87 | 3.88 | 64.26 | 1.30 | | |
| Weight% sigma (±) | | 0.10 | 0.24 | 0.39 | 0.28 | 0.57 | 0.24 | | |

*Table 24*. The chemical composition (at%) of arsenopyrite

| core | sample | S | Fe | Co | Ni | As | ∑(at%) | ∑(wt%) |
|---|---|---|---|---|---|---|---|---|
| DBH2955 | 62.60:2 | 29.86 | 27.61 | 3.13 | 1.94 | 37.46 | 100.00 | 102.01 |
| DBH2955 | 62.60:2 | 35.60 | 31.76 | 0.00 | 0.00 | 32.64 | 100.00 | 102.30 |
| DBH2955 | 62.60:2 | 31.79 | 26.75 | 3.14 | 0.00 | 38.32 | 100.00 | 100.84 |
| DBH2955 | 62.60:6 | 31.86 | 29.53 | 0.00 | 2.58 | 36.04 | 100.01 | 99.72 |
| DBH2955 | 62.60:6 | 31.64 | 29.98 | 0.00 | 2.39 | 35.99 | 100.00 | 100.73 |
| DBH2955 | 62.60:6 | 34.30 | 31.54 | 0.00 | 0.00 | 34.15 | 99.99 | 98.04 |
| DBH2955 | 62.60:7 | 32.78 | 30.64 | 0.00 | 1.00 | 34.62 | 99.04 | 102.81 |
| DBH2955 | 62.60:7 | 33.92 | 31.94 | 0.00 | 0.00 | 34.13 | 99.99 | 99.04 |
| DBH2955 | 62.60:9 | 34.04 | 32.58 | 0.00 | 0.00 | 33.38 | 100.00 | 102.66 |
| DBH2955 | 62.60:10 | 30.97 | 29.83 | 0.00 | 1.61 | 37.59 | 100.00 | 101.59 |
| DBH2955 | 62.60:11 | 31.13 | 30.57 | 1.57 | 0.00 | 36.73 | 100.00 | 101.22 |
| DBH2955 | 62.60:11 | 29.70 | 29.33 | 1.72 | 1.51 | 37.75 | 100.01 | 102.73 |
| DBH2955 | 62.60:17 | 32.30 | 30.95 | 1.41 | 0.00 | 35.33 | 99.99 | 100.14 |
| DBH2955 | 62.60:17 | 28.67 | 28.64 | 2.53 | 1.43 | 38.48 | 99.75 | 102.65 |
| DBH2955 | 62.60:17 | 30.73 | 29.49 | 1.92 | 0.87 | 36.99 | 100.00 | 102.31 |
| mean value (at%) | | 31.95 | 30.08 | - | - | 35.97 | | |
| minimum (at%) | | 28.67 | 26.75 | 0.00 | 0.00 | 32.64 | | |
| maximum (at%) | | 35.60 | 32.58 | 3.14 | 2.58 | 38.48 | | |
| Weight% sigma (±) | | 0.15 | 0.27 | - | 0.16 | 0.33 | | |

*Table 25*. The chemical composition (at%) of chalcocite

| core | sample | S | Fe | Cu | ∑(at%) | ∑(wt%) |
|---|---|---|---|---|---|---|
| DBH2955 | 62.60:2 | 34.86 | 0.83 | 64.29 | 99.98 | 97.40 |
| DBH2955 | 62.60:5 | 35.19 | 0.34 | 64.47 | 100.00 | 97.39 |
| DBH2955 | 62.60:7 | 35.03 | 1.85 | 63.02 | 99.90 | 98.01 |
| DBH2955 | 62.60:8 | 35.35 | 0.26 | 64.39 | 100.00 | 98.49 |
| DBH2955 | 62.60:8 | 34.79 | 0.38 | 64.83 | 100.00 | 98.17 |
| DBH2955 | 62.60:9 | 34.75 | 0.43 | 64.82 | 100.00 | 100.49 |
| DBH2955 | 62.60:9 | 35.09 | 0.36 | 64.55 | 100.00 | 99.47 |
| DBH2955 | 62.60:10 | 34.60 | 1.22 | 64.15 | 99.97 | 99.99 |
| DBH2955 | 62.60:10 | 33.86 | 2.24 | 63.54 | 99.64 | 97.55 |
| DBH2955 | 62.60:13 | 34.16 | 0.55 | 65.29 | 100.00 | 99.99 |
| DBH2955 | 62.60:13 | 34.43 | 0.00 | 65.57 | 100.00 | 98.64 |
| mean value (at%) | | 34.74 | - | 64.45 | | |
| minimum (at%) | | 33.86 | 0.00 | 63.02 | | |
| maximum (at%) | | 35.35 | 2.24 | 65.57 | | |
| Weight% sigma (±) | | 0.16 | 0.09 | 0.61 | | |

*Table 26*. The chemical composition (at%) of silver

| core | sample | Ag | Hg | ∑(at%) | ∑(wt%) |
|---|---|---|---|---|---|
| DBH2992 | 102.47:16 | 91.92 | 5.04 | 96.96 | 106.19 |
| DBH2992 | 102.47:16 | 94.41 | 4.97 | 99.38 | 104.10 |
| DBH2992 | 102.47:16 | 94.83 | 5.17 | 100.00 | 102.90 |
| DBH2992 | 102.47:16 | 94.82 | 3.55 | 98.37 | 104.97 |
| DBH2992 | 102.47:14 | 95.31 | 4.69 | 100.00 | 107.51 |
| DBH2993 | 114.40:2 | 99.52 | 0.00 | 99.52 | 109.29 |
| DBH2993 | 114.40:2 | 98.71 | 0.00 | 98.71 | 103.63 |
| DBH2993 | 114.40:2 | 100.00 | 0.00 | 100.00 | 107.13 |
| DBH2993 | 114.40:2 | 100.00 | 0.00 | 100.00 | 107.78 |
| mean value (at%) | | 96.61 | - | | |
| minimum (at%) | | 91.92 | 0.00 | | |
| maximum (at%) | | 100.00 | 5.17 | | |
| Weight% sigma (±) | | 0.53 | 0.33 | | |

*Table 27*. The chemical composition (at%) of allargentum

| core | sample | Ag | Sb | ∑(at%) | ∑(wt%) |
|---|---|---|---|---|---|
| DBH2992 | 110.71:2 | 85.80 | 14.20 | 100.00 | 107.40 |
| DBH2992 | 110.71:3 | 85.38 | 14.62 | 100.00 | 105.49 |
| DBH2992 | 110.71:3 | 82.95 | 17.05 | 100.00 | 101.83 |
| DBH2992 | 110.71:4 | 91.24 | 8.76 | 100.00 | 103.64 |
| DBH2992 | 110.71:5 | 90.40 | 8.39 | 98.79 | 102.12 |
| DBH2992 | 110.71:5 | 90.30 | 8.69 | 98.99 | 103.15 |
| DBH2955 | 62.60:9 | 81.80 | 18.92 | 100.72 | 107.83 |
| DBH2955 | 62.60:9 | 80.78 | 19.22 | 100.00 | 104.92 |
| DBH2955 | 62.60:10 | 85.13 | 13.52 | 98.65 | 107.28 |
| DBH2955 | 62.60:11 | 84.13 | 13.12 | 97.25 | 103.93 |
| DBH2955 | 62.60:12 | 84.97 | 15.03 | 100.00 | 106.18 |
| DBH2955 | 62.60:12 | 85.17 | 14.83 | 100.00 | 103.80 |
| DBH2955 | 62.60:14 | 85.55 | 14.45 | 100.00 | 104.59 |
| DBH2955 | 62.60:14 | 84.89 | 13.62 | 98.51 | 105.17 |
| DBH2955 | 62.60:15 | 81.28 | 18.72 | 100.00 | 104.87 |
| mean value (at%) | | 85.32 | 14.21 | | |
| minimum (at%) | | 80.78 | 8.39 | | |
| maximum (at%) | | 91.24 | 19.22 | | |
| Weight% sigma (±) | | 0.48 | 0.31 | | |

*Table 28*. The chemical composition (at%) of bismuth

| core | sample | Bi | ∑(at%) | ∑(wt%) |
|---|---|---|---|---|
| DBH2992 | 110.71:10 | 100.00 | 100.00 | 102.22 |
| DBH2992 | 110.71:1 | 98.72 | 98.72 | 99.46 |
| DBH2992 | 110.71:1 | 95.57 | 95.57 | 101.61 |
| DBH2992 | 110.71:4 | 98.08 | 98.08 | 102.44 |
| DBH2992 | 110.71:6 | 97.81 | 97.81 | 100.60 |
| DBH2992 | 110.71:6 | 96.44 | 96.44 | 102.76 |
| DBH2992 | 110.71:9 | 100.00 | 100.00 | 102.11 |
| DBH2992 | 110.71:9 | 100.00 | 100.00 | 101.91 |
| DBH2992 | 110.71:9 | 100.00 | 100.00 | 100.70 |
| DBH2955 | 62.60:12 | 99.27 | 99.27 | 99.41 |
| DBH2955 | 62.60:13 | 100.00 | 100.00 | 101.96 |
| mean value (at%) | | 98.72 | | |
| minimum (at%) | | 95.57 | | |
| maximum (at%) | | 100.00 | | |
| Weight% sigma (±) | | 0.65 | | |

*Table 29*. The chemical composition (at%) of parkerite

| core | sample | S | Ni | Bi | Fe | ∑(at%) | ∑(wt%) |
|---|---|---|---|---|---|---|---|
| DBH2992 | 108.72:10 | 27.97 | 41.70 | 27.80 | 2.54 | 100.01 | 97.16 |
| DBH2992 | 110.71:8 | 28.40 | 42.09 | 28.64 | 0.86 | 99.99 | 99.57 |
| Weight% sigma (±) | | 0.15 | 0.31 | 0.67 | 0.13 | | |

*Table 30*. The chemical composition (at%) of an unidentified intergrowth

| core | sample | O | Fe | Ag | Pb | U | ∑(at%) | ∑(wt%) |
|---|---|---|---|---|---|---|---|---|
| DBH2992 | 108.73:3 | 72.21 | 0.00 | 8.83 | 4.83 | 14.13 | 100.00 | 100.67 |
| DBH2992 | 108.73:3 | 69.49 | 0.52 | 9.94 | 5.37 | 14.69 | 100.01 | 96.23 |
| DBH2992 | 102.47:9 | 70.24 | 1.07 | 5.73 | 5.73 | 15.94 | 98.71 | 106.19 |
| Weight% | sigma (±) | 0.45 | - | 0.31 | 0.36 | 0.60 | | |

**Tidigare skrifter i serien ”Examensarbeten i Geologi vid Lunds Universitet”:**

194. Nilsson, Anders, 2006: Limnological responses to late Holocene permafrost dynamics at the Stordalen mire, Abisko, northern Sweden.
195. Nilsson, Susanne, 2006: Sedimentary facies and fauna of the Late Silurian Bjärsjölagård Limestone Member (Klinta Formation), Skåne, Sweden.
196. Sköld, Eva, 2006: Kulturlandskapets förändringar inom röjningsröseområdet Yttra Berg, Halland - en pollenanalytisk undersökning av de senaste 5000 åren.
197. Göransson, Ammy, 2006: Lokala miljöförändringar i samband med en plötslig havsyteförändring ca 8200 år före nutid vid Kalvöviken i centrala Blekinge.
198. Brunzell, Anna, 2006: Geofysiska mätningar och visualisering för bedömning av heterogeniteters utbredning i en isälvsavlagring med betydelse för grundvattenflöde.
199. Erlfeldt, Åsa, 2006: Brachiopod faunal dynamics during the Silurian Ireviken Event, Gotland, Sweden.
200. Vollert, Victoria, 2006: Petrografisk och geokemisk karaktärisering av metabasiter i Herrestadsområdet, Småland.
201. Rasmussen, Karin, 2006: En provenansstudie av Kågerödformationen i NV Skåne – tungmineral och petrografi.
202. Karlsson, Jonnina, P., 2006: An investigation of the Felsic Ramiane Pluton, in the Monapo Structure, Northern Moçambique.
203. Jansson, Ida-Maria, 2006: An Early Jurassic conifer-dominated assemblage of the Clarence-Moreton Basin, eastern Australia.
204. Striberger, Johan, 2006: En lito- och biostratigrafisk studie av senglaciala sediment från Skuremåla, Blekinge.
205. Bergelin, Ingemar, 2006: $^{40}Ar/^{39}Ar$ geochronology of basalts in Scania, S Sweden: evidence for two pulses at 191-178 Ma and 110 Ma, and their relation to the breakup of Pangea.
206. Edvarssson, Johannes, 2006: Dendrokronologisk undersökning av tallbestånds etablering, tillväxtdynamik och degenerering orsakat av klimatrelaterade hydrologiska variationer på Viss mosse och Åbuamossen, Skåne, södra Sverige, 7300-3200 cal. BP.
207. Stenfeldt, Fredrik, 2006: Litostratigrafiska studier av en platåformad sand- och grusavlagring i Skuremåla, Blekinge.
208. Dahlenborg, Lars, 2007: A Rock Magnetic Study of the Åkerberg Gold Deposit, Northern Sweden.
209. Olsson, Johan, 2007: Två svekofenniska graniter i Bottniska bassängen; utbredning, U-Pb zirkondatering och test av olika abrasionstekniker.
210. Erlandsson, Maria, 2007: Den geologiska utvecklingen av västra Hamrångesynklinalens suprakrustalbergarter, centrala Sverige.
211. Nilsson, Pernilla, 2007: Kvidingedeltat – bildningsprocesser och arkitektonisk uppbyggnadsmodell av ett glacifluvialt Gilbertdelta.
212. Ellingsgaard, Óluva, 2007: Evaluation of wireline well logs from the borehole Kyrkheddinge-4 by comparsion to measured core data.
213. Åkerman, Jonas, 2007. Borrkärnekartering av en Zn-Ag-Pb-mineralisering vid Stenbrånet, Västerbotten.
214. Kurlovich, Dzmitry, 2007: The Polotsk-Kurzeme and the Småland-Blekinge Deformation Zones of the East European Craton: geomorphology, architecture of the sedimentary cover and the crystalline basement.
215. Mikkelsen, Angelica, 2007: Relationer mellan grundvattenmagasin och geologiska strukturer i samband med tunnelborrning genom Hallandsås, Skåne.
216. Trondman, Anna-Kari, 2007: Stratigraphic studies of a Holocene sequence from Taniente Palet bog, Isla de los Estados, South America.
217. Månsson, Carl-Henrik & Siikanen, Jonas, 2007: Measuring techniques of Induced Polarization regarding data quality with an application on a test-site in Aarhus, Denmark and the tunnel construction at the Hallandsås Horst, Sweden.
218. Ohlsson, Erika, 2007: Classification of stony meteorites from north-west Africa and the Dhofar desert region in Oman.
219. Åkesson, Maria, 2008: Mud volcanoes -

a review. (15 hskp)

220. Randsalu, Linda, 2008: Holocene relative sea-level changes in the Tasiusaq area, southern Greenland, with focus on the Ta1 and Ta3 basins. (30 hskp)
221. Fredh, Daniel, 2008: Holocene relative sea-level changes in the Tasiusaq area, southern Greenland, with focus on the Ta4 basin. (30 hskp)
222. Anjar, Johanna, 2008: A sedimentological and stratigraphical study of Weichselian sediments in the Tvärkroken gravel pit, Idre, west-central Sweden. (30 hskp)
223. Stefanowicz, Sissa, 2008: Palyno-stratigraphy and palaeoclimatic analysis of the Lower - Middle Jurassic (Pliens-bachian - Bathonian) of the Inner Hebrides, NW Scotland. (15 hskp)
224. Holm, Sanna, 2008: Variations in impactor flux to the Moon and Earth after 3.85 Ga. (15 hskp)
225. Bjärnborg, Karolina, 2008: Internal structures in detrital zircons from Hamrånge: a study of cathodolumine-scence and back-scattered electron images. (15 hskp)
226. Noresten, Barbro, 2008: A reconstruction of subglacial processes based on a classification of erosional forms at Ramsvikslandet, SW Sweden. (30 hskp)
227. Mehlqvist, Kristina, 2008: En mellanjuras-sisk flora från Bagå-formationen, Bornholm. (15 hskp)
228. Lindvall, Hanna, 2008: Kortvariga effekter av tefranedfall i lakustrin och terrestrisk miljö. (15 hskp)
229. Löfroth, Elin, 2008: Are solar activity and cosmic rays important factors behind climate change? (15 hskp)
230. Damberg, Lisa, 2008: Pyrit som källa för spårämnen – kalkstenar från övre och mellersta Danien, Skåne. (15 hskp)
331. Cegrell, Miriam & Mårtensson, Jimmy, 2008: Resistivity and IP measurements at the Bolmen Tunnel and Ådalsbanan, Sweden. (30 hskp)
232. Vang, Ina, 2008: Skarn minerals and geological structures at Kalkheia, Kristiansand, southern Norway. (15 hskp)
233. Arvidsson, Kristina, 2008: Vegetationen i Skandinavien under Eem och Weichsel samt fallstudie i submoräna organiska avlagringar från Nybygget, Småland. (15 hskp)
234. Persson, Jonas, 2008: An environmental magnetic study of a marine sediment core from Disko Bugt, West Greenland: implications for ocean current variability. (30 hskp)
235. Holm, Sanna, 2008: Titanium- and chromium-rich opaque minerals in condensed sediments: chondritic, lunar and terrestrial origins. (30 hskp)
236. Bohlin, Erik & Landen, Ludvig, 2008: Geofysiska mätmetoder för prospektering till ballastmaterial. (30 hskp)
237. Brodén, Olof, 2008: Primär och sekundär migration av hydrokarboner. (15 hskp)
238. Bergman, Bo, 2009: Geofysiska analyser (stångslingram, CVES och IP) av lagerföljd och lakvattenrörelser vid Albäcksdeponin, Trelleborg. (30 hskp)
239. Mehlqvist, Kristina, 2009: The spore record of early land plants from upper Silurian strata in Klinta 1 well, Skåne, Sweden. (45 hskp)
239. Mehlqvist, Kristina, 2009: The spore record of early land plants from upper Silurian strata in Klinta 1 well, Skåne, Sweden. (45 hskp)
240. Bjärnborg, Karolina, 2009: The copper sulphide mineralisation of the Zinkgruvan deposit, Bergslagen, Sweden. (45 hskp)
241. Stenberg, Li, 2009: Historiska kartor som hjälp vid jordartsgeologisk kartering – en pilotstudie från Vångs by i Blekinge. (15 hskp)

LUNDS UNIVERSITET

Geologiska institutionen
Centrum för GeoBiosfärsvetenskap
Sölvegatan 12, 223 62 Lund